DURABILITY OF RESIDENTIAL CONCRETE USING FLY ASH WITH A HIGH ALKALI -SULFATE CONTENT

by

Tanya Owens

B.Sc.Eng., University of New Brunswick, 2004
B.Sc.Math, University of New Brunswick, 2001

A Thesis Submitted in Partial Fulfillment of
the Requirements for the Degree of

Master of Science in Engineering

in the Graduate Academic Unit of Dept. Civil Engineering

Supervisor: Michael Thomas, PhD, PEng, Dept. of Civil Engineering

Examining Board: Theodore W. Bremner, PhD, PEng, Dept. of Civil Engineering
Arun Valsangkar, PhD, PEng, Dept. of Civil Engineering
Ian Smith, PhD, P.Eng, Faculty of Forestry and Environmental Management

This thesis is accepted by the Dean of Graduate Studies

THE UNIVERSITY OF NEW BRUNSWICK

January 2014

©Tanya Owens, 2014

ABSTRACT

This project represents research performed to determine if Popcorn Calcite Deposition (PCD) occurs in residential concrete (i.e. concrete with relatively high water-to- cement ratio) produced with Ordinary Portland Cement (OPC) and fly ash with varying sulfate and alkali contents and if found, what is its affect on both mechanical strength and mass transport properties?

Paste, mortar and concrete samples were cast with varying water to cementitious material ratio (W/CM) between 0.5 and 0.9 and were tested to determine the effect of carbonation on a wide range of properties.

Carbonation in fly ash samples was shown to decrease the connectivity of calcium bearing phase, with it worsening as the W/CM increased. It was also observed carbonated fly ash samples underwent pore coarsening with this being more evident in samples made with high sulfate high alkali fly ash.

ACKNOWLEDGMENTS

I would like to acknowledge all those who supported and believed in me during this research project when “just another four months” turned into years. Most of all I would like to thank my supervisor Dr. Mike Thomas for all the support and guidance over the course of my research and encouraging me when it almost seamed easier to give up. I would also like to thank Christine Gilbert for all the help in casting and testing she provided during the laboratory portion of my research.

I would like to thank the National Science and Engineering Research Council (NSERC) and the Portland Cement Association (PCA) for their financial contribution enabling me to conduct this research.

I would like to thank all of those whom I work with whom afforded me the time and encouragement during my work schedule to complete paper.

Finally, I would like to thank my family and friends for their support as without them this would not have been possible, you all know who you are.

TABLE OF CONTENTS

ABSTRACT ..... **II**

ACKNOWLEDGMENTS ..... **III**

TABLE OF CONTENTS ..... **IV**

LIST OF TABLES ..... **VII**

1.0 INTRODUCTION **1**

1.1 BACKGROUND INFORMATION 1
1.2 PROBLEM STATEMENT 4
1.3 SIGNIFICANCE OF PROBLEM 5
1.4 GOALS AND OBJECTIVES 6

2.0 LITERATURE REVIEW **7**

2.1 RESIDENTIAL CONCRETE 7
2.2 HIGH WATER-TO-CEMENTITIOUS-MATERIAL RATIO 7
2.3 LOW CEMENTITIOUS MATERIAL CONTENT 8
2.4 CURING 8
2.5 CARBONATION 9
2.5.1 Mechanism 9
2.5.2 Factors Affecting Carbonation Rates 10
2.5.3 Effects of Carbonation on Hardened Properties 13
2.5.3.1 Pore Structure 13
2.5.3.2 Mechanical Properties/Hardness 16
2.5.3.3 Corrosion 20
2.5.4 Popcorn Calcite Deposition (PCD) 21
2.5.4.1 Composition of PCD 24
2.6 FLY ASH 24
2.6.1 Description 25
2.6.2 Classification 26
2.6.3 Hydration Reactions and Pozzolanic Activity 26
2.6.4 Benefits 27
2.6.5 Disadvantages 28

3.0 CASE HISTORY OF RESIDENTIAL CONCRETE FOUNDATIONS **30**

3.1 BACKGROUND 30
3.2 MATERIALS AND MIX DESIGN 32
3.3 SCANNING ELECTRON MICROSCOPE (SEM) EXAMINATION 32

4.0 EXPERIMENTAL METHODS **34**

4.1 METHODOLOGY 34
4.1.1 Paste 34
4.1.2 Mortar 34
4.1.3 Concrete 35
4.2 MATERIALS 36

4.2.1 Cement 36
4.2.2 Fly Ash 37
4.2.3 Aggregate 38
4.2.4 Admixtures 38
4.3 MIX PROPORTIONS 38
4.3.1 Paste 38
4.3.2 Mortar 39
4.3.3 Concrete 39
4.4 MIXING, CASTING AND CURING 42
4.4.1 Paste 42
4.4.2 Mortar 43
4.4.3 Concrete 45
4.5 TESTING 46
4.5.1 Paste 46
4.5.1.1 Percolation 46
4.5.1.2 Microhardness 49
4.5.2 Mortar 50
4.5.2.1 Flexural Strength 50
4.5.2.2 Compression Strength 51
4.5.2.3 Tensile Strength 51
4.5.2.4 Dynamic Young's Modulus of Elasticity 51
4.5.2.5 Porosity 52
4.5.3 Concrete 54
4.5.3.1 Compressive Strength 54
4.5.3.2 Rapid Chloride Permeability Test (RCPT) 54
4.5.3.3 Electrical Resistivity 55
4.5.3.4 Carbonation 56
4.5.3.5 Water Vapour Transmission (WVT) 56
4.5.3.6 Rate of Absorption (Sorptivity) 58
4.5.3.7 Rebound Hardness 61

5.0 SUMMARY OF RESULTS 63

5.1 PASTE 63
5.1.1 Percolation 63
5.1.2 Microhardness 69
5.2 MORTAR 72
5.2.1 Mechanical Properties 72
5.2.1.1 CO_2-Enriched Environment 73
5.2.1.2 Wet-Dry Cycled Environment 75
5.2.2 Dynamic Young's Modulus of Elasticity 78
5.2.3 Porosity 79
5.3 CONCRETE 82
5.3.1 Compressive Strength 82
5.3.2 Rapid Chloride Permeability Test 85
5.3.3 Electrical Resistivity 91
5.3.4 Carbonation 93
5.3.5 Vapor Transmission 97

5.3.6 Rate of Absorption (Sorptivity) 99
5.3.7 Rebound Hardness 103

6.0 DISCUSSION OF RESULTS 107

6.1 RESIDENTIAL FOUNDATIONS 107
6.2 CARBONATION OF PORTLAND CEMENT PASTE AND MORTAR 108
6.3 FLY ASH AND CARBONATION OF FLY ASH PASTE AND MORTAR 109
6.4 FLY ASH CONCRETE AND MASS TRANSPORT 117
6.5 IMPLICATIONS AND LIMITATIONS OF STUDY 120

7.0 CONCLUSION 121

8.0 RECOMMENDATION 122

9.0 REFERENCE 123

CURRICULUM VITA

LIST OF TABLES

Table 2.1 Time Required to Achieve a Discontinuous Pore Structure (Powers et al, 1959) 8
Table 4.1Chemical Analysis of Portland Cement (OPC) 36
Table 4.2 Calculated Bogue Compositions and Total Alkali Content of OPC..... 37
Table 4.3 Table Chemical Analyses and Alkali Content of Fly Ashes 37
Table 4.4 Alkali and Sulfur Content for Fly Ashes 38
Table 4.5 Phase I Mix Proportions. 41
Table 4.6 Phase II Mix Proportions 41
Table 4.7 Pore Solution Concentrations. 44
Table 4.8 Summary of Testing..... 54
Table 5.1 Percolation Data..... 67
Table 5.2 Microhardness Data 69
Table 5.3 Mechanical Strength Results in MPa..... 72
Table 5.4 Resonant Frequency Measurements 78
Table 5.5 Porosity 79
Table 5.6 Compressive Strength (MPa)..... 82
Table 5.7 Charge Passed (KCoulombs)..... 86
Table 5.8 Chloride Ion Penetrability Based on Charge Passed 86
Table 5.9 Resistivity (Kohm-cm) 92
Table 5.10 Depths of Carbonation Data 93
Table 5.11 Vapor Transmission Data 97
Table 5.12 Absorption Data..... 99
Table 5.13 Rebound Hardness Data..... 103

LIST OF FIGURES

Figure 2.1 Effects of curing and Fly Ash on Depth of Carbonation. 11
Figure 2.2.2 Influence of Relative Humidity, W/CM and temperature on Depth of Carbonation (Parrot, 1987,Wierig 1984). 13
Figure 2.3 Water Absorption Rate vs. Capillary Porosity (Parrott, 1992)..... 15
Figure 2.4Effects of Carbonation on Compressive Strength a) W/CM=0.4 b) W/CM=0.5 c) W/CM=0.6 and d) Depth of Carbonation..... 17
Figure 2.5 Hardness values on carbonated concrete (Chang, J.J et al. 2003)..... 19
Figure 2.6 Micro Hardness Data from Carbonated Concrete (Thaulow et al. 2001) 19
Figure 2.7 Micro hardness Data of Carbonated Residential Concrete (Thaulow et al., 2001). 20
Figure 2.8 Schematic Model of Carbonation to the left and Bicarbonation to the right (Thaulow et al. 2001). 22
Figure 2.9 Backscatter Electron Image of Popcorn Carbonation..... 23
Figure 3.1 Carbonation Zone in Concrete Containing Fly Ash. (Backscattered Electron Image)..... 33
Figure 4.1 CO_2-Enriched Environment..... 43
Figure 4.2 CO_2 Removal Systems 45
Figure 4.3 Burning Algorithm of Neighbouring Pixels..... 47
Figure 4.4 (a) Original Image, (b) Threshold Image, (c) Burned Image 48
Figure 4.5 Diamond Indent for Vickers Micro Hardness 49
Figure 4.6 RCPT Cell Set up 55
Figure 4.7 WVT Set up. 57
Figure 4.8 Sample Plot of Cumulative Mass Gained vs. Time..... 58
Figure 4.9 Absorption Schematic (ASTM 1585-04) 59
Figure 4.10 Sample Absorption vs. SQRT Time Plot 61
Figure 4.11 Patterns for Rebound Hammer Measurements..... 62
Figure 5.1 Backscatter Electron Images (BSE) left and Percolated Images Right of paste with W/CM=0.50 (400X Magnification)..... 65
Figure 5.2 Backscatter Electron Images (BSE) left and Percolated Images Right of paste with W/CM=0.90 (400X Magnification)..... 66
Figure 5.3 Percolation Relationships to W/CM..... 68
Figure 5.4 Ratio of Control Percolation to Fly Ash Mixes..... 68
Figure 5.5 Microhardness Non-Carbonated Paste 70
Figure 5.6 Microhardness Carbonated Paste. 70
Figure 5.7 Relative Microhardness Between Non-Carbonated and Carbonated Paste. 71
Figure 5.8 Relative Changes in Mechanical Strength between Non-Carbonated and Carbonated Mortar without Fly Ash (MOPC) 73
Figure 5.9 Relative Changes in Mechanical Strength between Non-Carbonated and Carbonated Mortar (MBR)..... 74
Figure 5.10 Relative Changes in Mechanical Strength between Non-Carbonated and Carbonated Mortar (MRP) 74
Figure 5.11 Relative Changes in Mechanical Strength between Non-Carbonated and Carbonated Mortar (MTB)..... 75

Figure 5.12 Relative Changes in Mechanical Strength between Non-Carbonated and Wet Dry Cycled Mortar (MOPC) 76
Figure 5.13 Relative Changes in Mechanical Strength between Non-Carbonated and Wet Dry Cycled Mortar (MBR) 76
Figure 5.14 Relative Changes in Mechanical Strength between Non-Carbonated and Wet Dry Cycled Mortar (MRP) 77
Figure 5.15 Relative Changes in Mechanical Strength between Non-Carbonated and Wet Dry Cycled Mortar (MTB) 77
Figure 5.16 Ratio of Squared Resonant Frequencies Between Non-Carbonated and Carbonated, Non-Carbonated and Wet-Dry Cycled. 79
Figure 5.17 Relative Changes in Porosity between Non-Carbonated and Carbonated Mortar 80
Figure 5.18 Relative Changes in Porosity between Non-Carbonated and Wet Dry Cycled Mortar 81
Figure 5.19 28-Day Compressive Strength..... 84
Figure 5.20 90-Day Compressive Strength..... 84
Figure 5.21 Continuously Cured Compressive Strength 85
Figure 5.22 1-Day Moist-Cured RCPT..... 87
Figure 5.23 3-Day Moist-Cured RCPT..... 88
Figure 5.24 7-Day Moist-Cured RCPT..... 88
Figure 5.25 Charge Passed for Concrete with W/CM=0.70 89
Figure 5.26Charge Passed for Concrete with W/CM=0.85 90
Figure 5.27 Relative Charge Passes between Control and Fly Ash Concrete (W/CM=0.70)..... 90
Figure 5.28 Relative Charge Passes between Control and Fly Ash Concrete (W/CM=0.85)..... 91
Figure 5.29 Relationships between Resistivity and Rapid Chloride Permeability 92
Figure 5.30 1-Day Cure Carbonation..... 94
Figure 5.31 3-Day Cure Carbonation..... 95
Figure 5.32 7-Day Cure Carbonation..... 95
Figure 5.33 90-Day Carbonation 96
Figure 5.34 365-Day Carbonation 96
Figure 5.35 Water Vapor Transmission..... 98
Figure 5.36 Relative Water Vapor Transmission Between Control and Fly Ash Concrete 98
Figure 5.37 Initial Absorption..... 100
Figure 5.38 Secondary Absorption 101
Figure 5.39 Relative Initial Absorption between the Control and Fly Ash Concrete 101
Figure 5.40 1-Day Moist-Cured Rebound Hardness Number 104
Figure 5.41 3-Day Moist-Cured Rebound Hardness Number 105
Figure 5.42 7-Day Moist-Cured Rebound Hardness Number 105
Figure 5.43 Relative Rebound hardness between 28-365 days W/CM 0.7 106
Figure 5.44 Relative Rebound hardness between 28-365 days W/CM 0.7 106
Figure 6.1Backscatter Electron Images of Carbonated Residential Concrete 107
Figure 6.2 Control Mechanical Strengths at 40-Weeks. 108

Figure 6.3 Relative Mechanical Strength between MBR and MCON Stored in CO_2 Enriched Atmosphere 110
Figure 6.4 Relative Mechanical Strength between MTB and MCON CO_2 Enriched Atmosphere 111
Figure 6.5 Relative Mechanical Strength between MRP and MCON CO_2 Enriched Atmosphere 111
Figure 6.6 Mechanical Strengths Non carbonated and Carbonated samples at 40-Weeks of a)BR, b) RP, and c) TB 113
Figure 6.7 Mechanical Strengths Wet Dry (tent) and Carbonated samples at 40-Weeks of a)Con, b) BR, c) RP, and d) TB 115
Figure 6.8 Carbonated Samples Relating % Coarse Porosity and %Percolation 117
Figure 6.9 Fly Ash compared to Control Compressive Strength at 90 days..... 118
Figure 6.10 Carbonation at 365 day..... 119

1.0 Introduction

1.1 Background Information

For many years, carbonation has been studied as a form of deterioration in concrete with respect to the corrosion of embedded reinforcing steel, scaling and shrinkage. Other reports on the effects of carbonation have lead to benefits such as improvement in strength, hardness and dimensional stability of cement products (ACI Committee 201, 2001).

Carbonation can be caused by carbon dioxide found in the atmosphere or in ground water. In both cases a reaction occurs between the dissolved carbon dioxide and calcium- bearing phases, mainly calcium hydroxide, producing calcium carbonate.

Fly ash has been used in concrete as a pozzolan for many years to improve fresh and hardened properties in addition to providing economic and environmental benefits. A pozzolan is defined by the American Society for Testing and Materials (ASTM) as "a siliceous or siliceous and aluminous material which in itself possesses little to no cementitious value but which will, in finely divided form and in the presence of moisture, chemically react with calcium hydroxide at ordinary temperature to form compounds possessing cementitious properties." Malhotra and Ramezanianpour (1994) also add that the alumino-silicates in the presence of moisture will react with the calcium ions to form calcium silicate hydrates.

Fly ash (fa) is the inorganic, non-combustible by-product of the coal-burning process (Mindess, et al. 2003). The composition of fly ash is dependant on the initial composition of the non-combustible minerals in the coal before the burning process. In North America fly ash is classified by either ASTM or Canadian Standards Association (CSA). First there is the classification set out in ASTM 618 which states that a Class F ash has a chemical composition where SiO_2 + Al_2O_3 + Fe_2O_3 ≥70 % and a Class C is where SiO_2 + Al_2O_3 + Fe_2O_3≥ 50%. Class C ashes are normally products or lignite of subbituminous coals and Class F are products of bituminous or anthracite coals (Malhotra and Ramezanianpour, 1994). Although this classification system makes no reference to calcium content, Class C is often termed high-calcium and Class F low-calcium fly ash. CSA A3000-03 has moved to classifying fly ash based on its calcium content as follows: Type F<8% CaO (low-calcium), Type CI 8-20% CaO (moderate-calcium), and Type CH >20% CaO (high-calcium).

Fly ash has been used and studied for many years in the Canadian concrete industry. It has been shown that with proper use, fly ash can improve several properties of concrete leading to increased durability. The majority of fly ashes used and studied in the Atlantic Provinces are low-calcium ashes and in Western Canada they are moderate-calcium ashes. Typically these ashes have a relatively low alkali and sulfate content (Na_2O_{eq} <4% and SO_3 <3%). Currently the fly ash produced or imported into Canada can have mineral compositions that vary substantially from those used in the past. Fly ash now used can have calcium

contents exceeding 30% CaO , alkali content up to 10% Na_2O_{eq}, and/or sulfates contents up to 6%. These differences in composition may have a significant impact on the performance and durability of concrete.

Even though fly ash is classified on the bases of its major oxides, other oxides such as SO_3, Na_2O_{eq}, and MgO play a role in its performance. Because of stricter regulations against emissions produced by power plants, scrubbers are installed to reduce the amount of sulfur dioxide escaping from the stacks. During this process the fly ash may be mixed with scrubber residue increasing the free lime and sulfate content. There are limits placed on some of these oxides when used in certain applications. Such limits would include maximum alkali content when being used with a reactive aggregate. CSA 3001-03 limits the sulfate content of the fly ash to ≤5% SO_3 unless it is demonstrated by performance testing using CSA 3004-C4 that higher levels of sulfate do not result in deleterious expansion.

Back in the mid-1980's fly ash with particular characteristics such as high alkali-sulfate content, in particular sodium sulfate ($NaSO_4$), was used in a large number of residential foundations (basement walls). Along with the use of fly ash, this concrete had a low cement content and was also suspected to have a excessively high water-to-cementitious-ratio (W/CM), up to or over 0.90. This concrete has reportedly experienced severe mechanisms of deterioration such as efflorescence, sub-florescence, spalling and scaling, which was later attributed to the characteristics of the fly ash. Several explanations such as chemical and physical

sulfate attack, carbonation, and/or freeze thaw actions have been proposed to explain this deterioration.

During the investigation of this deterioration it was noted that the calcium carbonate formed due to carbonation was micro-structurally different from that typically formed by the carbonation process. The calcium carbonate formed discrete nodules in a decalcified silica gel. Even though the calcium carbonate precipitate was uncharacteristic of carbonated concrete, it has been observed in several other structures and was termed popcorn carbonation or popcorn calcite deposition (PCD). This is due to the small-nodule form of calcium carbonate having the appearance of popcorn. This carbonation zone has been reported to be soft and friable. There have been several connections made between PCD and thaumasite sulfate attack found in other structures. (Sibbick, 2003; Hagelia et al. 2003)

1.2 Problem Statement

In most deteriorated concretes a combination of mechanisms are responsible for the damage. It is well known in the cement and concrete industry that the most controlling factor in concrete production that influences durability is the W/CM. With an increase in W/CM the concrete is more permeable to water and aggressive chemicals, which increases the risk of premature deterioration due to physical and chemical attack. (Neville, 1993; Mindess et al. 2003)

Many studies have been performed on the durability of fly ash with low W/CM, varying curing time, and different replacement levels. However, little research has been done with high W/CM (> 0.7). One of the concerns surrounding the use of fly ash is its effect on increasing the rate of carbonation. Currently the main concern when dealing with carbonation is its effect with regards to reinforcing steel. As concrete carbonates the pH of the pore solution is reduced which destroys the resistance of the reinforcing steel to corrosion. However, carbonation is rarely investigated when dealing with residential construction (e.g. foundation walls are rarely structurally reinforced with rebar). It is unknown whether the form of carbonation, PCD, found in the residential concrete foundations was a result of fly ash composition, high W/CM, or a combination of the two. It is also unknown what effect PCD has on the mass transport properties and mechanical strength of concrete.

1.3 Significance of Problem

The use of fly ash in low replacement levels in different applications has been accepted in various concrete applications in North America since the mid 1970's. When properly used, fly ash has been shown to enhance fresh and hardened properties of concrete. However, in some applications such as residential construction, fly ash is being used in combination with more relaxed regulations placed on the concrete itself. If several conditions, such as high W/CM, low cement content and short cure time, are present with the use of fly ash with

different compositions, deleterious processes may occur. These parameters need to be evaluated to ensure the proper use of fly ash for these applications.

1.4 Goals and Objectives

The goal of this project was to determine if the carbonation, PCD, found in residential concrete containing high alkali-sulfate fly ash is a result of the chemical composition of the fly ash, high W/CM, or a combination of these factors.

The objectives of this project were as follows:

1. To examine the effect of W/CM (0.70 and 0.85) and varying fly ash composition on strength, surface hardness, carbonation rates, permeability, absorption, and vapor transmission of concrete.
2. To determine the effects of "accelerated" carbonation on flexural, tensile, compressive strength, and porosity of mortars produced with fly ash differing in composition.
3. To determine the effect of "natural" carbonation and cyclic wetting and drying on flexural, tensile, and compressive strength of mortars produced with fly ash differing in composition.
4. To determine the difference in the microstructure and connectivity of calcium carbonate in carbonated paste varying in W/CM, and fly ash composition.
5. To determine the difference in micro-hardness in carbonated and non-carbonated paste varying in W/CM and fly ash composition.

2.0 Literature Review

2.1 Residential Concrete

There are several characteristics of residential foundation construction that makes the concrete more susceptible to rapid deterioration. This includes mix design factors such as high water to cementitious material ratios (W/CM) and low cementitious material contents. In the field, construction practices of adding water on site to enhance slump and short curing times can adversely affect the performance of the concrete structure.

2.2 High Water-to-Cementitious-Material Ratio

Water to cementitious material ratio (W/CM) is one of the most critical parameters that influence the durability of concrete. The W/CM influences the permeability of the cementing systems; more specifically it affects the quantity of capillary pores, which is the governing factor in the movement of water, aggressive chemicals, and gases through concrete. As the W/CM decreases, so does the capillary porosity. The permeability is influenced by the connectivity of the capillary pores. As hydration continues, cement hydration products form in the capillary pores, and this leads for the creation of a discontinuous and tortuous pore system (Mindess et al. 2003). That being said, concrete with a W/CM greater than 0.7 will never experience complete discontinuity of capillary pores. See Table 2.1 for the relationship between W/CM and curing time required to produce a discontinuous capillary pore system.

Table 2.1 Time Required to Achieve a Discontinuous Pore Structure (Powers et al, 1959)

W/C	Time
0.40	3 Days
0.45	7 Days
0.50	14 Days
0.60	6 Months
0.70	1 Year
>0.70	Impossible

With the increase in porosity created by increased W/CM, researchers have also shown that as the W/CM increases the compressive strength decreases. Duff Abrams, in 1918, developed a simplistic model for determining the compressive strength at a fixed age. Strength of concrete is governed by two variables: the degree of hydration and the capillary porosity. As the concrete industry increases the use of minerals and chemical admixtures, this model grows more complex.

2.3 Low Cementitious Material Content

The lowest strength requirement for residential concrete is 15-20 MPa for footings, walls, and interior slabs (CSA A438, 2000). With today's cements, this is easily achievable with relatively low cement contents. With the designed water demand and construction practices, W/CM may exceed values recommended for protection against deterioration.

2.4 Curing

Cement hydration relies on the availability of water to undergo the chemical reaction. The prolonged availability of water or protection against evaporation is

termed curing. This concept of curing has been well established in the concrete research community and concrete industry. However, when concrete reaches the residential construction industry, there is less effort extended to properly cure concrete due to the fact it is “just a foundation” and the formwork is needed for the next project or to keep crews working.

2.5 Carbonation

2.5.1 Mechanism

In the first stage of the carbonation process carbon dioxide from the atmosphere or ground water, diffuses through the concrete and dissolves in the capillary pore water of concrete to form bi-carbonate (HCO_3^-); see Equation 2.1 for the reaction. The bi-carbonate ions react further with hydroxyl ions to form carbonate ions (CO_3^-) as shown in Equation 2.2. This lowers the pH of the pore solution, which is normally greater then 13, to less then 8; this is also referred to as neutralization. During this process calcium hydroxide dissolves into the pore solution and increases the pH to 12.5. The calcium then reacts with the carbonate ions to form calcite (calcium carbonate ($CaCO_3$)). See Equation 2.3 for reaction. Along with calcium hydroxide, other calcium phases (such as calcium-silicate-hydrate, C-S-H, and various calcium aluminate hydrates) are also partially stripped of their calcium; this process is known as de-calcification (Meyers S.L.1949 Found in Verbeck 1958).

$$CO_2 + OH^- \rightarrow HCO_3^- \qquad \text{Equation 2.1}$$

$$HCO_3^- + OH^- \rightarrow CO_3^- + H_2O \qquad \text{Equation 2.2}$$

$$Ca(OH)_2 + CO_3^- \rightarrow CaCO_3 + H_2O \qquad \text{Equation 2.3}$$

As a result of the de-calcification of the other calcium-bearing phases silica gel, hydrated aluminum and iron oxides are left behind. After complete carbonation, sulfate originally present in the cement will convert from calcium sulfoaluminate phases to gypsum (Parrott, 1978).

2.5.2 Factors Affecting Carbonation Rates

The main factors that affect the rate of carbonation are W/CM, cement content, type and amount of supplementary cementing materials, and curing time. These factors influence the permeability, as discussed above, and the mass of calcium hydroxide available for reaction (Parrott 1987, Malhotra and Ramezanianpour ,1994) . Other environmental factors that influence the rate of carbonation are the degree of saturation with water, the concentration of CO_2 present in the atmosphere or ground water, and temperature.

As the W/CM ratio is decreased, the volume of capillary porosity is decreased, which leads to an increased discontinuous pore system. This discontinuity reduces the rate at which carbon dioxide can diffuse through concrete and cause a reaction between the dissolved carbon dioxide and calcium-bearing phases in concrete. The carbonation reaction is further reduced by increased curing time. At short curing times the surface layer of concrete is allowed to reduce in moisture content and stop further hydration. This reduction in the degree of hydration will increase the porosity, increase permeability, and decrease the amount of hydration

products that need to be consumed in order for the carbonation reaction to propagate (Parrott, 1987). Curing time is more critical for concrete containing fly ash, which will be discussed later. The increase in the rate of carbonation due to curtailing curing time or increasing fly ash content can be seen in Figure 2.1

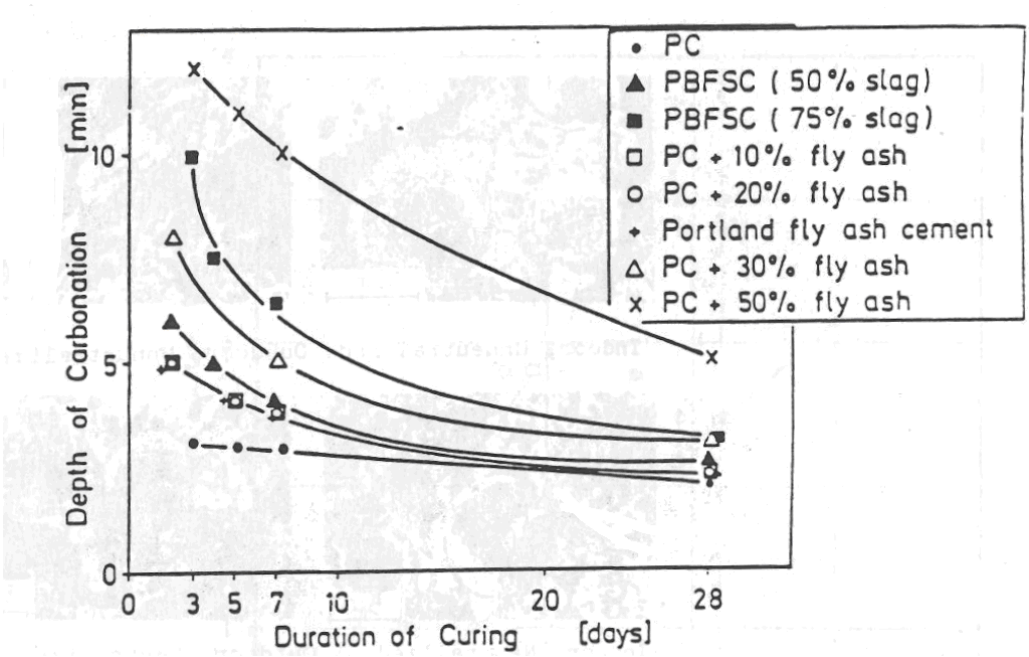

Figure 2.1 Effects of curing and Fly Ash on Depth of Carbonation. (Parrot, 1987)

As mentioned above, permeability influences the migration of water and aggressive chemicals through concrete. This includes atmospheric CO_2 and CO_2 dissolved in ground water. In the case of carbonation, Fick's law of diffusion governs the diffusion of CO_2 through the concrete. The permeability influences the diffusion coefficient and the concentration of carbon dioxide influences the rate of diffusion (Parrot, 1987)

Cement content also affects the rate of carbonation as the actual mass percent of calcium hydroxide found in the system is decreased as the mass of cement used decreases. The amount of calcium hydroxide found in concrete is also influenced by the replacement of cement with supplementary cementing materials. In the case of mass percent replacement, the fact that cement is being replaced by another material reduces the quantity of calcium hydroxide produced. More importantly in the case of pozzolans, the very nature of the reaction, siliceous material reacting with calcium hydroxide, results in the consumption of calcium hydroxide present. Also, the use of fly ash increases the permeability at early ages and if the concrete is not cured adequately the state of high permeability will be maintained throughout service. The effects of fly ash on carbonation will be examined in more depth later in this report.

It has been well established that concrete will carbonate at a faster rate when the relative humidity is between 40% and 75% the optimum being approximately 65%, as shown in Figure 2.2 (Parrott 1987). This is required for the CO_2 from the atmosphere to dissolve into the pore water to form the bicarbonate before any interaction between it and the solid phases of calcium can occur. If the relative humidity is too low, no significant reaction can occur. On the other hand, if the concrete is saturated carbonation can still occur, however since the carbon dioxide diffuses through the concrete, water in the pores will limit the gaseous diffusion and the rate of carbonation is reduced. (Parrott, 1987)

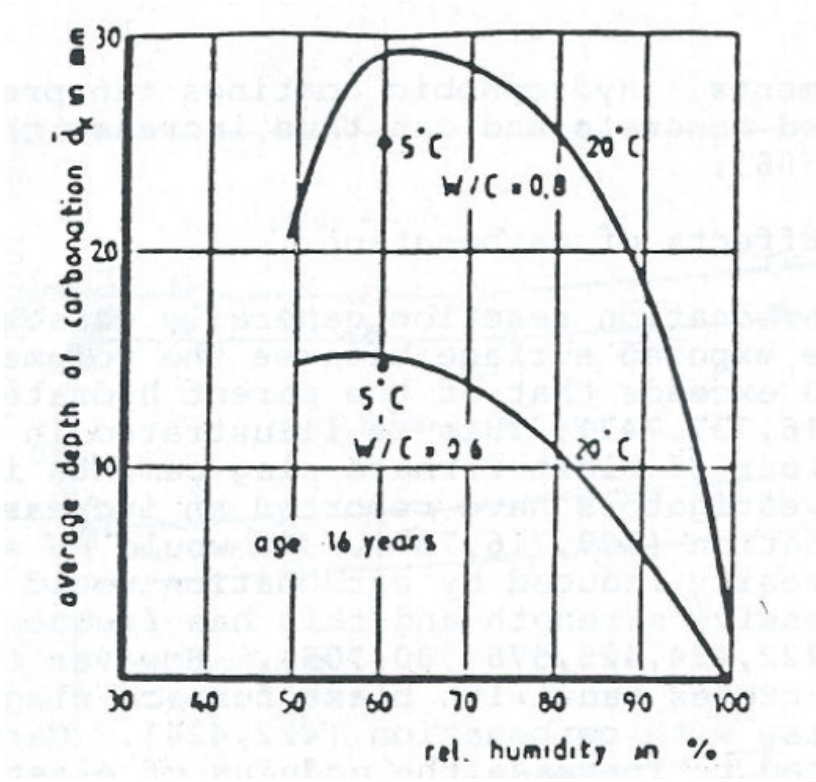

Figure 2.2 Influence of Relative Humidity, W/CM and temperature on Depth of Carbonation (Parrot, 1987,Wierig 1984).

2.5.3 Effects of Carbonation on Hardened Properties

2.5.3.1 Pore Structure

One of the most important properties when designing concrete from a materials perspective, aside from structural requirements, is it resistance to the transport of water and aggressive chemicals. When water passes through concrete it may lead to chemical and/or physical deterioration to the cementing system. There are many variables in concrete production that influence transport properties. Some of the most recognized variables include W/CM ratio, curing time, and the use of supplementary cementing materials. Other factors that influence the ability of concrete to transport water and aggressive chemicals include chemical and

physical attack such as; sulfate attack, alkali silica reaction, corrosion and freeze-thaw that create cracks that act as conduits for further transport.

One of the normal effects of carbonation on hardened concrete is a reduction in porosity. This reduction is explained by the increase in solid volume when the calcium-bearing hydrates are converted into calcium carbonate (Parrott 1987, Ngala and Page, 1997). This reduction in porosity has lead to observed increases in compressive strength. There have been several studies showing this reduction of porosity due to carbonation.

Ngala and Page (1997) showed in paste, produced at W/CM ratios of 0.5, 0.6, and 0.7 with OPC (Ordinary Portland Cement), OPC/30% FA (Fly Ash) and OPC/65% BFS (Blast Furnace Slag), a decrease in total porosity due to carbonation; however, there was a redistribution of pore sizes. They showed an increase in the proportion of large capillary pores in all paste mixes and found the increase in the OPC to be negligible when compared to the 140% and 230% increase in the paste produced with fly ash and slag respectively. Parrott (1992) also observed this increase in capillary porosity in concrete containing fly ash and slag that was affected by carbonation. Ngala and Page (1997), reported in Bier (1986), described the coarsening of the pore structure as the formation of silica gel produced due to the decomposition of C-S-H as a result of prolonged carbonation. This difference was also associated with the differences in original composition, amount of hydrates produced, and the pozzolanic reaction of fly ash

and the hydraulicity of slag that reduces the calcium hydroxide and increases the C-S-H gel that decomposes into the silica gel (Ngala and Page, 1997). Kobayashi (1993) also reported that carbonation decomposes not only $Ca(OH)_2$ but also C-S-H in various structures across Japan.

Parrot (1992) showed that in zones of carbonation for ordinary Portland cement there was a decrease in capillary porosity and rate of absorption; however, there was increase in capillary porosity and the rate of absorption for cement containing fly ash and slag. An increase in capillary porosity leads to an increase in the rate of absorption as shown in Figure 2.3.

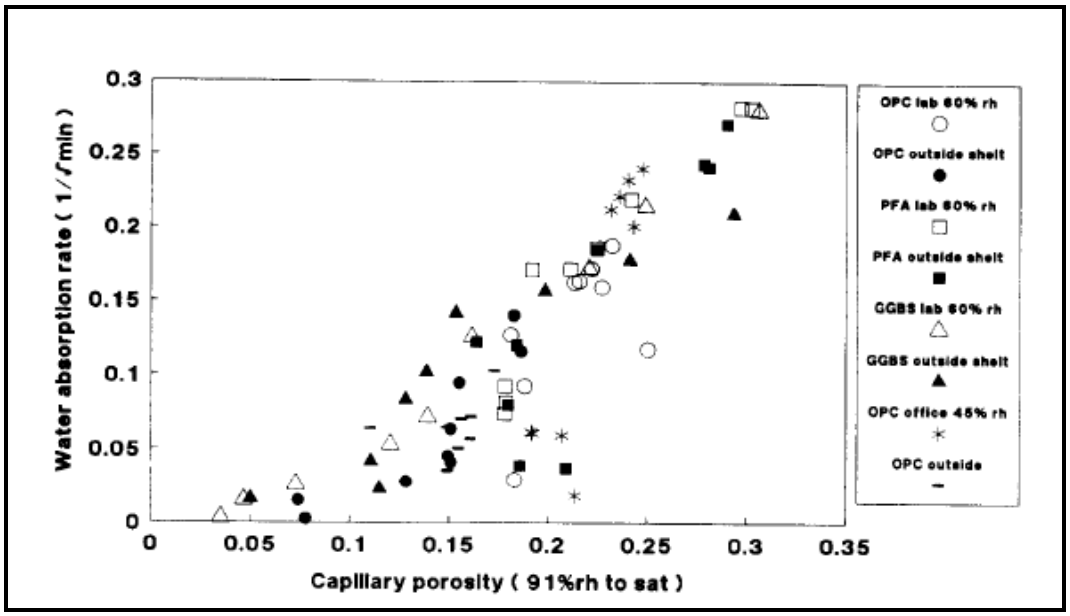

Figure 2.3 Water Absorption Rate vs. Capillary Porosity (Parrott, 1992)

Although there is an increase in capillary porosity, there is a critical point at which capillary pores become continuous. This increase in absorption can be seen

above 0.1% to 0.15%. Parrott (1992) describes this point as the transition between when porosity in the cement goes from being discontinuous to continuous.

2.5.3.2 Mechanical Properties/Hardness

Chang et al (2003) reported several observations when concrete was allowed to carbonate (1 atmosphere 50% CO_2 concentrations) from the ends only and from the sides only when compared to the control that was exposed to atmospheric CO_2 concentration of 0.03%. He found that when allowed to carbonate, the concrete experienced an increase in compressive strength. These results can be seen in Figure 2.4. Furthermore, the concrete that was allowed to carbonate from the side surfaces experienced a greater depth of carbonation and showed a larger increase in compressive strength. He also showed that at higher W/CM the depth of carbonation was greater at any given time as seen in Figure 2.4 d).

Chang et al. (2003) concluded that this increase in compressive strength could be attributed to the formation of a stronger calcite replacing weaker calcium hydroxide. Also, not mentioned by Chang et al. (2003) but discussed earlier in this paper, carbonation decreases the porosity that leads to an increase in the compressive strength.

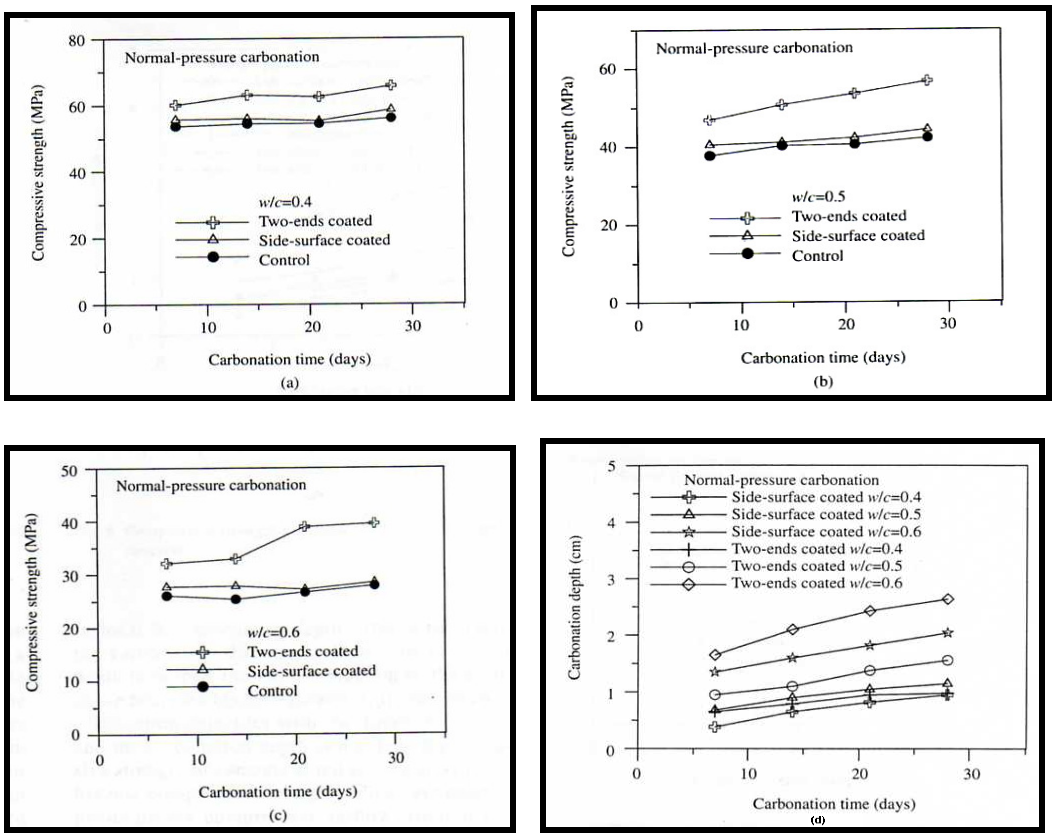

Figure 2.4Effects of Carbonation on Compressive Strength a) W/CM=0.4 b) W/CM=0.5 c) W/CM=0.6 and d) Depth of Carbonation (Chang et al., 2003)

Microhardness is used to evaluate the quality of materials by forcing an indenter into the surface of the material and measuring the size of the indentation (Igarashi et at, 1996). There are several different types of testing used to determine micro hardness of a material such as Vickers, Knoop, Berkovitch, and Bernell. The most commonly used is Vickers which has a diamond indenter and has a hardness value that is the ratio between the load and the contact area, giving units of stress (Igarashi et al., 1996).

Microhardness, more specifically Vickers, was developed for metals but is now being used to determine mechanical responses of other materials such as ceramics

and cement pastes (Igarashi et al., 1996). There are several areas where hardness measurements are used in the study of cement paste. One of these is the quantification of the micro-structural gradients across the interfacial transition zone (ITZ), the zone between cement paste and aggregate particles. This zone has been shown to have a varying W/CM ratio and microstructure when compared to the bulk paste (Asbridge et al, 2002). Secondly, it has been used to determine if bond degradation between the reinforcing steel and the concrete is due to softening of the concrete (Chang , 2001). Thirdly, which is of interest in this study, it is used to evaluate the change in hardness due to carbonation (Chang et al, 2003).

Along with compressive strength discussed earlier, Chang (2001) also examined the change in microhardness of non-carbonated to carbonated concrete. They measured the hardness with relation to depth from the surface and found that carbonation enhanced the hardness as shown in Figure 2.5. The data in Figure 2.5 also show that hardness increases as the W/CM decreases.

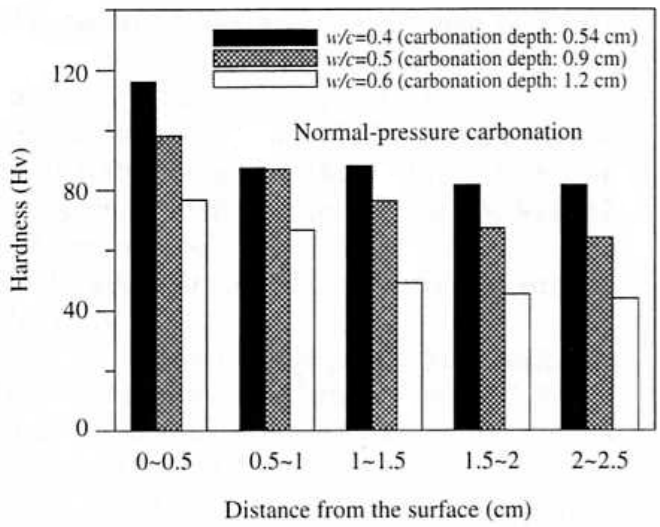

Figure 2.5 Hardness values on carbonated concrete (Chang, J.J et al. 2003)

Thaulow et al (2001) also showed that carbonated concrete showed an increase in hardness when compared to non-carbonated concrete as shown in Figure 2.6

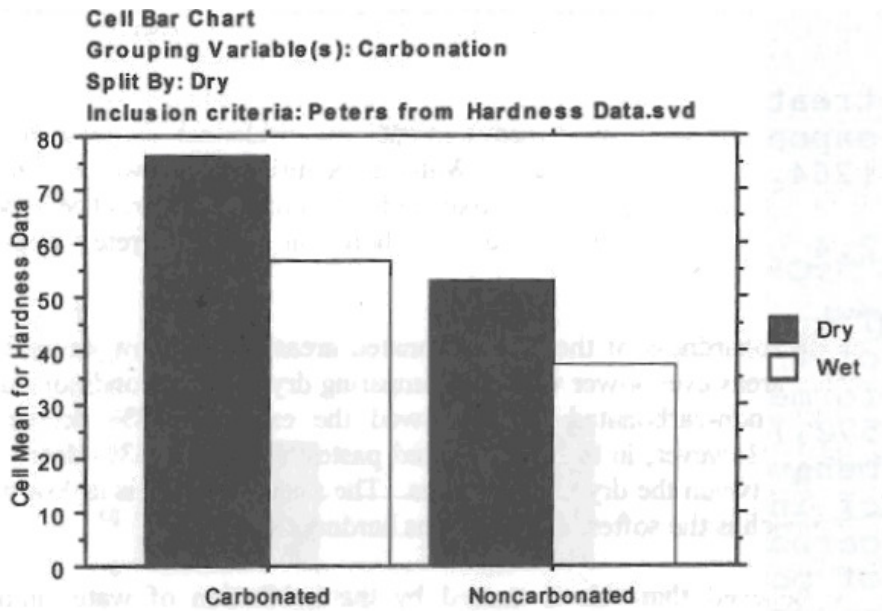

Figure 2.6 Micro Hardness Data from Carbonated Concrete (Thaulow et al. 2001)

However, when examining concrete obtained from residential foundation walls with high W/CM and fly ash they found that there was a decrease in hardness due to carbonation. See Figure 2.7 for hardness of carbonated residential concrete.

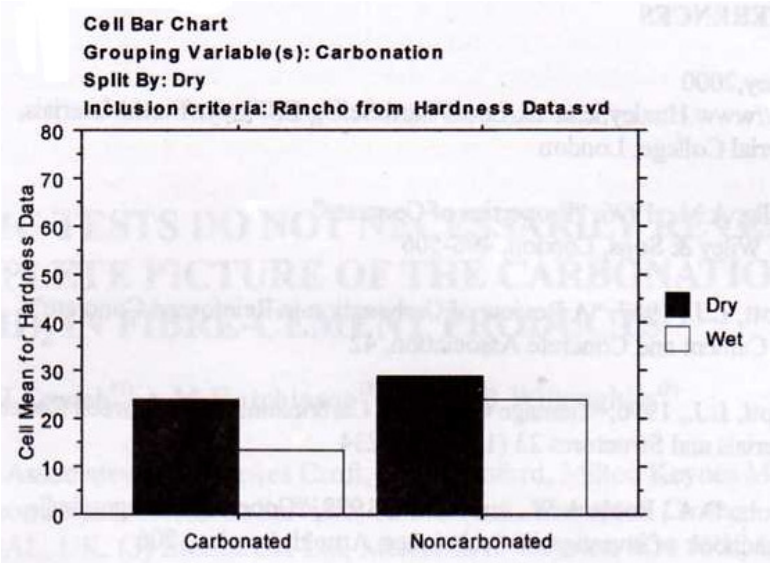

Figure 2.7 Micro hardness Data of Carbonated Residential Concrete (Thaulow et al., 2001).

Thaulow et al (2001) attributed this reduction in hardness to the bicarbonate or popcorn carbonation observed in the residential concrete. He further explained this due to the presence of water in the decalcified silica gel resulting in a softening of the cement paste.

2.5.3.3 Corrosion

As discussed above, carbonation decreases the alkalinity of the pore solution. Once this alkalinity drops the passive layer coating the reinforcing steel no longer protects the steel from corrosion. This topic has been researched significantly but is not relevant to this study which is concerned with the effects of carbonation on the properties of non-reinforced concrete.

2.5.4 Popcorn Calcite Deposition (PCD)

Research has shown that carbonation produces calcium carbonate that occupies more space then the calcium hydroxide it replaces. As the calcium carbonate occupies more space, the porosity is reduced and certain properties are improved such as increased strength and reduced permeability. However, other effects such as a decrease in pore solution pH, have a detrimental effect on reinforced concrete. Steel in concrete with a pH>13 has a passive layer that protects the steel from corrosion. When the concrete has undergone the carbonation process the pH is reduced to below 8, which destroys this passive layer and allows the rebar to become vulnerable to corrosion if all other conditions are met (i.e. oxygen and water are required to sustain corrosion).

It has been observed in various concretes that the calcium carbonate formed as a result of carbonation sometimes takes on the characteristics of "popcorn" like clusters. This type of calcite deposition has been termed popcorn carbonation or popcorn calcite deposition (PCD) and has been noted to be soft and friable. It has been thought that this type of carbonation is associated with the alkalinity of the cementitious materials. One conjecture is that with higher alkalinity, CO_2 dissolves faster and decomposes the calcium phases at a faster rate. This carbonation process not only consumes calcium from calcium hydroxide but other calcium phases such as C-S-H and C-A-H, leaving behind a silica-aluminum gel low in calcium. This can be seen pictorially in Figure 2.8 (Thaulow et al., 2001).

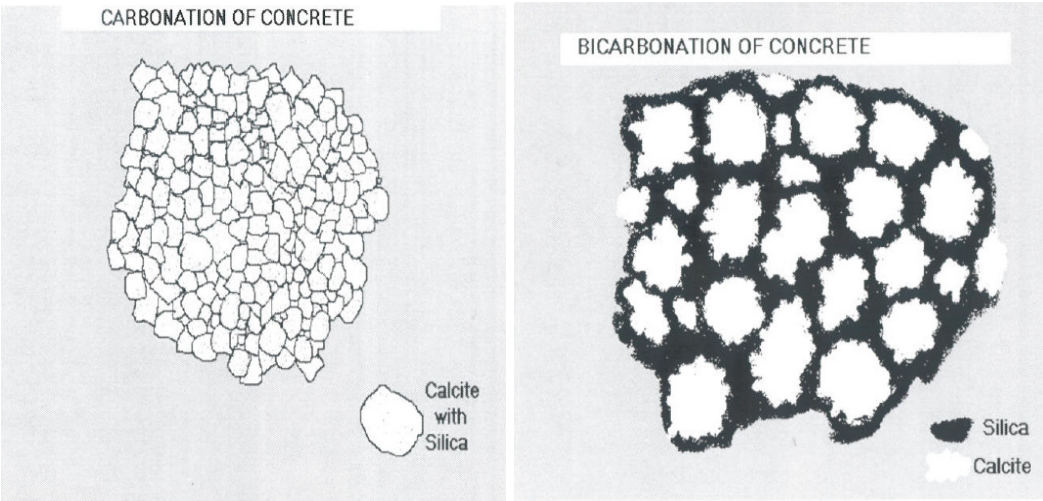

Figure 2.8 Schematic Model of Carbonation to the left and Bicarbonation to the right (Thaulow et al. 2001).

In the past, researchers have investigated varying forms of material failures and degradation processes involving Portland cement based materials. Some of these processes include sulfate attack, thaumasite form of sulfate attack, seawater attack, acid attack, alkali-silica reaction, leaching due to excessive groundwater flow and the action of aggressive carbon dioxide. With these degradation processes they all, to varying degrees, involve the reduction of alkalis within the cement based materials (Sibbick and Crammond 2003). Thaulow et al. (2001)) have also associated this reduction in pH with the unusual formation of calcium carbonate deposition termed popcorn calcite deposition (PCD).

As discussed above, carbonation is the process in which carbon dioxide from the environment dissolves into the pore solution and creates a reduction in its pH. In this low alkali environment, various calcium phases become soluble. In the cases of most carbonation reactions, calcium hydroxide is consumed and forms calcium

carbonate. Further research has shown other calcium phases, such as calcium silicate, calcium aluminates and even un-hydrated cement particles, carbonate and undergo decalcification. (St. John et al in Thaulow et al., 2001)

As other calcium phases carbonate, residual silica forms a silica gel matrix in which the carbonate precipitates as "popcorn" shaped crystals. This popcorn like appearance can be seen in Figure 2.9. This process is referred to as popcorn calcite deposition, also known as popcorn carbonation or bi-carbonation.

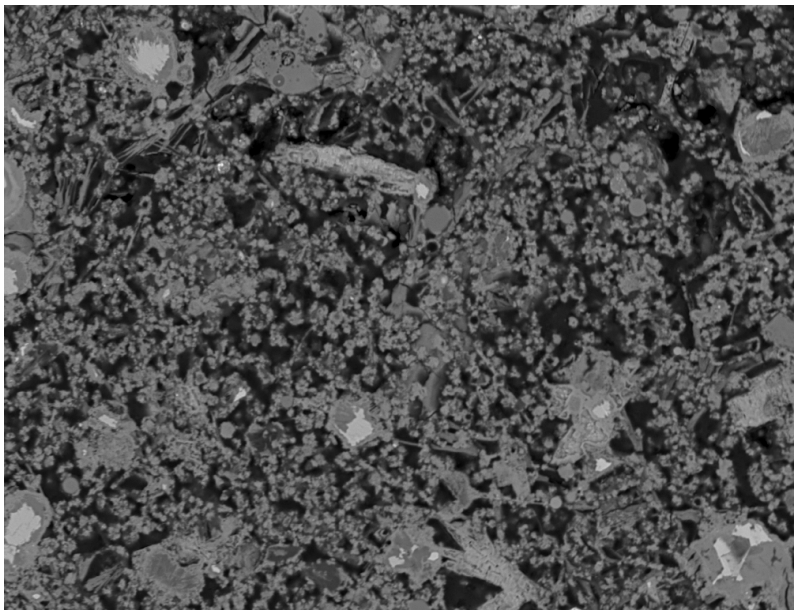

Figure 2.9 Backscatter Electron Image of Popcorn Carbonation

This type of carbonation has been observed in several other alkali-consuming or pH-reducing processes. It is hard to determine if this is a new or an existing problem due to the fact that the concrete or mortars affected by this process are sometimes left soft and friable and if the sample is not carefully collected, the affected material will be lost. Another reason why this may not be detected is due

to the fact that if no other symptoms of deterioration are present an investigation may not be initiated. There have been several reported cases of PCD over the past decade, when other processes have been examined. One of these associated forms of deterioration in which PCD has also been identified in concrete and mortar is the thaumasite form of sulfate attack (Hagelia et al. 2003)

2.5.4.1 Composition of PCD

In some cases, the calcium carbonate formed is pure calcite crystals and in other cases it may have traces of silica present (note less stable forms of calcium carbonate, namely aragonite and vaterite, may form initially under some circumstances but will eventually change to calcite). As this process occurs through the porous silica matrix, silica gets entrapped in the calcium carbonate as an impurity. This silica gel also contains aluminum, iron and magnesium derived from other calcium-bearing phases.

2.6 Fly Ash

Due to the ever increasing use of fly ash in concrete, much attention must be paid to the composition and possible long-term durability issues. Fly ash and other supplementary cementing materials has been the subject of research for many decades. However, due to ever advancing technology and environmental concerns, the properties of some of these SCM's are changing. With these changes, those responsible for producing material specifications need to limit or restrict the use of materials with particular chemical properties such as sulfates,

calcium oxide, LOI (Loss of Ignition) and moisture content. These are currently governed in Canada by CSA 3001-08 *Cementitious Materials for use in Concrete.*

It is the purpose of this project to determine if fly ashes with varying composition with respect to sulfates and alkalis have an adverse effect on concrete when it undergoes carbonation.

2.6.1 Description

Fly ash is a fine residue produced as a result of the combustion of pulverized coal in electric power generating plants. During the combustion process the mineral impurities found in the coal fuse together and solidify into glassy spherical particles during the cooling period. These particles are collected from the exhaust gases by mechanical and electrostatic preceptor. (Malhotra and Ramezanianpour, 1994)

Fly ash is considered a pozzolan which is defined by the American Society for Testing and Materials (ASTM) as " a siliceous or siliceous and aluminous material which in itself possesses little to no cementitious value but which will, in finely divided form and in the presence of moisture, chemically react with calcium hydroxide at ordinary temperature to form compounds possessing cementitious properties" Malhotra and Ramezanianpour (1994) also adds that the alumino-silicates in the presence of moisture will react with the calcium ions to for calcium silicate hydrates.

2.6.2 Classification

The initial composition of the noncombustible material in the coal burned determines the final composition of fly ash. The main elements found in fly ash are silicon, aluminum, iron, calcium, and magnesium.

Fly ash is classified based on its composition and ASTM and CSA use different criteria. ASTM 618 states that a Class F ash has a chemical composition such that $SiO_2 + Al_2O_3 + Fe_2O_3 \geq 70$ % where as Class C ash has a composition such that $SiO_2 + Al_2O_3 + Fe_2O_3 \geq 50\%$. Class C ashes are normally products of lignite of subbituminous coals and Class F are products of anthracite bituminous coals (Malhotra and Ramezanianpour, 1994). Although this classification system makes no reference to calcium content, Class C is termed high-calcium and Class F low-calcium ash. The Canadian Standards Association (CSA) A3000-03 have moved to classifying fly ash based on its calcium content as follows: Type F<8% CaO, Type CI 8-20% CaO, and Type CH >20% CaO.

2.6.3 Hydration Reactions and Pozzolanic Activity

The reaction of Portland cement and water creates calcium silicate hydrate (C-S-H), calcium hydroxide (CH), ettringite, monosulphate and minor amounts of other calcium-aluminates and calcium-alumino-ferrite phases. Some of the high calcium fly ashes possess self hardening properties due to the presence of tricalcium aluminate (C_3A) and dicalcuim silicate (C_2S), similar to that found in Portland cement. However, the rate of formation of C-S-H from the glass phase is

comparatively slow (Ghosh and Pratt, 1981 in Malhotra, 1995). Lower calcium fly ashes will only produce C-S-H or C-A-H when calcium hydroxide is available to react pozzolanically with the alumino-silicate glass in the fly ash.

Many investigators have reported that fly ash retards the hydration of the C_3A and the degree depends on the sulfate content of the fly ash, the amount of dissolved alkalis, and the calcium adsorption capacity. Sulfates in fly ash retard the hydration more than the equivalent amount of added gypsum which may be due to other ions besides sulfate being dissolved from the fly ash. (Malhotra and Ramezanianpour, 1994)

2.6.4 Benefits

There are many advantages and some disadvantage to fresh and hardened properties of concrete produced with fly ash. There are also advantages of using fly ash from an economical and environmental point of view Fly ash on average costs less then cement, which reduces material cost by reducing the quantity of cement used is making concrete. For every ton of cement produced a ton of CO_2 is emitted into the environment. (Marceau et al. 2006). When fly ash replaces cement it reduces the quantity of CO_2 associated with the concrete. Also the cost of waste disposal is decreased, i.e. reduced fly ash disposed into landfills.

Not only does fly ash reduce the cement required by simple replacement, but fly ash also increases the workability, which in turn reduces the actual water and cement content needed to achieve the desired level of workability. Fly ash,

especially lower calcium ash, also reduces the heat of hydration by acting as a fine aggregate during the early hydration, which is particularly important in mass concrete structures (Malhotra and Ramezanianpour 1994).

It was found that when cement was replaced with fly ash early measurements of permeability showed that the fly ash was detrimental, however at later ages once the pozzolanic activity started, the concrete with fly ash was less permeable than the concrete produced with Portland cement only. Decreasing the permeability increases the durability of concrete against frost attack, sulfate attack, alkali-aggregate reaction and the resistance of concrete to corrosion of embedded steel reinforcement (Joshi and Lohtia 1997). Along with reducing the permeability by reducing the movement of water and aggressive chemicals, fly ash also plays a significant role in reducing the alkalis available for reaction with aggregate (Joshi and Lohtia, 1997).

2.6.5 Disadvantages

Due to the slower strength gain, particularly with lower calcium fly ashes, there is often resistance to the use of fly ash in concrete due to fears that its use will adversely impact construction schedules. Fly ash requires longer curing times in order to promote continued hydration and pozzolanic activity (Malhotra and Mehta, 2002).

Another disadvantage of using fly ash is its effect on the rate of carbonation. Due to the pozzolanic reaction of fly ash consuming calcium hydroxide from the

cementitious system, along with the simple replacement of cement, the mass of calcium hydroxide required for the carbonation process to consume is reduced. This reduction will increase the rate in which carbonation will propagate in concrete. This effect is most important when dealing with exposed reinforced concrete as discussed earlier.

3.0 Case History of Residential Concrete Foundations

3.1 Background

Between 1986 and 1987, a large number of residential house foundations were constructed using fly ash with an unusual composition. The fly ash used had a high alkali and sulfate content. The average during the 1986/87 period was 8.13 % Na_2O_{eq} and 5.5 %SO_3 (Thomas, 2008). Not only did this concrete contain this fly ash but it also was suspected to have an abnormally high W/CM (>0.7 and possibly as high as 0.9). After as little as 18 months, signs of deterioration such as efflorescence, spalling and scaling were occurring in some foundations.

At the time of construction the Canadian Standards for residential concrete was CSA A438-M1983 "Concrete Construction for Housings and Small Buildings", which was a simplified form of A23.1-M77 "Concrete Materials and Methods of Concrete Construction". CSA A438 allowed the use of fly ash as permitted in CSA CAN3 A23.5-M82 "Supplementary Cementing Materials and Their use in Concrete Construction". However, the overriding standard in the construction of these residential foundations was the Ontario Building Code 1983.

In CSA A438, clause 3.6.2 "Slump Control on Site" addition of water on site, not exceeding 12L/m^3, was permitted if maximum slump was not achieved. Unless strictly enforced, the addition of water may have exceeded this limit to achieve the desired level of workability. With this un-metered addition, W/CM can reach

up to and over 0.80 in the field. For example, concrete designed with 200 kg cementitious material and 140 kg water would have W/CM=0.70, but with an addition of 12-15 l/m^3 on site the W/CM would increase to 0.78 or more.

The basic requirements for residential concrete in these foundations came from the Ontario Building Code and CSA A23.1, where no specific mention of the use of fly ash was made. The following are a list of the basic requirements for concrete in residential concrete:

- A minimum 28-day compressive strength for concrete for foundation walls of 15 MPa in A438, and 14 MPa in the Ontario Building Code.
- Air content between 5 and 8%.
- A maximum slump of 100 mm for the Ontario Building Code and 150 mm in CSA A438.
- CSA A438 provides warnings against segregation at maximum slump.
- CSA A438 recommends a minimum of 20 MPa be used to reduce cracking, improve water tightness, and reduce dampness.

The sulfate restriction on supplementary cementing materials was specified in A23.5 as 5.0 % SO_3 maximum.

3.2 Materials and Mix Design

The materials used by the concrete supplier was Type GU cement, Class C Fly Ash (20% replacement, which was suspected to be as high as 40%), coarse aggregate (crushed limestone), fine aggregate (natural siliceous) that consisted of up to 25% limestone crusher screenings, water and water reducing and air-entraining admixtures. The mix design W/CM was 0.66, however this was suspected to be as high as 0.90. (Thomas, 2008)

The fly ash used was by ASTM standards Class C and by CSA standards Class CI and had high alkali and sulfate contents, with average values of 8.1% Na_2O_{eq} and 5.5% SO_3. X-ray diffraction analysis indicated that much of the alkalis and sulfates present were in the form of thenardite (sodium sulfate, Na_2SO_4).

3.3 Scanning Electron Microscope (SEM) Examination

Researchers have differing opinions with regards to the actual mechanism(s) that was the main form of deterioration in the basement foundations; proposed mechanisms included freeze-thaw and internal sulfate attack. However during the investigation, it was noted that an unusual form of carbonation was observed. This form of carbonation can be seen in Figure 3.1, where discrete “islands” of calcium carbonate are dispersed in decalcified silica gel. The backscatter-electron image was taken by the author from a polished sample prepared from a core extracted from one of the foundation walls. The carbonated material was weak and friable.

Carbonation usually forms a continuous framework of calcite that maintains the integrity of the matrix.

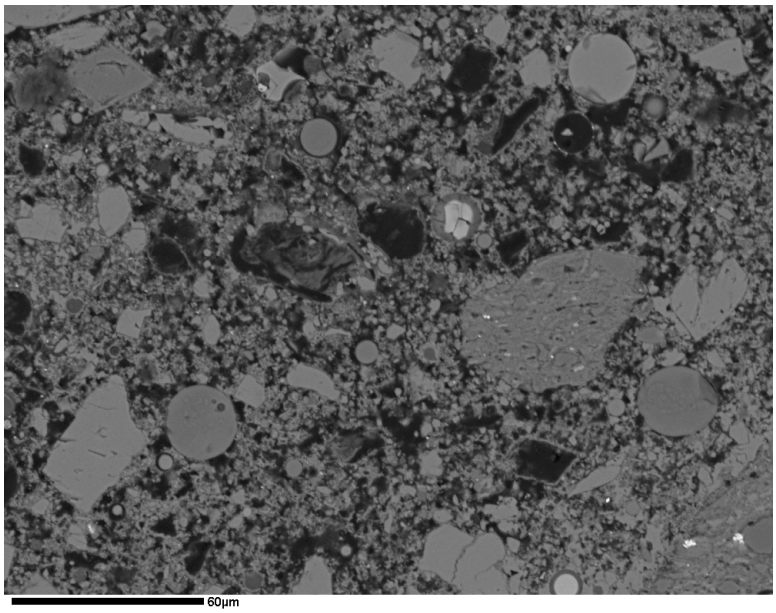

Figure 3.1 Carbonation Zone in Concrete Containing Fly Ash. (Backscattered Electron Image)

Although rare, this form of carbonation, which has been referred to as "popcorn calcite deposition" (PCD), has been previously reported in the literature as discussed in the preceding chapter. The extent to which PCD contributed to the damage of the concrete foundations was never established although it was alleged during the ensuing litigation that the use of fly ash and a high W/CM may have played a role in the formation of PCD. These allegations provided some of the inventive for conducting this research project.

4.0 Experimental Methods

4.1 Methodology

For this project paste, mortar and concrete specimens were cast using three different class CI fly ashes replacing type GU Portland cement by 20%.

4.1.1 Paste

Paste specimens were produced with W/CM equal to 0.50, 0.70, and 0.90. They were placed in two different environmental conditions; 100% N_2 and 1% CO_2 chambers with a temperature of 23ºC and 65%RH. These paste specimens were produced to investigate the effect of carbonation on the microstructure using scanning electron microscope (SEM) and microhardness using Vickers hardness indenter.

4.1.2 Mortar

Mortar specimens were cast, with a W/CM equal 0.70, to evaluate the change in various mechanical strength properties including flexural, compressive and tensile strength. Mortar specimens were also used to evaluate changes in porosity and dynamic modulus. The different environments the mortar samples were placed in were a CO_2-free chamber and a 1%-CO_2 chamber. For the first nine weeks half of the samples from each environment were immersed in water for a period of four hours every seven days. The samples were soaked in separate water for each of the four mixes and each time thereafter the samples were soaked in the same

water in order to limit leaching of alkalis and to keep the alkali concentration in the pore solution as close to the original concentration as possible.

During this nine week period the RH in each of the chambers was ≥75%. The optimum relative humidity for carbonation is 40 to 65% RH (Parrot, 1987). The cause of this high humidity was a combination of the liberation of water absorbed by the specimens during the wetting cycle and the inability of the saturated salt solution to absorb that water.

In order to eliminate this, specimens that were being immersed in water and then being placed in the two chambers (CO_2 free and 1% CO_2) were then placed in an environmental chamber where the RH was maintained at 65%. The CO_2 in the environmental chamber was not controlled and was equal to atmospheric levels. The period of drying was then changed from seven days to 14 days in order for the internal RH in the specimens to reduce sufficiently for carbonation to take place.

4.1.3 Concrete

Concrete cylinders were cast using two different W/CM ratios. The first was a W/CM= 0.70 with a water-reducing admixture, representing a residential concrete mix that meets the national specification, and the second was a W/CM=0.85 with no water reducer, representing a residential mix that has had water added in order to reach the desired slump on site. The concrete specimens were tested for strength, rapid chloride permeability, resistivity, water vapor transmission,

absorption, and surface hardness (using a rebound hammer). The rebound hammer was used to determine change in surface hardness due to carbonation.

4.2 Materials

4.2.1 Cement

The ordinary Portland cement (OPC) used was the same cement source that was used in the production of the residential concrete in question and met the requirements of CSA A3001-03 GU and ASTM C150 Type I. The chemical analysis can be found in Table 4.1.

Table 4.1Chemical Analysis of Portland Cement (OPC)

%Oxides	OPC
SiO_2	20.08
Al_2O_3	4.58
TiO_2	0.21
P_2O_5	0.13
Fe_2O_3	3.06
Ca0	63.09
MgO	2.37
Na_2O	0.2
K_2O	0.78
Mn_2O_3	0.21
SrO	0.12
SO_3	3.35
LOI	1.45
Total	99.63

The calculated Bogue composition and total alkali content can be found in Table 4.2.

Table 4.2 Calculated Bogue Compositions and Total Alkali Content of OPC

C_3S	C_2S	C_3A	C_4AF	Na_2O_{eq}
59.5	12.6	6.9	9.3	0.73

4.2.2 Fly Ash

The three fly ashes used were all Type CI as defined by CSA A3001-03. A Type CI fly ash is defined by CSA (Table 5) as an ash with a CaO content between 8-20%. The chemical analysis and alkali content of the fly ashes can be found in Table 4.3.

Table 4.3 Table Chemical Analyses and Alkali Content of Fly Ashes

%Oxides	BR	TB	RP
SiO_2	34.09	46	40.69
Al_2O_3	19.52	19.65	21.72
TiO_2	1.32	0.74	1.5
P_2O_5	0.75	0.3	1.05
Fe_2O_3	5.95	4.99	6.08
CaO	17.6	13.51	19.12
MgO	4.12	3.04	4.73
Na_2O	8.47	7.08	1.55
K_2O	0.78	1.17	1.11
Mn_2O_3	0.04	0.03	0.03
SrO	0.83	0.41	0.3
SO_3	4.58	1.62	1.02
LOI	0.49	0.67	0.67
Total	98.53	99.21	99.57
BaO	1.8	1	0.7
Na_2O_{eq}	9	7.88	2.3

The fly ashes were chosen based on two differing compositions, which were alkali and sulfate content. Table 4.4 shows the varying compositions for each fly ash used. Unfortunately a fly ash with high sulfate and low alkalis to complete the matrix could not be found.

Table 4.4 Alkali and Sulfur Content for Fly Ashes

	Designation	Type (CaO%)	Na2Oeq	SO3%
BR	HAHS	CI (17.6)	High (9.00)	High (4.58)
TB	HALS	CI (19.65)	High (7.88)	Low (1.62)
RP	LALS	CI (19.12)	Low (2.30)	Low (1.02)

4.2.3 Aggregate

The fine aggregate used for mortar was Ottawa graded sand and met the requirements of ASTM C 788. The fine aggregate used for concrete was natural sand (from the Zeeland pit in NB) and had a specific gravity of 2.60 and water absorption value of 1.32%. The coarse aggregate (from the Blagdon Quarry in NB) was a crushed stone with a maximum nominal size of 20 mm, specific gravity of 2.6 and absorption value of 0.7%. Both coarse and fine aggregates used met the requirements of CSA A23.1-04.

4.2.4 Admixtures

The admixtures used in this project included a Type A normal-range water reducer. Even though the concrete produced for this project was not subjected to freeze thaw cycles, air-entraining admixture was used to achieve 5-8% air content. The super plasticizer used was a Type F high-range water reducer. All admixtures used met the requirements of ASTM C 494.

4.3 Mix Proportions

4.3.1 Paste

The mix proportions of materials used to produce paste specimens were as follows: 1000g cement and 900g water for W/CM=0.90; 1000g cement and 700g

water for W/CM=0.70; and 1000g cement and 500g water for W/CM=0.50. For the specimens containing fly ash, a 20% by mass replacement of cement was used. For labelling purpose a "P" was placed before the cementitious material labels described in Table 4.1 and 4.3. For example a paste containing fly ash BR and W/CM=0.70 was labelled PBR7.

4.3.2 Mortar

The mix proportions for the mortar specimens were 1000g cement, 3750g Ottawa graded sand, and 700g water (W/CM=0.70). For the specimens containing fly ash, a 20% replacement by mass of cement was used. The mass of sand, 3750g, used was determined by achieving an acceptable flow with mixes containing fly ash in order to minimize segregation. Superplastisizer was then added to the control mortar (without fly ash) to achieve the same consistency of the mortars produced with fly ash while using the same sand content. For labelling purpose an "M" was placed before the cementitious material labels described in Table 4.1 and 4.3. For example a paste containing fly ash BR was labelled MBR.

4.3.3 Concrete

The testing scheme for concrete was divided into two phases. For both phase one and two, concrete had W/CM= 0.70 and 0.85. The cementitious content was 200 kg/m^3 and the water content, combined with a water reducer, was changed in order to achieve the varying W/CM. In phase II the cement content in the control was raised to 220 kg/m^3 in order to raise the water content to ensure an adequate

slump. Phase I was to evaluate compressive strength where as Phase II was to evaluate all other test performed on concrete samples.

The mix proportions for concrete used in phase I can be found in Table 4.5.

The mix proportions for concrete used in phase II can be found in Table 4.6.

Table 4.5 Phase I Mix Proportions.

		Quantities kg/m^3				Quantities ml/100kg			Slump	
Mix ID	FA Type	Cement	Fly Ash	Water	W/CM	WRA	AEA	SPN	(mm)	% Air
A1		200	0	140	0.7	300	25	600	25	4
A2		200	0	170	0.85	0	25	0	75	5
B1	BR (HAHS)	160	40	140	0.7	300	45	0	125	9
B2	BR (HAHS)	160	40	170	0.85	0	35	0	200	7
R1	RP (HALS)	160	40	140	0.7	300	35	300	75	4.5
R2	RP (HALS)	160	40	170	0.85	0	40	0	150	5
T1	TB (LALS)	160	40	140	0.7	300	40	0	50	7
T2	TB (LALS)	160	40	170	0.85	0	40	0	75	5

Table 4.6 Phase II Mix Proportions

		Quantities kg/m^3				Quantities ml/100kg		Slump	
Mix ID	FA Type	Cement	Fly Ash	Water	W/CM	WRA	AEA	(mm)	% Air
CL		220	0	154	0.7	250	20	50	6
CH		200	0	170	0.85	0	20	100	6
BL	BR (HAHS)	160	40	140	0.7	250	20	100	6
BH	BR (HAHS)	160	40	170	0.85	0	20	200	7
TL	RP (HALS)	160	40	140	0.7	250	20	50	5
TH	RP (HALS)	160	40	170	0.85	0	20	200	5
RL	TB (LALS)	160	40	140	0.7	250	20	50	7
RH	TB (LALS)	160	40	170	0.85	0	20	100	4

4.4 Mixing, Casting and Curing

4.4.1 Paste

Paste specimens were mixed in a standard household food blender. The cementitious materials were added to the water and were mixed at medium speed for 90 seconds after which they were allowed to sit for one minute. Then the blender was turned on to high speed for another two minutes. The paste slurry was then placed in a desiccator, under vacuum for 20 minutes to remove air entrapped during the mixing. After the paste was removed from the desiccator, it was stirred by hand for one minute to eliminate segregation. The paste was poured into plastic containers which were sealed and then rotated end over end at a speed of 2 rpm for 24 hours to eliminate segregation during hydration. After this 24-hour period, samples were allowed to cure for an additional 6 days and then removed from the plastic containers and allowed to dry for 28 days in an environmental chamber (RH~ 60%). The samples were cut into 25-mm thick slices and placed into two different environmental conditions, a 100%-N_2 chamber and a 1% CO_2 accelerated carbonation chamber. For the 100% N_2 chamber, N_2 was passed though the chamber to replace the air containing CO_2. Specimens were checked regularly by creating a fractured surface and spraying with 1% phenolphthalein indicator solution. This was done to ensure that all CO_2 was flushed from the chamber thereby preventing carbonation of the specimens. The set up for the 1%-CO_2 chamber is shown in Figure 4.1. Carbon dioxide from a pressurized gas cylinder and compressed air supply were passed through flow meters which were adjusted to control the flow rates such that the flow of air was

99 times greater than the flow of CO_2, thus achieving a mixture of 1%-CO_2. A saturated salt solution of potassium carbonate was placed in the base of the chamber to control relative humidity to 43%. Two computer type fans were installed at different locations within the chamber to ensure adequate air circulation. An air lock was fitted to the top of the chamber to allow air to escape without allowing atmospheric air to enter.

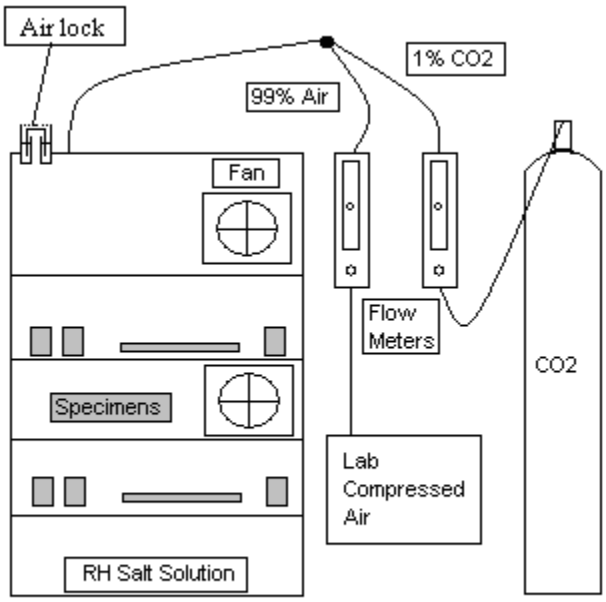

Figure 4.1 CO_2-Enriched Environment

4.4.2 Mortar

Mortar specimens were mixed following ASTM C 305 *Practice for Mechanical Mixing of Hydraulic Cement and Paste Samples of Plastic Consistency*. The mortar specimens cast were 25x25x 300mm mortar bars, 50x50x300mm prisms and "dog-bone" briquettes which were 25x25 mm at the smallest cross section (see ASTM C 190-85 *Standard Test Method for Tensile Strength of Hydraulic-Cement Mortars*.) The specimens were cured over water in moulds for one day

and then for an additional 2 days in solution replicating the pore solution of each mix. The replicated pore solution was determined from paste samples, W/CM=0.70, cured for 28 days. The pore solution was obtained using a pore press and analyzed using ion chromatography. See Table 4.7 for pore solutions results.

It was assumed that the potassium and sodium ions were accompanied by hydroxyl ions to achieve electro neutrality. This is a reasonable assumption for mature cement paste where the pore solution is composed almost entirely by Na^+, K^+ and OH^- ions.

Table 4.7 Pore Solution Concentrations.

	Morality (mol/L)	
	K^+	Na^+
POPC28	0.32	0.25
PBR28 (HAHS)	0.33	0.76
PRP28 (LALS)	0.26	0.15
PTB28 (HALS)	0.23	0.34

After this curing regime, the 50x50x300mm prisms were cut into 25 mm thick slices. All specimens were placed into two different environmental conditions, a CO_2-free chamber and a 1%-CO_2 enriched environment. For the CO_2-free environment, air was passed through a saturated calcium hydroxide solution and then through a saturated sodium hydroxide solution stripping the CO_2 from the compressed air supply. For the 1%-CO_2 enriched environment flow tubes were used to control the CO_2 concentration. See Figure 4.1 for CO_2 enriched environment and Figure 4.2 for set up used to remove CO_2 from air. In both conditions relative humidity was controlled by a saturated solution of potassium

carbonate following ASTM E 104-02 *Standard Practice for Maintaining Constant Relative Humidity by Means of Aqueous Solution*. The published RH for saturated potassium carbonate at a temperature of 25ºC is 43.13%. However, due to large liberation of water from the specimens in the drying stage, the actual measured relative humidity in the chamber was ~60%.

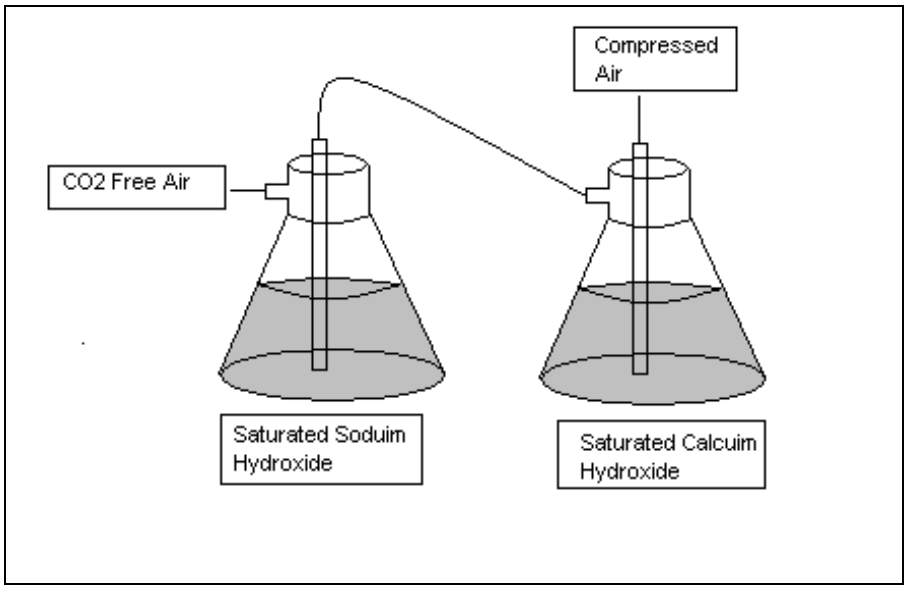

Figure 4.2 CO_2 Removal Systems

4.4.3 Concrete

Concrete specimens were mixed in a counter-action mechanical mixer. The coarse aggregate, cementitious materials and fine aggregate were added to the mixer in that order and the air-entraining admixture was sprinkled over the sand. These materials were then mixed dry for 30 seconds. The water (including water-reducing admixture where required) was then added over a 30-second period. The concrete was then mixed for another two minutes and stopped for one minute. It was at this point that superplasticizer was added if the slump was not sufficient to permit proper consolidation. The concrete was then mixed for another minute

before discharging after which the fresh concrete was tested for air content and slump. The air content was tested in accordance of ASTM C 231 *Test Method for Air Content of Freshly Mixed Concrete by the Pressure Method* and slump was measured following ASTM C 143/C 143M *Test Method for Slump of Hydraulic Cement Concrete*.

Prisms (50mm x 50mm x 300mm) and slabs (250mm x 300mm x 72mm) specimens were cast as per ASTM C 192/C 192M-98 *Making and Curing Concrete Test Specimens in The Laboratory.* All specimens were then moist-cured for either 1, 3, or 7 days. Cylinders (100mm∅ x 200 mm) that had nominally the same material proportions as listed in Table 4.5 were cast at a later date and cured for 1, 7, 28 and 90 days. After curing, specimens were placed in an environmental chamber for 90 days at ~60% RH and 20-25ºC and then placed on an outdoor exposure site where samples were protected from direct precipitation.

4.5 Testing

4.5.1 Paste

Paste specimens were examined at approximately one year of age to examine the change in microstructure. The micro structural properties measured were the "percolation" of the calcium phases and the microhardness of the carbonated and uncarbonated paste.

4.5.1.1 Percolation

Percolation is defined as the degree of connectivity of a disordered medium. Usually when researchers investigate percolation or connectivity of cementing

systems they are mainly concerned with capillary pores as they govern permeability and the mass transport of water and aggressive agents. Bentz, D developed a FORTRAN program, *burn2d*, that determines whether or not a defined phase percolates a two dimensional image. This program uses "a burning algorithm"; this means a "fire" is started on two sides, top and left edge, of the image and the phase of interest is "burned". In the case of a digital image the grey level is changed to indicate the phase that was burned. The only way the fire can precede to burn the defined phase is if its neighbor is the same phase. In the program used a neighbor is described as a pixel adjacent to the facets of the burned pixel. See Figure 4.3 for schematic. If there are no neighboring pixels of the same phase the fire does not proceed on that path.

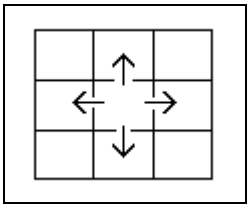

Figure 4.3 Burning Algorithm of Neighbouring Pixels

For this study paste samples were examined using a scanning electron microscope (SEM) to capture backscattered electron images of polished paste samples using the DPIC software used with the SEM. Then using the imaging software ImageJ, calcium phases were thresholded within a grey scale that represented the calcium phases present after carbonation. Each image was converted into a black and white image; black representing calcium phases and white representing everything else such as empty pores and silica and alumina gel. An example of an original image, an image after thresholding and an image after burning can be

seen in Figure 4.4. For the burned image the non-calcium phase is observed as white, the percolated calcium phases are gray and the non-percolated calcium phases are black.

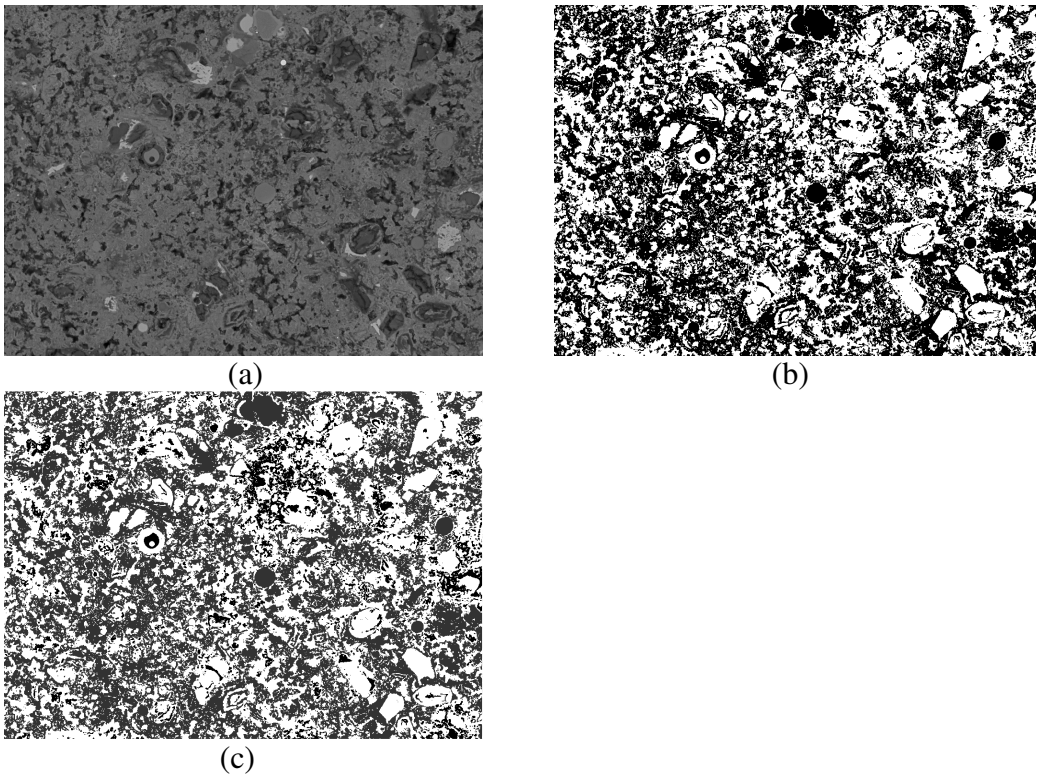

Figure 4.4 (a) Original Image, (b) Threshold Image, (c) Burned Image.

The *burn2d* program was adapted by Steve Cogswell of the microscopy and microanalysis facility at the University of New Brunswick to determine the percent of calcium phase present and the percent calcium that was connected to the percolated path. The images were then run through the adapted Fortran program *burn2d*. Equation 4.1 calculated the percent calcium and Equation 4.2 calculated percent calcium percolated.

% Calcium = (Burned Pixels + Non-Burned Pixels)/ Total Pixels X 100% **Equation 4.1**

% Percolated = Burned Pixels/Non-Burned Pixels X 100% **Equation 4.2**

4.5.1.2 Microhardness

Microhardness differences between non-carbonated and carbonated specimens were also determined on paste specimens. This test was performed using a Leitz Miniload 2 with the Vickers diamond indenter and the test was conducted in accordance with *ASTM E 384 Standard Test Method for Microindentation Harndness of Material*.

The paste specimens were cut using a diamond wafer saw and were polished using 800P (21.8μm), 1200P (15.3 μm) and P2500 (8.4 μm) sand papers to obtain an adequate surface with minimum damage. Between each step the specimens were rinsed with ethyl alcohol, cleaned off with compressed air and placed in an ultrasonic bath, containing ethyl alcohol, to prevent damage to the polished surface. After polishing, a gold sputtering was applied to the surface to increase the visibility of the diamond indentation. Figure 4.5 shows an example of diamond indentation produced.

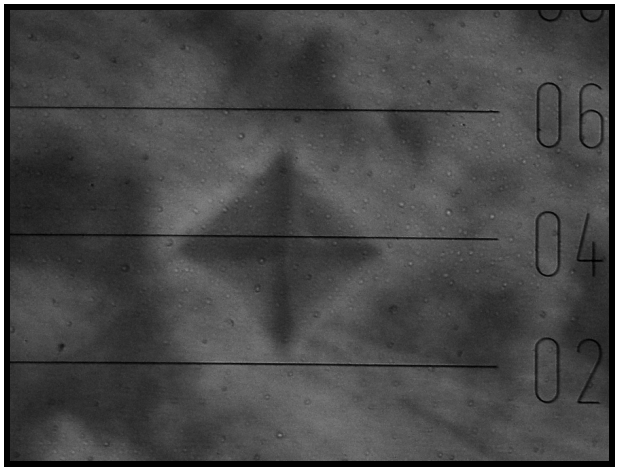

Figure 4.5 Diamond Indent for Vickers Micro Hardness

The load, P (N), was applied for 30 seconds after which the diagonals of the indentation, d (μm), of the diamond in perpendicular directions were measured and averaged. The hardness, H_v (MPa), was calculated as shown in Equation 4.3:

$$H_v = 1.8544\ P/d^2 \qquad \textbf{Equation 4.3}$$

The units for hardness are MPa but should not be confused with the measure of strength. Since the cement paste is not ideally elastic-plastic, the normal relationship between hardness and strength cannot be made easily. For the purpose of this study, hardness values will be used for comparison purposes only.

4.5.2 Mortar

Mortar samples were tested for flexural, compressive and tensile strength at 7, 14 and 40 weeks of age. At 40 weeks the dynamic Young's modulus of elasticity was also measured. The 40-week time period was determined as the point at which specimens in the CO_2 enriched environment were fully carbonated.

4.5.2.1 Flexural Strength

For determining flexural strength of mortar specimens ASMT C 348-02 *Standard Test Method for Flexural Strength of Hydraulic-Cement Mortars* was followed with some modification. The specimen size was 25mm x 25mm x 300mm instead of the specified 40 mm x 40mm x 160 mm. This size was chosen in order to achieve full carbonation of the specimen within an acceptable period of time.

4.5.2.2 Compression Strength

After specimens were tested in flexure pieces of the prism were tested for compressive strength following *ASTM C 349-02 Standard Test Method for Compressive Strength of Hydraulic-Cement Mortars (Using portions of Prisms Broken in Flexure)*. As a result of the modification of mortar bars, the same reduction in sample dimension, 40mm to 25mm, occurred.

4.5.2.3 Tensile Strength

Briquette specimens were tested for tensile strength following *ASTM C 190 Standard Test Method for Tensile Strength of Hydraulic Cement Mortars*.

4.5.2.4 Dynamic Young's Modulus of Elasticity

The dynamic Young's modulus of elasticity was measured following *ASTM C 215 Standard Test Method for Fundamental Transverse, Longitudinal, and Torsional Resonant Frequencies of Concrete* with some modifications. In this study, the transverse resonant frequency was determined on mortar specimens with a cross section of 25x25 mm and length of 300mm. The specimens tested were then used for flexural strength measurements.

To calculate E, Dynamic modulus, Equation 4.4 is used.

$$E=CMn^2 \qquad \textbf{Equation 4.4}$$

However, for the purpose of this study C, the shape constant, and the mass of specimen M (kg) remained relatively constant. Therefore, only the squares of the

measured transverse frequency n (Hz) were used for comparing non-carbonated, carbonated and wet dry cycled mortar specimens.

4.5.2.5 Porosity

The porosity of samples were determined after complete carbonation of the specimens that were in the enriched CO_2 environment (40 week), At this age three 50x50x25mm slices were taken from each of the three exposure conditions (N_2 (CO2 free), enriched CO_2 and controlled relative humidity). The specimens were then saturated with water by immersion until they reached constant mass, change less then 0.01g, determined by weekly measurements. It took four weeks to achieve constant mass. The mass of each specimen was then determined in air ($m_{w,sat}$) and suspended in water ($m_{w,sus}$). The specimens were then allowed to dry for one week at room temperature. They were than immersed in isopropanol until they reached constant mass. Four-angstrom (0.4 nm) molecular sieves were used to remove the water to maintain the purity of the isopropanol. Constant mass was determined when weekly masses were measured and the changes were less then 0.01g. This took approximately six weeks. The mass of each specimen in air ($m_{p,sat}$) was determined. The specimens were then placed into an oven at a temperature of 105°C until constant dry mass (m_{dry}) was reached. This took approximately five days. The total porosity, n_t, was calculated by Equation 4.5. and the isopropanol porosity, n_p, was calculated by Equation 4.6.

$$n_t = (m_{sat} - m_{dry}) / (m_{sat} - m_{sus})$$ **Equation 4.5**

$$n_p = ((m_{w,sat} - m_{p,sat}) x (m_{sat} - m_{sus})) / (\rho_w - \rho_p)$$ **Equation 4.6**

Where ρ_w is the density of water ρ_p is the density of isopropanol.

The total porosity, n_t, provides a measure of the total pore space occupied by the evaporable water. This includes very small "gel pores" (generally < 10 nm) in the C-S-H gel that are not considered to contribute to mass transport in concrete (Mindess et al. 2003). Larger molecules of isopropanol only exchange with water in larger pores and the isopropanol porosity, n_p, is considered to be more representative of the capillary pores that contribute to mass transport,

After the specimens were dried they were then conditioned at a relative humidity of 11%. This was achieved by placing the specimens over a saturated lithium chloride solution. Constant mass was determined when weekly masses were measured and the change was less then 0.01g. This took four weeks to achieve and the mass of the sample at 11% relative humidity ($m_{11\%}$) was then determined. The porosity was then calculated using Equation 4.7.

$$n_{11\%} = (m_{sat}-m_{11\%})/ (m_{sat}-m_{sus})$$ **Equation 4.7**

When specimens are dried at 105°C water between the C-S-H layers are removed and the structure is collapse creating additional pore space (Ramachandran et al., 1981). This space is unavailable for transport and conditioning to 11% RH fills the single monolayer of water in the C-S-H structure. This procedure does not restore the structure but can be used to give a further indication (i.e. in addition to isopropanol porosity) of the porosity that is available for mass transport.

4.5.3 Concrete

Concrete was cured and tested at different ages. A summary of the testing, curing, and storage regimens can be found in Table 4.8.

Table 4.8 Summary of Testing

Testing	Curing Time (Days)	Exposure after curing	Age at Testing (Days)
Compressive strength (Phase l)	1, 7, 28, and 90	60% RH up to 90 days	1, 7, 28, 90, 180 and 365
RCPT, Resistivity, Carbonation and Rebound Hammer (Phase ll)	1, 3, 7, and 28	then placed in Outdoor exposure	28, 90, 180, and 365
WVT (Phase ll)	1, 3, and 7		90
Absorption(Phase ll)	1, 3, and 7		180

4.5.3.1 Compressive Strength

The compressive strength of concrete was measured at 1, 7, 28 and 90 days. The compressive strength was measured in accordance of *ASMT C39 Standard Test Method for Compressive Strength of Cylindrical Concrete Specimens*.

4.5.3.2 Rapid Chloride Permeability Test (RCPT)

The RCPT was tested in accordance of *ASTM 1202 Standard Test Method for Electrical Indication or Concrete's Ability to Resist Chloride Ion Penetration* with some modifications. The specimens were tested for 30 minutes and results were interpolated to obtain a charge passed over the required six-hour test period. This time was shortened due to the excessive charge passed during the test. The temperature of the specimen and apparatus increased with the large charge passed. RCPT was performed on concrete with varying moist-cure times of 1, 3, 7 and 28

days; and were tested at 28, 90, 180, and 365 days. The schematic for RCPT is seen below in Figure 4.6.

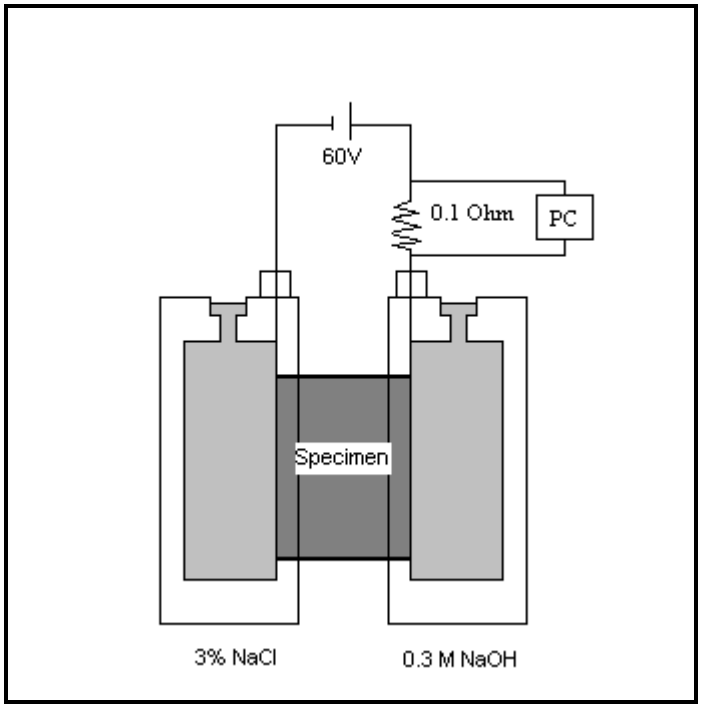

Figure 4.6 RCPT Cell Set up

4.5.3.3 Electrical Resistivity

Currently there is no standard for measuring the resistivity of concrete. For this project the resistivity was determined using the same test set up used in the RCPT, but instead of the 60 volts applied over 6 hours and current measured, an alternating current, I, of 100μA was applied through the sample and voltage, V, was measured. The resistance, R (Kohm), is calculated by Ohm's Law, R= V/I. Resistivity, ρ (Kohm-cm), is then calculated using the equation ρ= RA/L. Where A is the cross-sectional area (cm^2), and L is the length (cm) of the concrete test specimen. Resistivity measurements were performed on concrete with varying

moist-cure times of 1, 3, 7 and 28 days; and were tested at 28, 90, 180, and 365 days.

4.5.3.4 Carbonation

To determine the depth of carbonation, test specimens were sprayed with a 1% phenolphthalein indicator solution on a freshly fractured surface. This pH indicator will turn magenta pink when the pore solution of concrete is greater then 9.2, and will remain colourless if the pH is lower then 9.2. In non-carbonated concrete the pore solution is typically greater than 13 due to the presence of alkali hydroxides, primarily sodium and potassium hydroxide (Parrott, 1987). In concrete that has undergone carbonation the pH is reduced to approximately 8 (Parrott, 1987).

After the fresh surface has been sprayed with the indicator solution, measurements from each face to the point where the concrete changes to the magenta colour were taken and averaged to determine the depth of carbonation.

Carbonation measurements were performed on concrete with varying moist-curing times of 1, 3, 7 and 28 days; and were tested at 28, 90, 180, and 365 days.

4.5.3.5 Water Vapour Transmission (WVT)

The transmission of vapour was determined in accordance with *ASTM E 96-00 Standard Test Method for Water Vapor Transmission of Materials*. The following steps were included due to the nature of the test specimens. Two 23mm slices

were taken from a 100mm ϕ x 200 mm cylinder. These samples were taken at sample age of 180 days, and the curing times of the samples were 1, 3, and 7 days. After the slices were cut they were placed in an environment of ~60% RH and laboratory temperature for a period of one month in order to reach constant weight. The samples were then sealed between two chambers at different humidity's. The bottom surface of the concrete was exposed to 100% RH by means of a container filled with water at a level ~75mm below the specimen. On the other side of the specimen a saturated magnesium nitrate salt solution controlled the humidity to 51%. See Figure 4.7 for specimen schematic. The specimens were placed in an environment where the temperature was controlled at 32 ± 2°C. The temperature was elevated above ambient to allow temperature control by heating without the need for cooling.

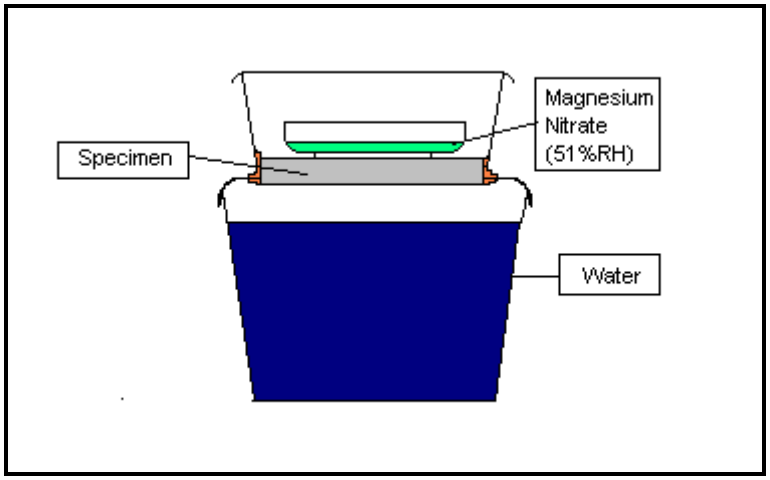

Figure 4.7 WVT Set up.

To determine the quantity of moisture transmitted through the specimen, the mass of the top portion, which included the specimen and the salt solution, was measured. The mass was measured at intervals of one week or greater in order to obtain mass gains greater then 100 times the balance sensitivity. The initial

measurements will indicate the amount of water absorbed and transmitted by the specimen. After steady-state was achieved, the change in mass was only water transmitted through the specimen. This took approximately 21 days to achieve. The cumulative mass gained was then plotted against time, an example of which can be seen below in Figure 4.8.

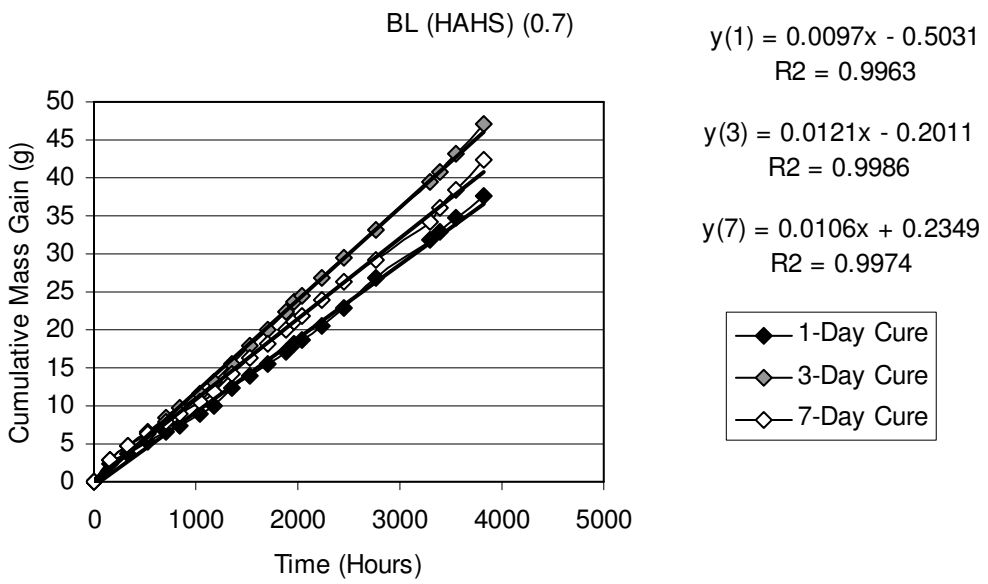

Figure 4.8 Sample Plot of Cumulative Mass Gained vs. Time

The flux was calculated using Equation 4.8 where WVT is the water vapor transmission ($g/h \cdot m^2$), G is the cumulative mass gain (g), t is the time (h) and A is the test area (m^2).

$$WTV = G/tA \qquad \textbf{Equation 4.8}$$

4.5.3.6 Rate of Absorption (Sorptivity)

The rate of absorption or sorptivity was determined by measuring the increase in mass over time of a specimen when one surface was exposed to water. The increase in mass is dominated by the capillary suction. The schematic of the

absorption specimen set up can be seen below in Figure 4.9. The specimens were 180 days old and initial curing was 1, 3, and 7 days. The rate of absorption was determined in accordance of *ASTM C 1585-04 Standard Test Method for Measurement of Rate of Absorption of Water by Hydraulic Cement Concretes.*

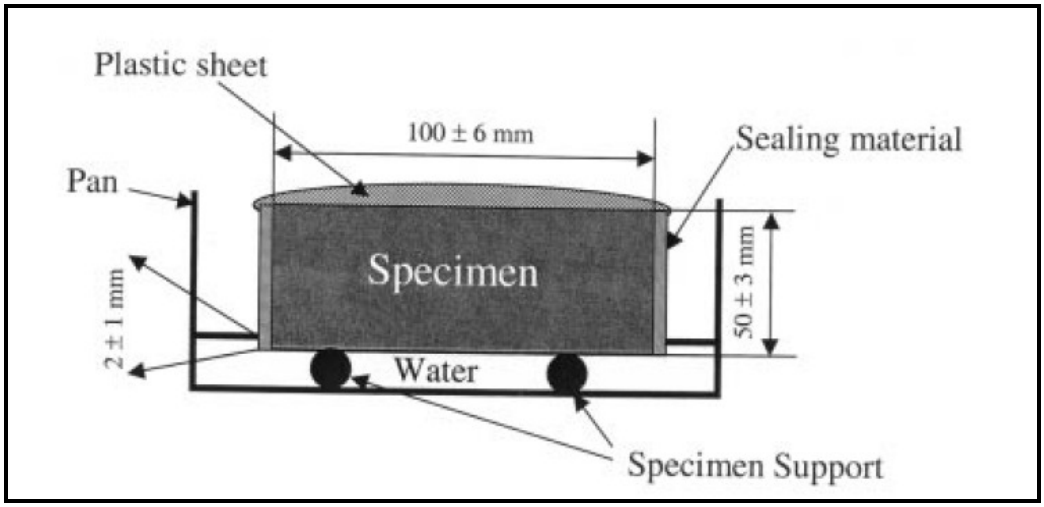

Figure 4.9 Absorption Schematic (ASTM 1585-04)

The specimens used were the two 50-mm thick slices used for the RCPT. After performing the RCPT the specimens were place in the relative humidity controlled environment for two weeks. They were then placed in an oven at 50°C and 80% relative humidity for three days. The 80% RH was obtained with a saturated potassium bromide solution. The specimens were then placed in a sealed container at 23°C for at least 15 days. It has been shown that this storage results in an equilibration of the moisture distribution within the test specimen between 50 and 70% RH. This is similar to the relative humidities found near the surface in some field concrete (ASTM C 1584-04).

The curved side and one end of the specimens were then sealed with duct tape and plastic wrap. The sample was then placed in an open container such that the bottom surface was in contact with water (Figure 4.9). The mass was determined at one, five, 10, 20, 30, and 60 minutes, then every 60 minutes up to six hours, than once a day up to three days, and then one measurement between seven and nine days.

The absorption is calculated by Equation 4.9 where I is the absorption (mm), m_t is the change in mass at time t (g), a is the exposed surface area (mm^2), and d is the density of water (g/mm^3).

$$I = m_t/(a/d)$$ **Equation 4.9**

Absorption is then plotted against the square root of time and the initial absorption ($mm/hr^{1/2}$) was determined from the slope of the regression line plotted for data points between one minute and six hours. The secondary absorption ($mm/hr^{1/2}$) was determined from the slope of the regression line plotted for data points between one day and seven days. A sample absorption plot showing initial and secondary absorption regression line plots can be found in Figure 4.10.

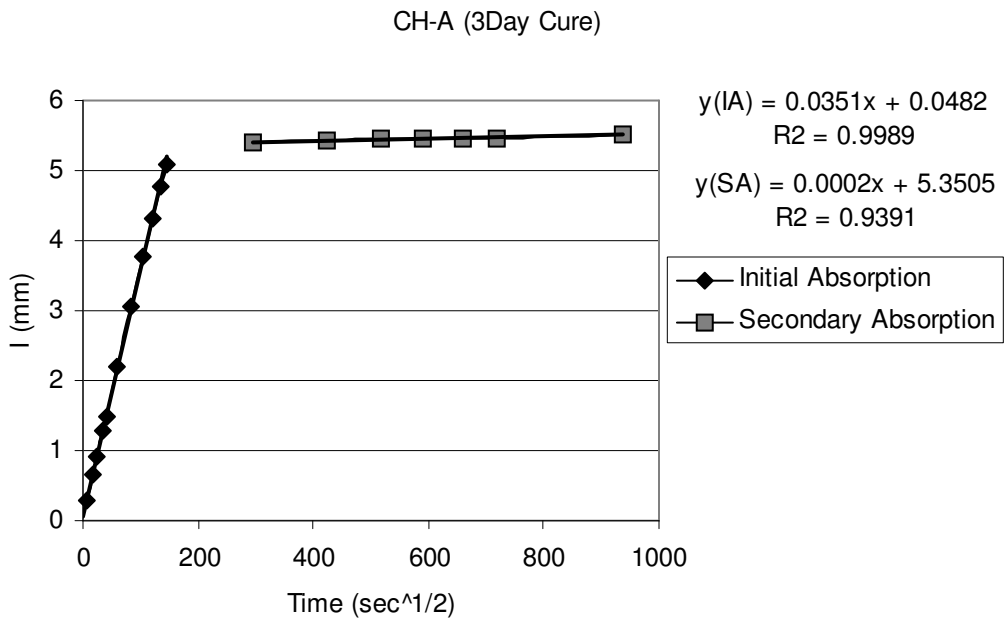

Figure 4.10 Sample Absorption vs. SQRT Time Plot

4.5.3.7 Rebound Hardness

The rebound value was obtained using the Schmidt rebound hammer in accordance with *ASTM C805 Standard Test Method for Rebound Number for Hardened Concrete.* The rebound number should not be confused with a measure of compressive strength. For this study the rebound number is only used as a measure for comparison of relative strength of concrete to determine changes in surface hardness that might occur due to carbonation. The rebound number was obtained from 12 (4x3) locations, in a downward angle, on both the cast and finished surface of the 250 x 300 x 75mm slabs. The pattern of testing can be seen below in Figure 4.11.

X	X	X	X
X	X	X	X
X	X	X	X

Figure 4.11 Patterns for Rebound Hammer Measurements

Rebound measurements were performed on concrete with varying cure times of 1, 3, 7 and 28 days; and were tested at 28, 90, 180, and 365 days.

5.0 Summary of Results

5.1 Paste

There were two methods used to compare the difference in the performance of cementing systems using the 3 different Type CI fly ashes; these were percolation and microhardness.

5.1.1 Percolation

Percolation in this application is defined as the amount of calcium phases that were connected when two edges (either the top and left edges or the bottom and right edges) of the images obtained from SEM were used as the starting point of the burning algorithm. A sample of images before and after this process can be seen in Figure 5.1 for a carbonated paste with W/CM=0.5 and in Figure 5.2 for carbonated paste with W/CM=0.9. The images on the left are backscattered electron (BSE) images of the carbonated paste; the images on the right are "percolated images" in which the burning process (started on the top and left edges) has reached the calcium phases which are connected. The white color represents silica gel, grey represents percolated calcium phases, and black represents non-percolated calcium phases.

.

In Figure 5.1 in can be observed that the control and fly ash mixes all have a connective calcium phase matrix. However, the control appears to be denser. When comparing the percolated images in Figure 5.1 to those in Figure 5.2 a

more porous, less connective calcium phases is evident in the paste with the higher W/CM.

Discrete calcite “blobs” dispersed in a non-calcium matrix (predominantly silica gel) are clearly visible figure 5.2 (c) for BR (HAHS) fly ash and to a lesser extent in Figure 5.2 (e) and (g) for RP (LALS) and TB (HALS) ashes respectively. The lack of connectivity can be seen in the respective percolated images. Once the burning has begun, it does not proceed though the samples as in 5.2 (a) the control sample.

Table 5.1 shows results calculated from these analyses. The proportion of calcium-bearing phases (“% Calcium” in Table 5.1) was determined by image analysis by selecting threshold grey levels to include hydrated and unhydrated phases containing calcium. The last column in the table (column heading “% Percolated”) represents the proportion of the calcium-bearing phases in the image that are connected when the burning algorithm was started on two adjacent faces; the data is the average for burning started on the top and left faces and then the bottom and right faces.

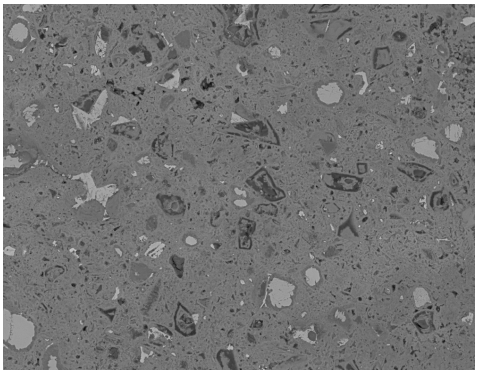

(a) PCON BSE Image

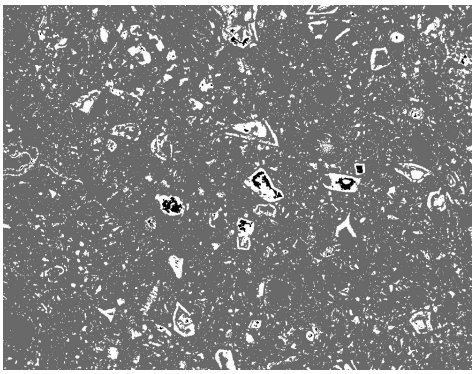

(b) PCON Percolated Image

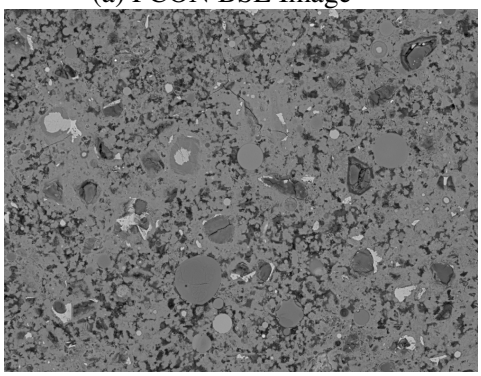

(c) PBR (HAHS) BSE Image

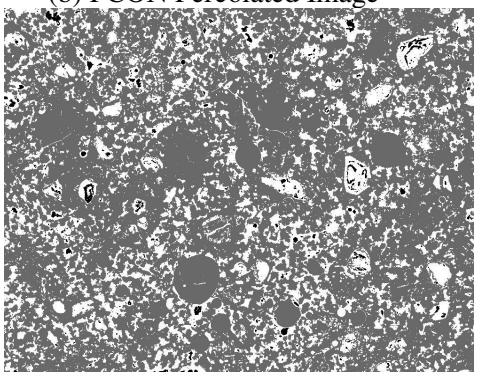

(d) PBR (HAHS) Percolated Image

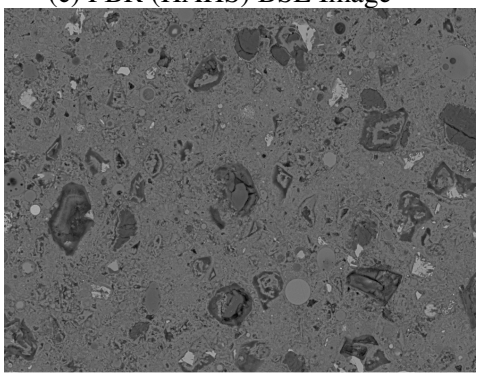

(e) PRP (LALS) BSE Image

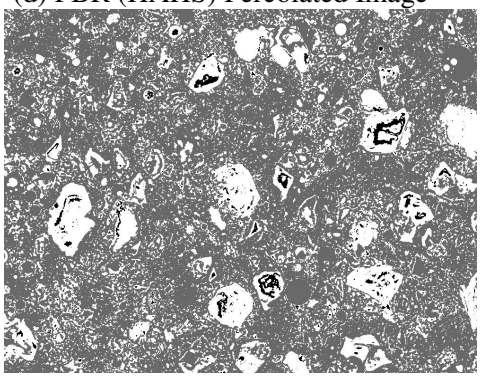

(f) PRP (LALS) Percolated Image

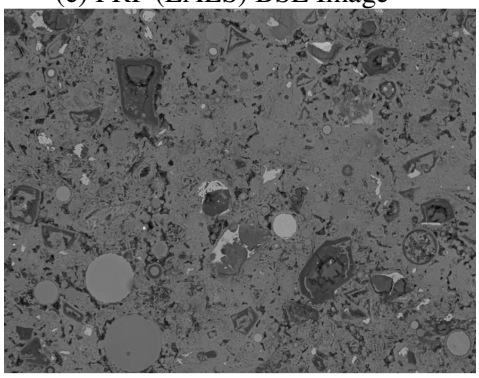

(g) PTB (HALS) BSE Image

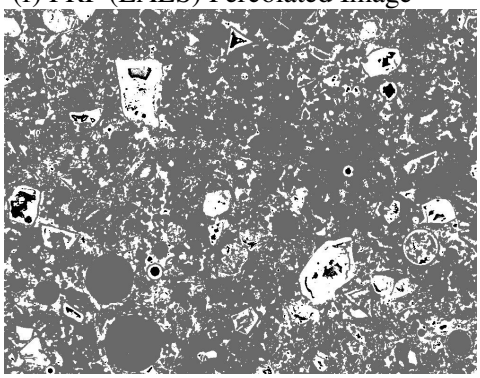

(h) PTB (HALS) Percolated Image

Figure 5.1 Backscatter Electron Images (BSE) left and Percolated Images Right of paste with W/CM=0.50 (400X Magnification)

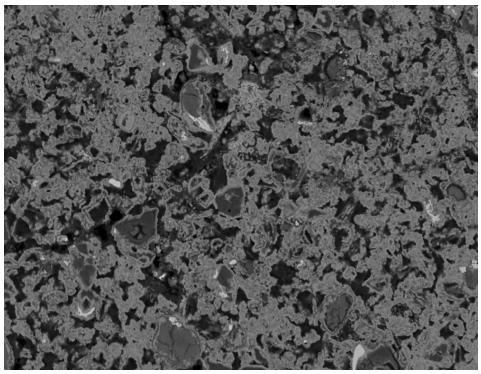

(a) PCON BSE Image

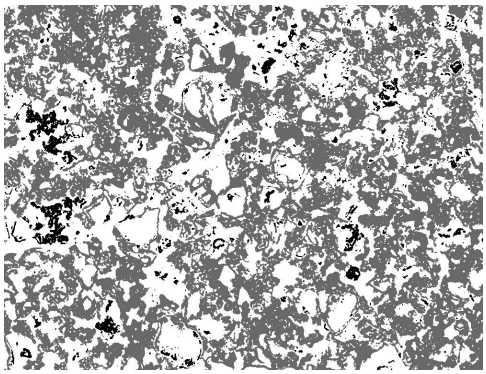

(b) PCON Percolated Image

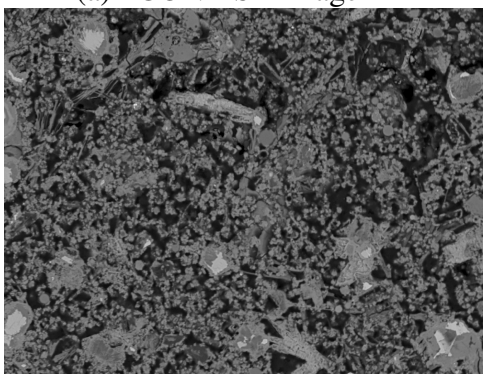

(c) PBR (HAHS) BSE Image

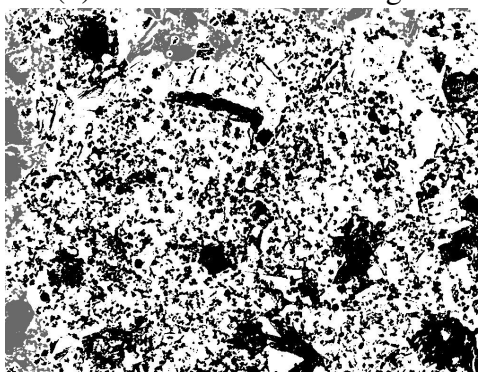

(d) PBR (HAHS) Percolated Image

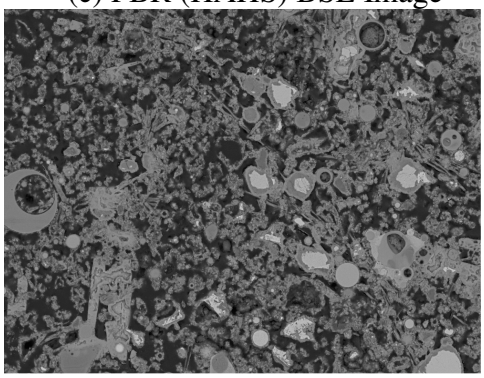

(e) PRP (LALS) BSE Image

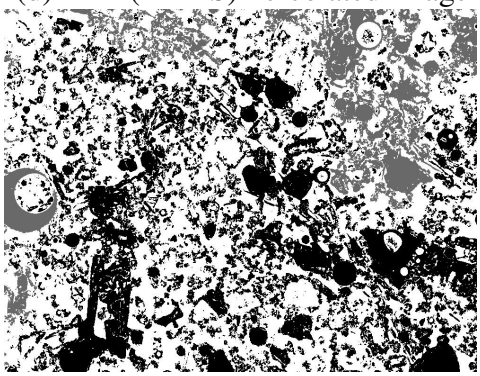

(f) PRP (LALS) Percolated Image

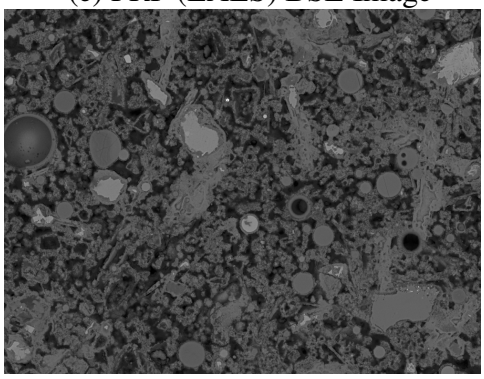

(g) PTB (HALS) BSE Image

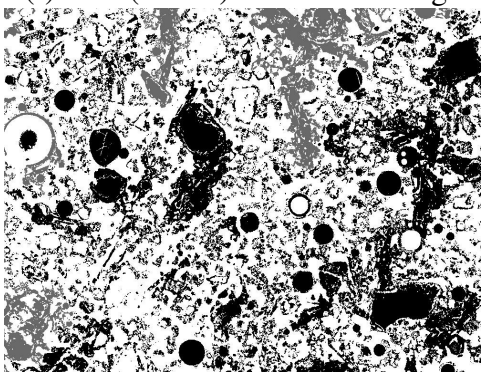

(h) PTB (HALS) Percolated Image

Figure 5.2 Backscatter Electron Images (BSE) left and Percolated Images Right of paste with W/CM=0.90 (400X Magnification)

Table 5.1 Percolation Data

	W/CM	%Calcium	% Percolated
POPC	0.5	84.7	99.3
	0.7	57.8	91.5
	0.9	51.4	82.9
PBR (HAHS)	0.5	78.3	98.4
	0.7	48.2	57.1
	0.9	44.1	22.4
PRP (LALS)	0.5	75.6	98.4
	0.7	64	96.2
	0.9	44.5	21.6
PTB (HALS)	0.5	78.9	98.4
	0.7	60.6	94.3
	0.9	39.2	13.2

The percolation data in Table 5.1 indicate that at a W/CM equal to 0.50, all mixes performed relatively the same showing almost complete connectivity of the calcium phases. As the W/CM was increased to 0.70, the connectivity in POPC, PRP (LALS), and PTB (HALS) remained above 90%. However, the PBR (HAHS) connectivity was reduced to 57%. This indicates that as the W/CM increased to 0.70 for the BR fly ash, the connectivity of the calcium phase was greatly reduced. When the W/CM was increased to 0.90, the connectivity of the control specimens stayed high at 83% whereas all the mixes produced with fly ash experienced a low connectivity in the range of 13-22%. This indicates that the calcium carbonate produced after carbonation is disconnected in pastes produced with these three fly ashes at W/CM=0.90.

The connectivity of the calcium phases in relation to W/CM and cementitious systems can be seen in Figure 5.3. Figure 5.4 shows the connectivity of the

calcium phases in the fly ash pastes normalized to that of the control pastes at the same W/CM.

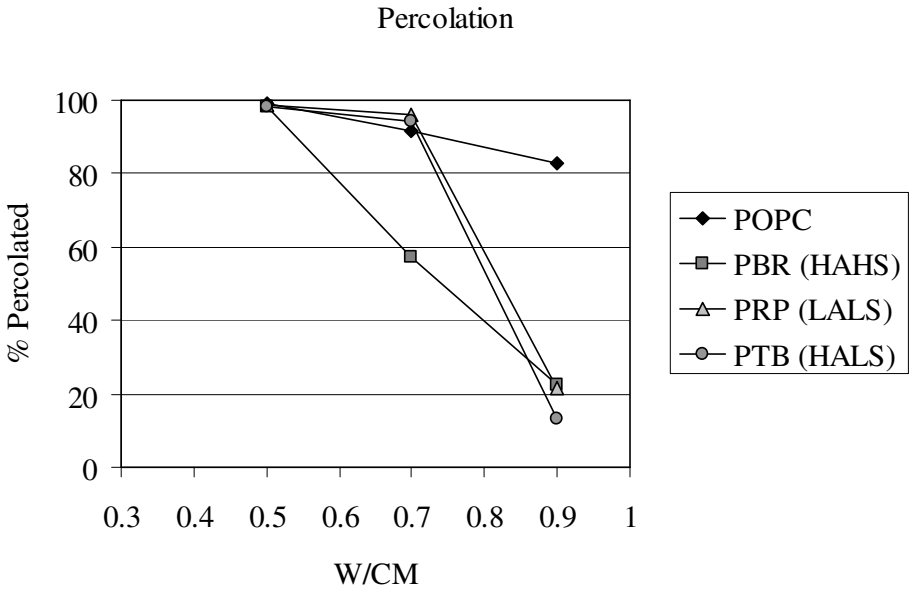

Figure 5.3 Percolation Relationships to W/CM

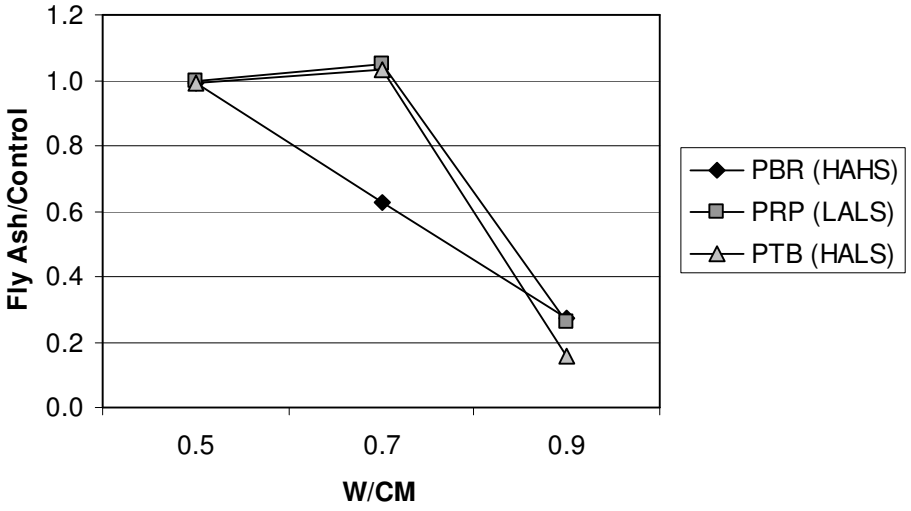

Figure 5.4 Ratio of Control Percolation to Fly Ash Mixes.

5.1.2 Microhardness

Microhardness results are summarized in Table 5.2. Data are not reported for the carbonated paste with W/CM=0.90 and RP (LALS) and TB (HALS) fly ashes due to issues with sample preparation. When it came time to perform the control non-carbonated there were no samples from the N_2 enriched environment.

Table 5.2 Microhardness Data

	Carbonated			Non-Carbonated		
W/CM	0.5	0.7	0.9	0.5	0.7	0.9
POPC	59.7	17	5.8	36.3	15.1	-
PBR (HAHS)	44.6	19.7	7.2	27	15.5	8.1
PRP (LALS)	45.1	15.5	-	21	12.6	6
PTB (HALS)	43.8	17	-	28.8	10	6.6

As shown earlier, Chang (2003) provided evidence that when hydrated cement products carbonate there is an increase in microhardness. He also showed that as the W/CM decreased there is also an increase in microhardness. The same relation was observed in the paste produced in this study and can be seen in both non-carbonated and carbonated paste in Figure 5.5 and Figure 5.6 respectively.

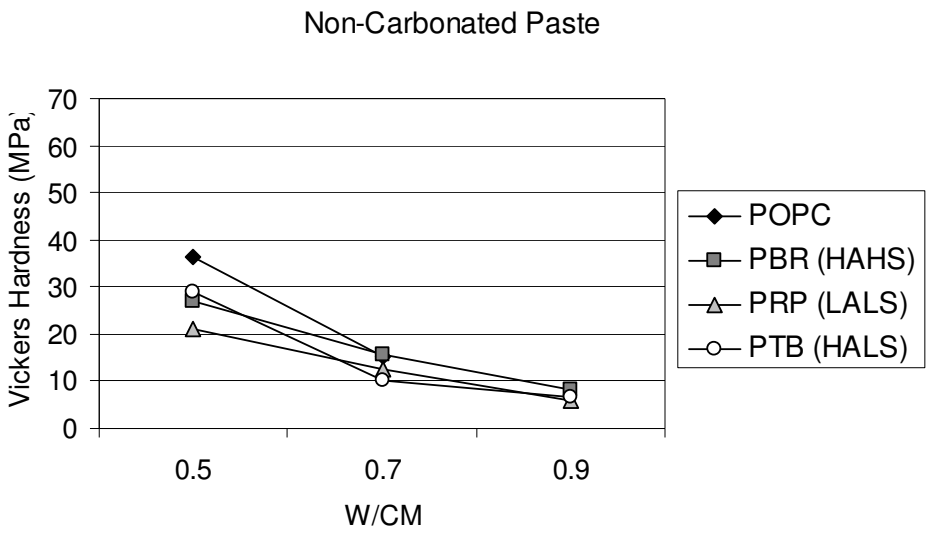

Figure 5.5 Microhardness Non-Carbonated Paste

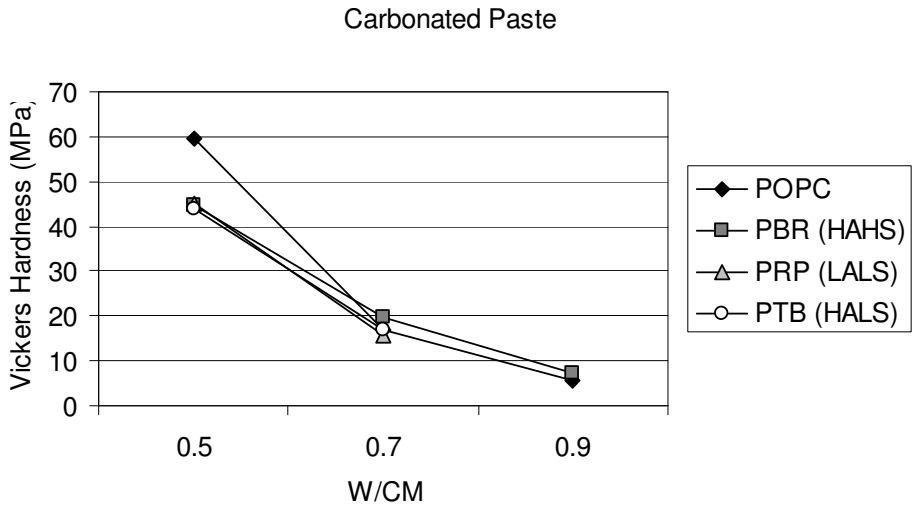

Figure 5.6 Microhardness Carbonated Paste.

The increase in hardness due to carbonation tends to diminish as the W/CM ratio increases. This trend can be observed below in Figure 5.7. This reduced impact can be seen in both the POPC (Control) and the paste produced with different fly ashes.

It is noted that for PBR (HAHS) at W/CM=0.9 that the non-carbonated paste was harder then the carbonated paste. It should be noted that at high W/CM difficulties in preparation were encountered due to the softness of the paste. There were also difficulties in measurement of the diamond indents due to the increases in porosity and less than adequate preparation. Therefore, not only the carbonation process but also the process of measuring it may have contributed to this observed decrease in hardness.

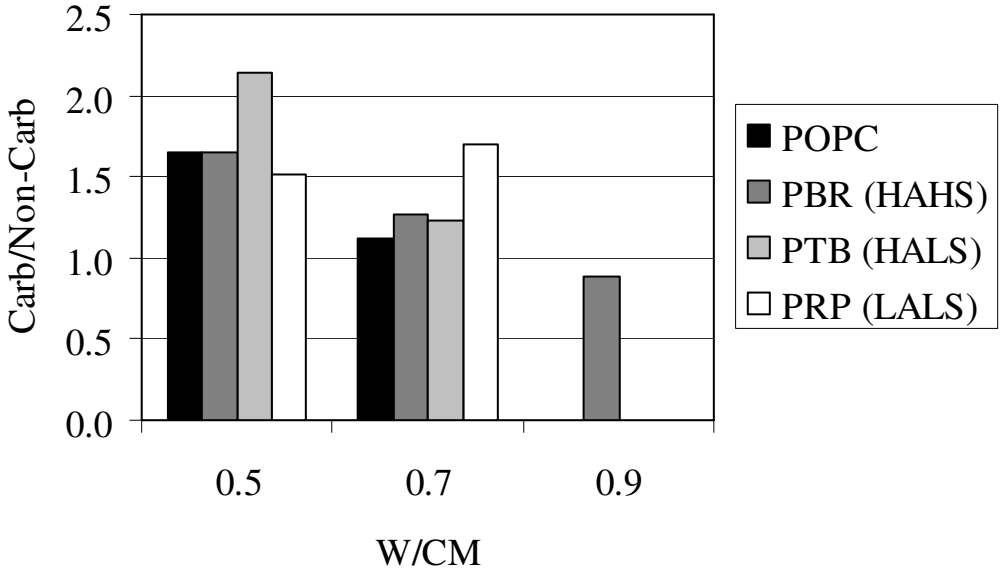

Figure 5.7 Relative Microhardness between Non-Carbonated and Carbonated Paste.

5.2 Mortar

5.2.1 Mechanical Properties

Flexural, compressive, and tensile strength results are summarized below in Table 5.3. A summary of exposure conditions are as follows:

N_2 - Mortars exposed to CO_2-free atmosphere by circulating nitrogen through chamber.

CO_2 Enriched - Mortars exposed to 1% CO_2

W-D (65% RH tent) - Mortars initially exposed to 1% CO_2 for 9 weeks then placed in 65% RH tent. During both environmental conditions the samples were saturated in a solution that represented the corresponding pore solution for 4 hours every 7 days.

Table 5.3 Mechanical Strength Results in MPa

Mix	Exposure Condition	7-Weeks			14-Weeks			40-Weeks		
		Flex.	Comp.	Ten.	Flex.	Comp	Ten.	Flex.	Comp.	Ten.
MOPC	N_2	3.5	20.8	1.5	3.2	18.5	1.8	2.8	15.5	1.9
	CO_2	3.4	19.8	1.3	3.1	22.2	2.2	5.9	28	3.3
	W-D	3.9	22.6	1.6	3.6	25	1.8	2.5	28.5	1.7
MBR (HAHS)	N_2	3.4	21.4	1.3	2.7	18	1.7	3.2	16.9	1.9
	CO_2	3	21.2	1.1	2.7	20.5	1.3	2.8	23.4	1.5
	W-D	3	22.1	1.7	2.9	22.1	1.5	1.8	25.2	1.1
MRP (LALS)	N_2	3.2	18.4	2	3.2	17.5	1.4	2.7	14.7	1.9
	CO_2	3.1	20.4	1.3	3.1	17.2	1.5	4	18.9	1.9
	W-D	4	23.6	1.1	3.2	22.6	1.1	2.9	20.6	1.8
MTB (HALS)	N_2	3	18.1	1.4	3.5	18.9	1.5	3.2	17.8	1.6
	CO_2	2.6	16	1.6	3.2	20.9	1.1	5.1	21.2	2.6
	W-D	3.4	22.4	1.8	3.4	25	1.3	1.2	28.5	1

5.2.1.1 CO_2-Enriched Environment

As carbonation took place in the control sample, MOPC, flexural, compressive, and tensile strength all increased. These increases of 110%, 80% and 175%, respectively, can be seen in Figure 5.7, which shows the strengths of samples stored in CO_2 expressed as a ratio of the strengths for the same samples stored in N_2. Such increases in strength can be expected as hydrated cement products carbonate (Parrott, 1987)

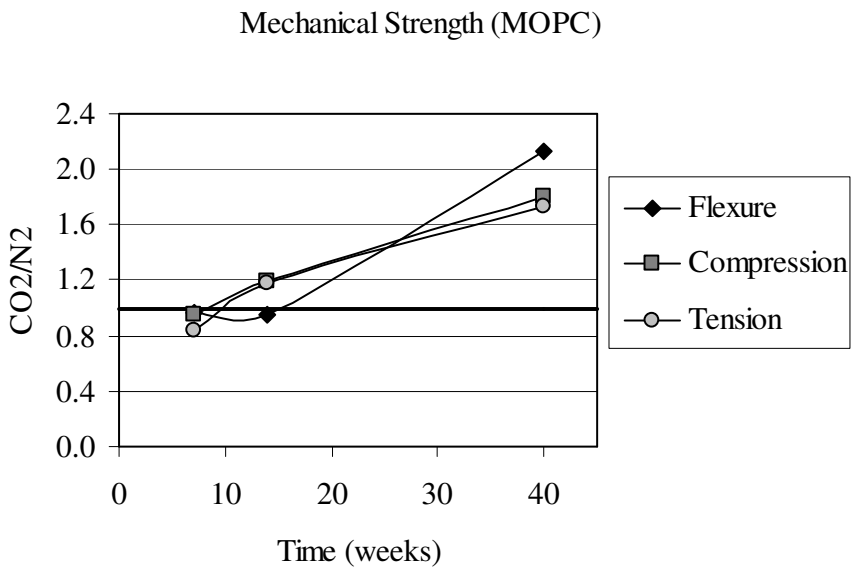

Figure 5.8 Relative Changes in Mechanical Strength between Non-Carbonated and Carbonated Mortar without Fly Ash (MOPC)

However, the mortar made with BR (HAHS) fly ash only experiences an increase in compressive strength of 40% after carbonation whereas the flexure and tensile strengths both show a decrease of 13% and 21%, respectively, after carbonation. The CO_2/N_2 relationship between mortars mechanical strengths produced with BR fly ash can be seen in Figure 5.9.

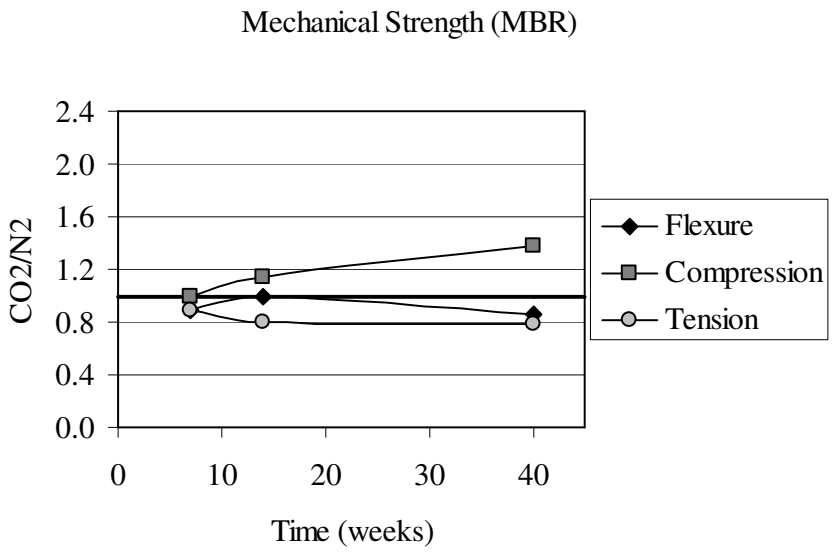

Figure 5.9 Relative Changes in Mechanical Strength between Non-Carbonated and Carbonated Mortar (MBR, HAHS)

Mortars produced with the RP (LALS) fly ash exhibited some increase in compressive and flexural strength as the cement hydrates carbonated but showed a decrease in tensile strength. The CO_2/N_2 relationship between mortars mechanical strengths produced with RP fly ash can be seen in Figure 5.10.

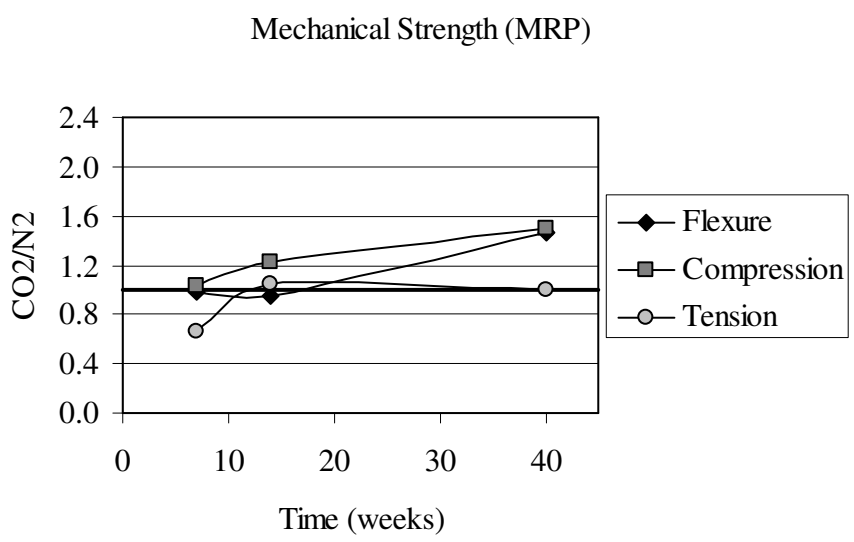

Figure 5.10 Relative Changes in Mechanical Strength between Non-Carbonated and Carbonated Mortar (MRP, LALS)

The mortar produced with the TB fly ash exhibited an increase in compressive, tensile, and flexural strengths of 60%, 20% and 62% respectively as the hydrated cement products carbonated over time. The CO_2/N_2 relationship between mortars mechanical strengths produced with TB (HALS) fly ash can be seen in Figure 5.11. The increase is less than that observed for the control mortar (MOPC).

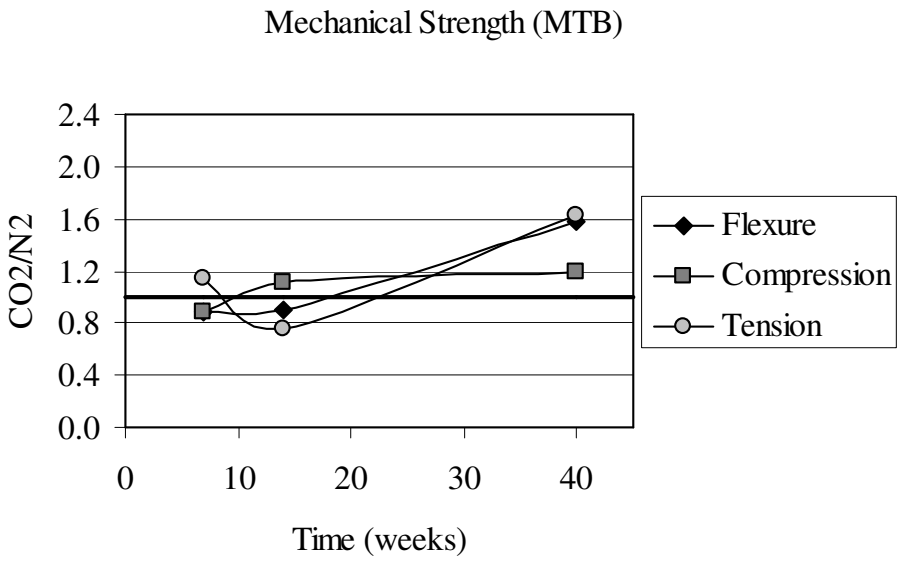

Figure 5.11 Relative Changes in Mechanical Strength between Non-Carbonated and Carbonated Mortar (MTB, HALS)

5.2.1.2 Wet-Dry Cycled Environment

It should be noted that the specimens that were wet-dry cycled were not completely carbonated and only showed a depth of carbonation of approximately 5-7 mm. For the specimens that were wet-dry cycled there was a different response to carbonation in all of the mixes except for the mix produced with the RP (LALS) fly ash. As can be shown in Figures 5.12, 5.13, 5.14, and 5.15 as the specimens experienced more wet-dry cycles and carbonated further, the compressive strength increased. This increase was also seen in the specimens that

were not wet dry cycled. However, in the specimens that were wet-dry cycled, there seemed to be a deleterious effect on the flexural and tensile strength in both the control samples and samples produced with the BR (HAHS), RP (LALS) and TB (HALS) fly ashes.

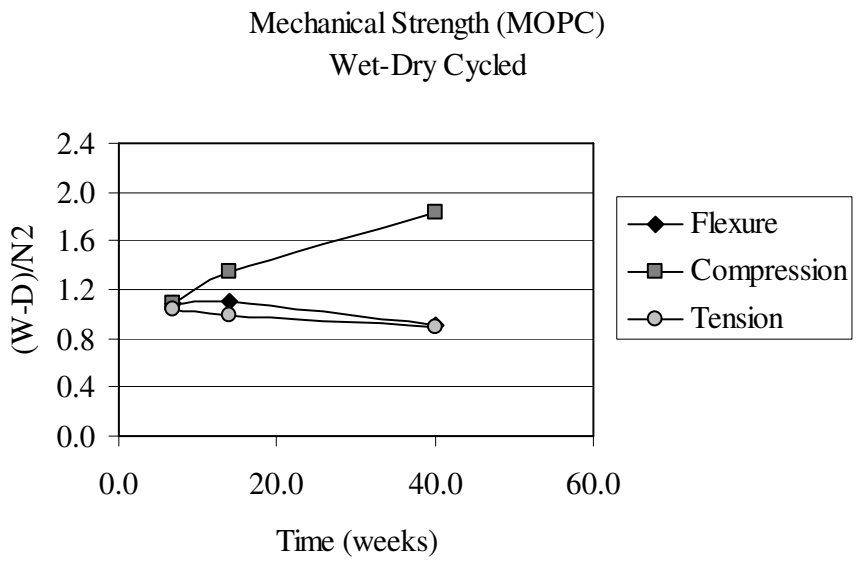

Figure 5.12 Relative Changes in Mechanical Strength between Non-Carbonated and Wet Dry Cycled Mortar (MOPC)

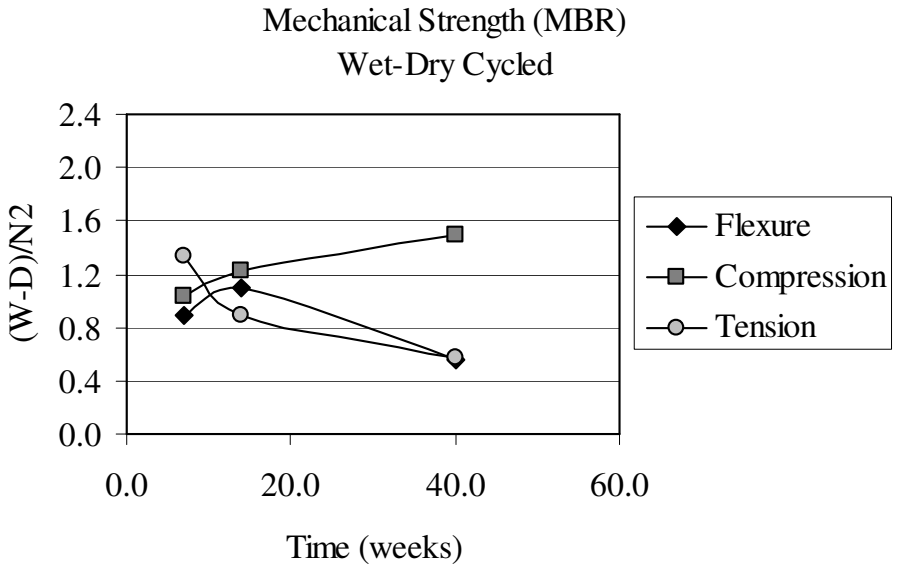

Figure 5.13 Relative Changes in Mechanical Strength between Non-Carbonated and Wet Dry Cycled Mortar (MBR, HAHS)

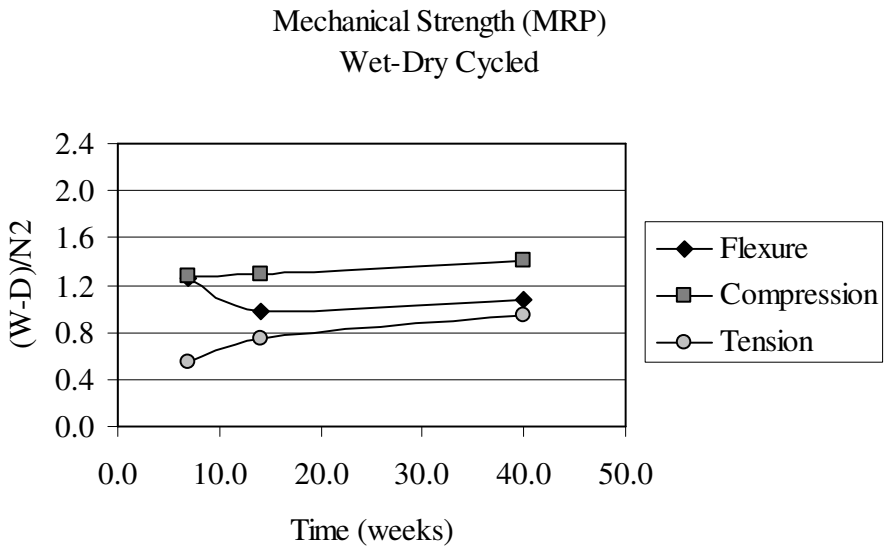

Figure 5.14 Relative Changes in Mechanical Strength between Non-Carbonated and Wet Dry Cycled Mortar (MRP, LALS)

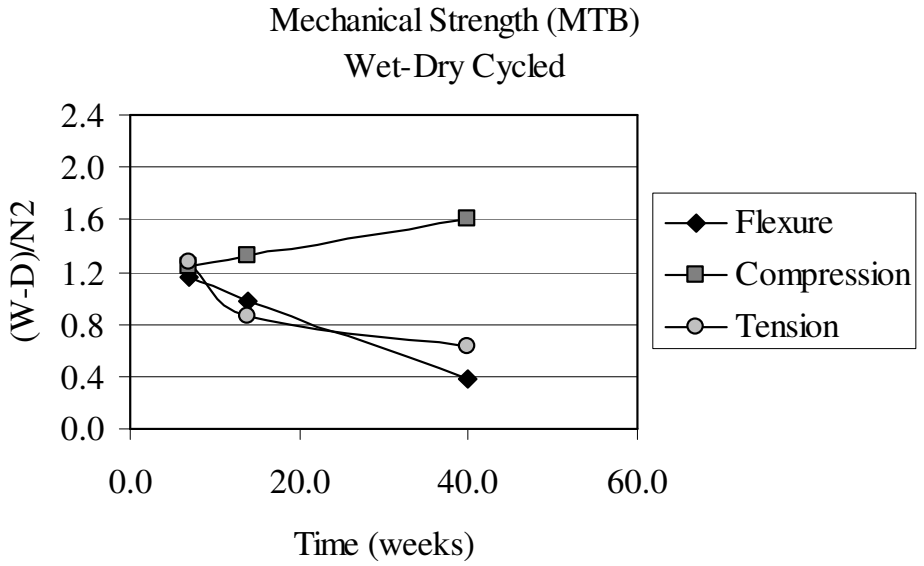

Figure 5.15 Relative Changes in Mechanical Strength between Non-Carbonated and Wet Dry Cycled Mortar (MTB, HALS)

5.2.2 Dynamic Young's Modulus of Elasticity

The results for resonant frequency measurements can be found in Table 5.4.

Table 5.4 Resonant Frequency Measurements

		Resonant Frequency (Hz)
MOPC	N_2	860
	CO_2	933
	W-D	947
MBR (HAHS)	N_2	893
	CO_2	813
	W-D	808
MRP (LALS)	N_2	850
	CO_2	840
	W-D	860
MTB (HALS)	N_2	853
	CO_2	837
	W-D	850

A comparison of the squares of the resonant frequencies of the non-carbonated vs. carbonated mortars and non-carbonated vs. wet-dry cycled mortars can be found in Figure 5.16. The control mortars when carbonated and wet-dry cycled performed better then the control non-carbonated. However, this is not the case for all the mortars produced with fly ash. For the mortars produced with the TB (HALS) and RP (LALS) fly ash there seems to be a small difference in performance due to carbonation or wet-dry cycling. The mortar produced with the BR fly ash experienced some deleterious effect due to carbonation and wet-dry cycling.

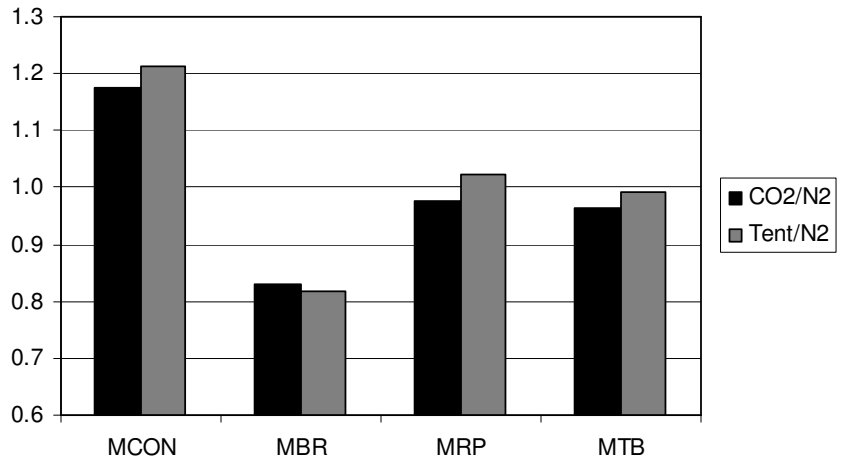

Figure 5.16 Ratio of Squared Resonant Frequencies Between Non-Carbonated and Carbonated, Non-Carbonated and Wet-Dry Cycled.

5.2.3 Porosity

The results for porosity are presented in Table 5.5.

Table 5.5 Porosity

	N_2 (Non Carbonated)			CO_2 (Carbonated)			Wet Dry Cycled		
	n-Water	n-Prop	n-11	n-Water	n-Prop	n-11	n-Water	n-Prop	n-11
MOPC	18.7	14.6	18	17.5	16.1	17	17.6	13.3	17
MBR (HAHS)	17.7	11	16.9	18.3	18.5	17.7	17.9	17.7	17.3
MRP (LALS)	18.6	12.8	17.8	17.3	17.1	16.8	16.7	13.8	16
MTB (HALS)	18.6	13	17.8	17.9	16.2	17.4	17.9	15.6	17.3

Figure 5.17 compares the different porosity measurements for non-carbonated (N_2) specimens with the carbonated (CO_2) specimens from the same mix. The total porosity (n-water) is reduced by approximately 10% for the control (MOPC) specimens and for those with fly ash RP (LALS) and TB (HALS) (MRP and MTB in Figure 5.17). However, in the mortar with fly ash BR there is a slight

increase in total porosity. Despite the reduction in total porosity for three of four mortars, carbonation appears to have increased the volume of the coarser capillary-size pores (as measured by n-prop) for all four mortars, the increase being significantly greater for the mortar with fly ash BR (MBR, HAHS).

Ngala and Page (1997) showed with mercury intrusion porosimetry that when paste samples underwent carbonation the porosity decreased but a redistribution of pore size occurred. They showed a slight but insignificant increase in coarse capillary pores in the OPC paste but found an increase of 140% in coarse capillary pores in paste produced with a Type F fly ash. The results presented here for isopropanol porosity are consistent with the findings of Ngala and Page (1997).

Differences between n-water and n-11 for a given mortar indicate the amount of gel porosity in the system. The differences are slightly smaller in the carbonated paste (see Table 5.5) as a result of the carbonation and destruction of C-S-H.

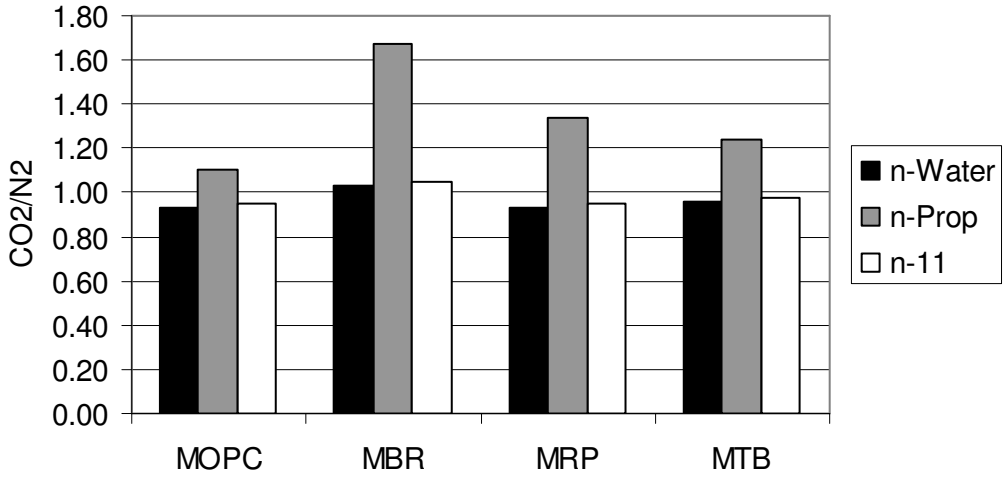

Figure 5.17 Relative Changes in Porosity between Non-Carbonated and Carbonated Mortar

Even though the specimens that were wet-dry cycled did not experience full carbonation a reduction in total porosity for samples CON, RP (LALS) and TB (HAHS) can be seen in Figure 5.18. This may be attributed to further hydration of the cement during and shortly after the wetting period.

Sample BR, as in the carbonated samples, showed a slight increase in total porosity. The volume of capillary pores, as measured by n-prop porosity, decreased with wet-dry cycling for the control but increased for the fly ash mortars, especially the BR (HAHS) fly ash.

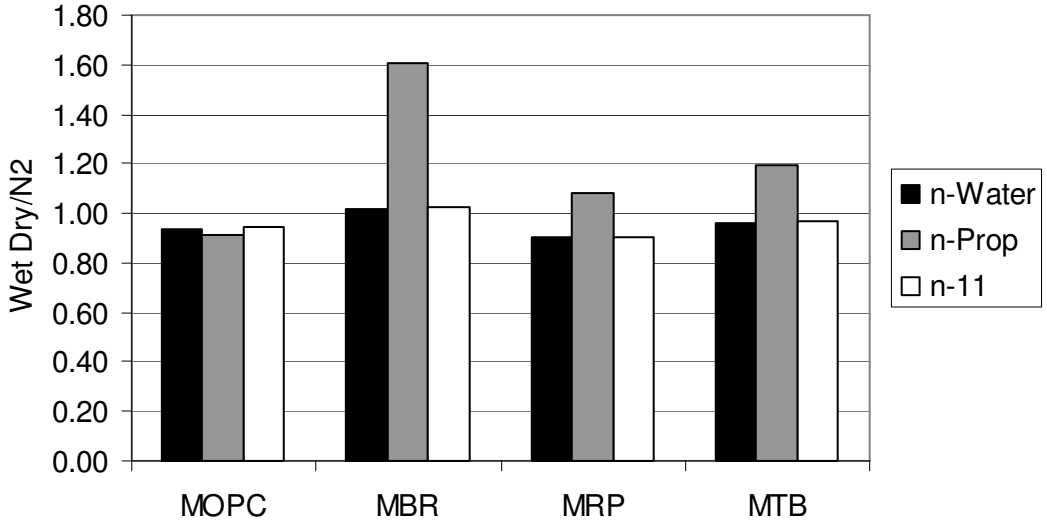

Figure 5.18 Relative Changes in Porosity between Non-Carbonated and Wet Dry Cycled Mortar

5.3 Concrete

5.3.1 Compressive Strength

The results for compressive strength are presented in Table 5.6. As stated Phase I was conducted to evaluate compressive strength of each fly ash compared to changes in W/CM.

Table 5.6 Compressive Strength (MPa)

			Age Tested (Days)							
			1	7	28			90		
			Time Cured (Days)							
Mix ID	W/CM	FA Type	1	7	1	7	28	1	7	90
A1	0.7		5.4	23.2	18.4	26	28.4	17	23.3	30.8
A2	0.85		3.9	13.5	12.3	17.1	20.8	11.3	15.6	21.5
B1	0.7	BR (HAHS)	3.6	13.3	11.4	14.3	19.1	11.2	12.3	20.6
B2	0.85	BR (HAHS)	2.2	8.5	7.6	10	14.4	7.2	10.1	14.9
T1	0.7	TB (HALS)	3.4	15.3	11.6	18.2	25.2	11.9	16	27.7
T2	0.85	TB (HALS)	2.4	8.2	8.1	12	16.8	7.9	9.6	20.3
R1	0.7	RP (LALS)	2.6	17.1	13.2	19.6	25.9	12.3	17.2	27.2
R2	0.85	RP (LALS)	1.9	9.6	7.6	11.6	16.9	7.7	11.2	19.2

For residential concrete the CSA A438 M84 requirement is a minimum 28-day compressive strength of 15 MPa for foundation walls with no maximum W/CM. It can be seen in Figure 5.19 that all but one mix, B2 (HAHS), achieved a compressive strength of 15 MPa at 28 days provided the samples were moist-cured. Mix B2 (HAHS) had a 28-day (moist-cured) compressive strength of 14.4 MPa and had an air content of 9%. This air content is above the range of 5-8%

specified in CSA A438-M84 and this increase in air will result in a decrease in compressive strength[1].

It can be seen in Figure 5.19, 5.20, and 5.21 that the control at W/CM of 0.70 and 0.85 yielded a higher compressive strength then all the mixes produced with the three different fly ashes at both W/CM of 0.70 and 0.85. The reason the mixes produced with fly ash have lower compressive strengths is because of the slow pozzolanic reaction of the fly ash with the calcium hydroxide. It can also be seen in the concrete produced with the same type of cementitious materials that the concrete mixed with W/CM of 0.70 gave a higher compressive strength then the concrete produced with W/CM of 0.85, which is expected. It can also be noted that at 28 and 90 days, the samples increased in strength as the curing time increased.

For all mixes, as the curing time increased from 28 to 90 days, the compressive strength only marginally increased. For the samples cured for 7 days, when tested at 7, 28 and 90 days, there was increase strength between 7 and 28 days for all samples, however between 28 and 90 days a decrease in compressive strength was noted.

[1] The compressive strength of concrete is reduced by approximately 5.5 % for each 1% air in the mix. **(Neville, A M, 1993)**

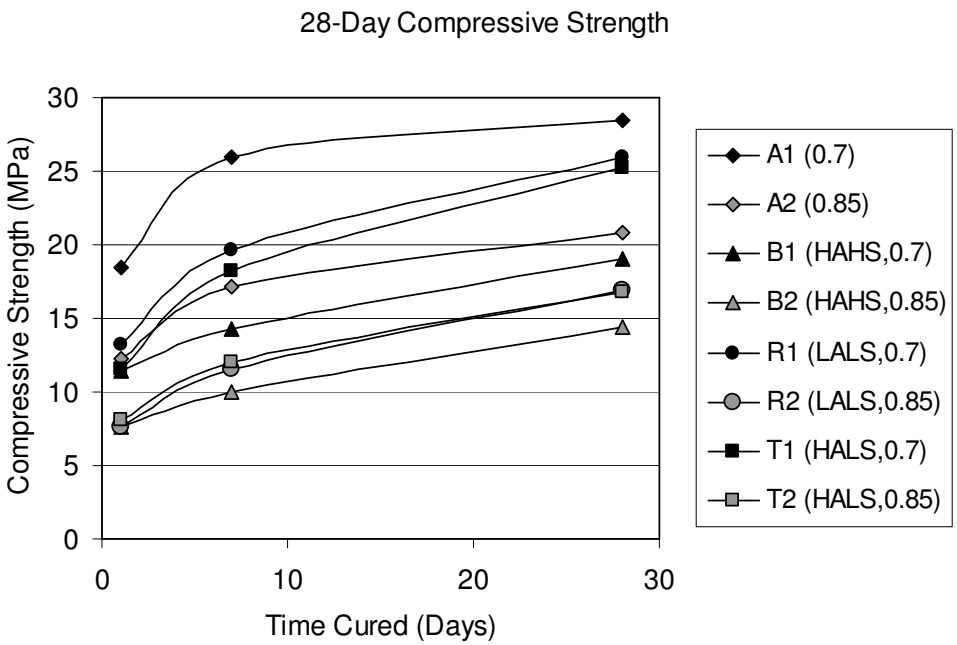

Figure 5.19 28-Day Compressive Strength

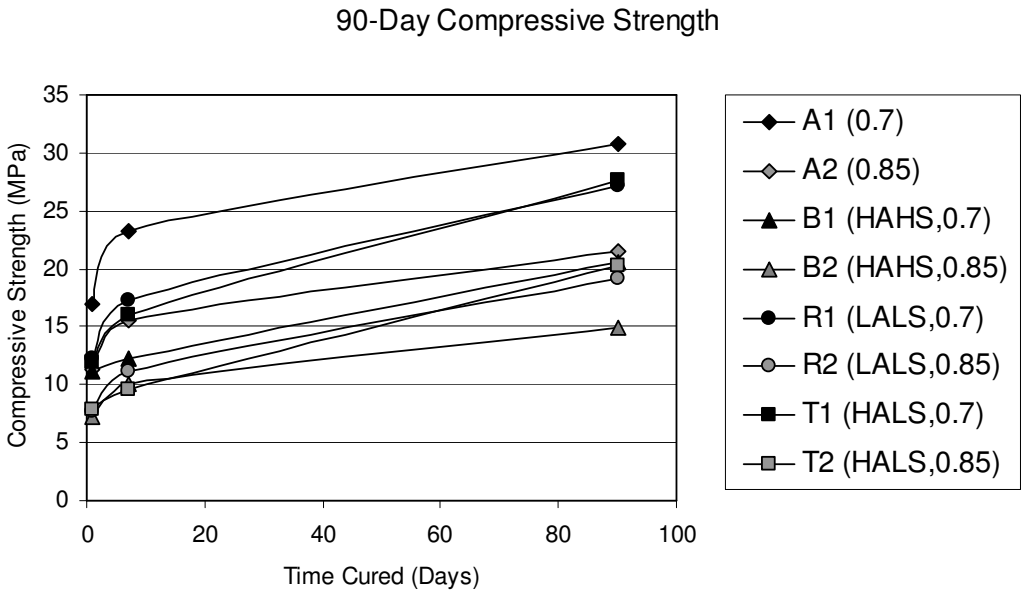

Figure 5.20 90-Day Compressive Strength

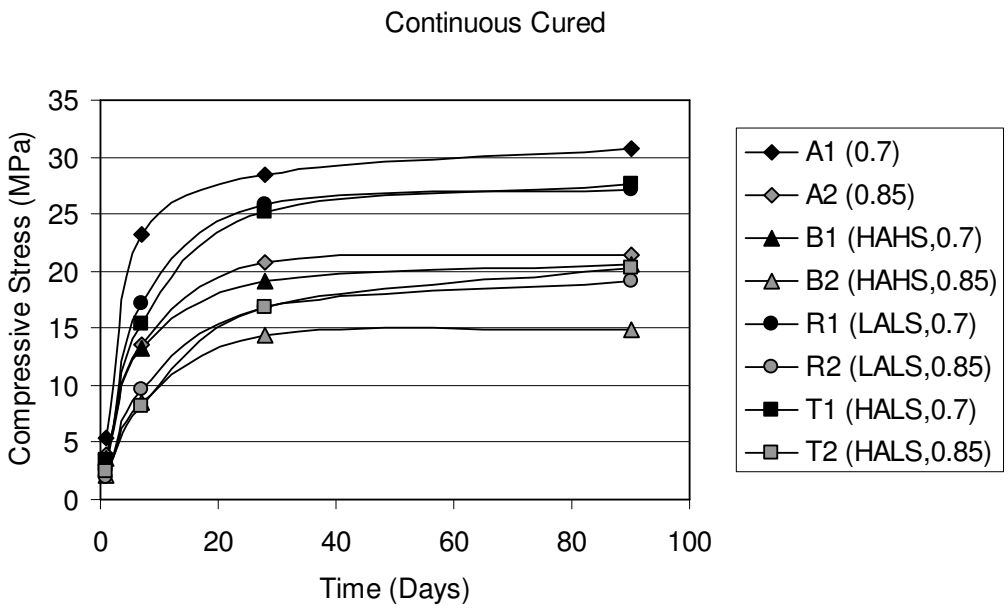

Figure 5.21 Continuously Cured Compressive Strength

5.3.2 Rapid Chloride Permeability Test

The results for the rapid chloride permeability test can be found in Table 5.7. For specimens CL, CH, BL (HAHS), and BH (HAHS) at 28 days moist-cured, RCPT measurements were not performed due to miss communication with lab personnel. For specimen RH, there was no 365 day measurement taken for the 3 day moist cure due to the measurement being taken on the wrong specimen.

Table 5.7 Charge Passed (KCoulombs)

	Time Tested (Days)												
	28				90			180			365		
	Time Cured (Days)												
	1	3	7	28	1	3	7	1	3	7	1	3	7
CL	6.5	5.4	5.4	0	6.2	7.3	6.9	3.6	3.8	3.8	6	5.3	4.7
CH	6.5	5.3	5.9	0	6.4	7.9	6.3	4.1	4.9	5.1	6.1	4.2	5.8
BL (HAHS)	10.3	9.3	8.8	0	9.7	10.2	10.5	3.8	4.5	5.1	5.6	5.7	7.9
BH (HAHS)	13.9	11.4	14.3	0	14	11.5	14.7	8.1	6.4	7.1	7.9	8.3	8.8
RL (LALS)	9.8	5.4	6.8	7.5	6.4	7.2	7	4.9	7	5.9	5.3	4.2	5.2
RH (LALS)	7.3	7.6	6.8	7.4	7.3	8.2	7.7	4.7	5	4.3	4.7	0	5.2
TL (HALS)	5.7	4.8	7.1	4.3	6.8	6.9	6	4.8	4.2	3.9	2.9	4	4.4
TH (HALS)	4.7	6.3	6.3	4.1	9.4	7	8.2	5.2	5	4.9	4.4	5.6	3.6

Table 5.8, taken from ASTM C1202 relates the charge passed to the ability of the concrete to resist chloride ion penetration.

Table 5.8 Chloride Ion Penetrability Based on Charge Passed

Charge Passed (Coulombs)	Chloride Ion Penetrability
>4,000	High
2,000-4,000	Moderate
1,000-2,000	Low
100-1,000	Very Low
<100	Negligible

All concrete tested, according to ASTM C1202 *Standard Test Method for Electrical Indication or Concrete's Ability to Resist Chloride Ion Penetration*, showed moderate or high chloride ion penetrability with most of the results being greater than 4000 Coulombs ("high penetrability"), in many cases significantly higher. It can be seen in Figure 5.22, 5.23, and 5.24 that the W/CM in most cases

has an effect on the charge passed. As expected, concrete with a W/CM of 0.85 had more charge passed then concrete produced with W/CM 0.70, although there was little effect of the W/CM on the control concrete. It can also be seen that after 90 days, the concrete performs better. This can be attributed to further hydraulic and pozzolanic reaction. It can also be due to carbonation of the specimens that results in a reduction in ion concentration in pore solution and densification of porosity for some mixes.

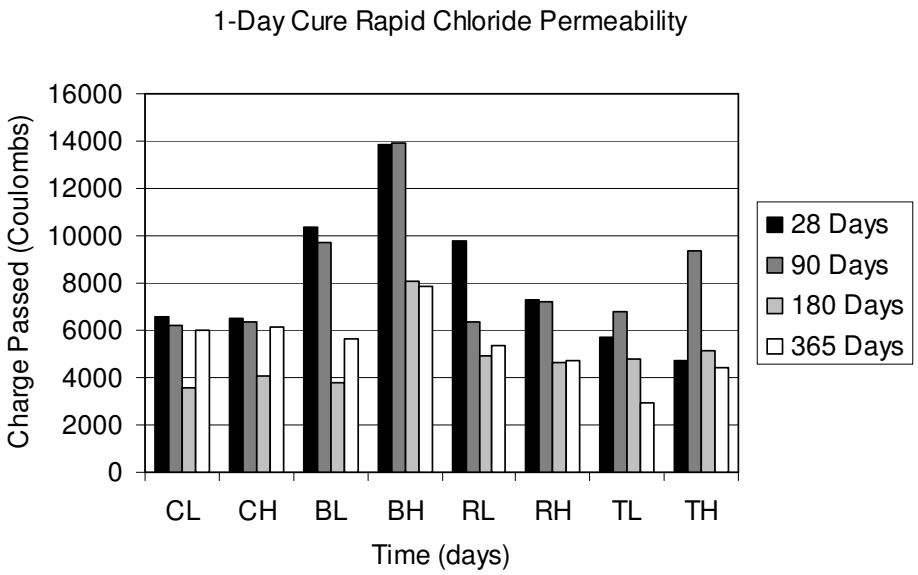

Figure 5.22 1-Day Moist-Cured RCPT

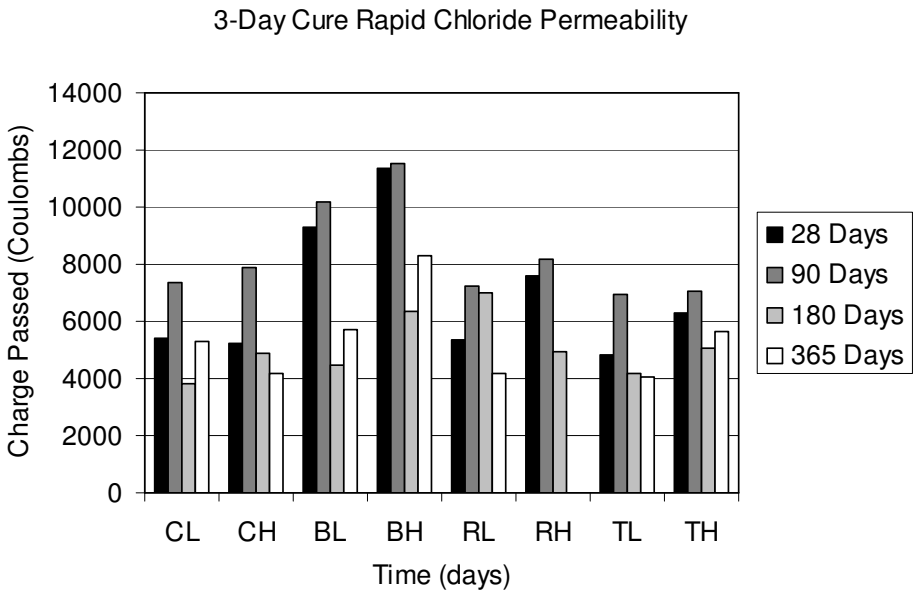

Figure 5.23 3-Day Moist-Cured RCPT

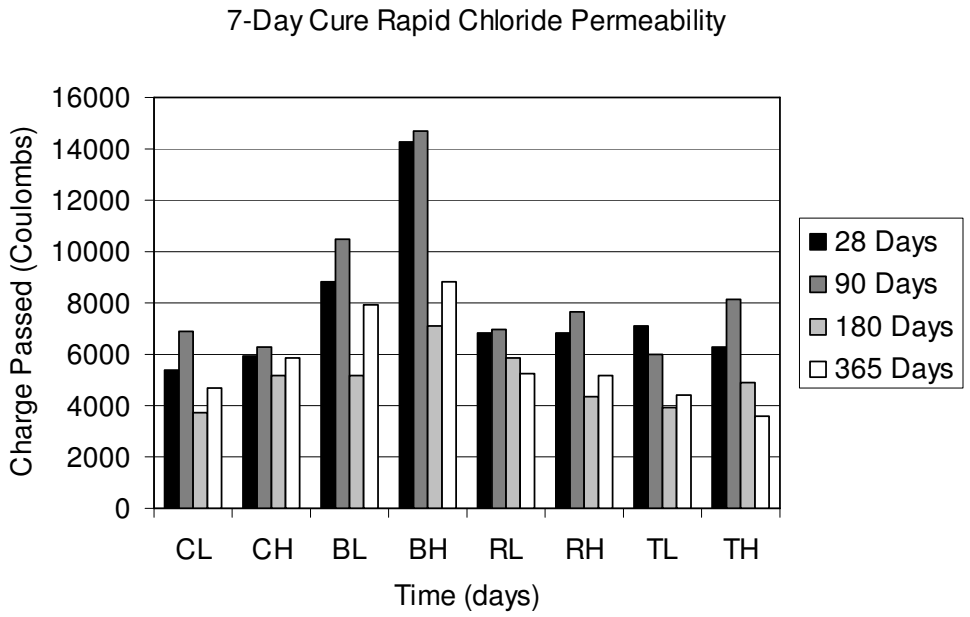

Figure 5.24 7-Day Moist-Cured RCPT

Figure 5.25 and 5.26 show the effect of moist curing period on the RCPT value for the mixes with W/CM= 0.70 and 0.85 respectively. Figure 5.27 and 5.28 show the same data for the fly ashes normalized using the data for the comparative

control mixes. These figures show that all the concrete produced with fly ash with moist-curing period of one, three and seven days performed worse then the control. There was a few times in which the concrete produced with fly ash performed better then the control. One note should be made about the concrete produced with BR fly ash is that for both W/CM 0.70 and 0.85 (more so 0.85) the charge passed is significantly more then the control and the concrete produced with both the TB (HALS) and RP (LALS) fly ash. Surprisingly, there does not seem to be any apparent relationship between the moist curing period and the amount of charge passed.

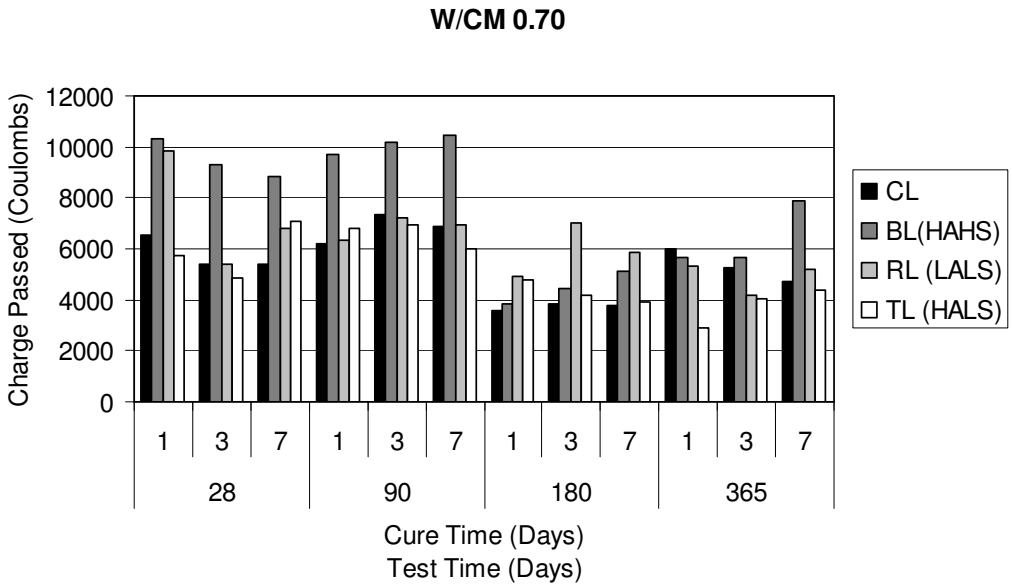

Figure 5.25 Charge Passed for Concrete with W/CM=0.70

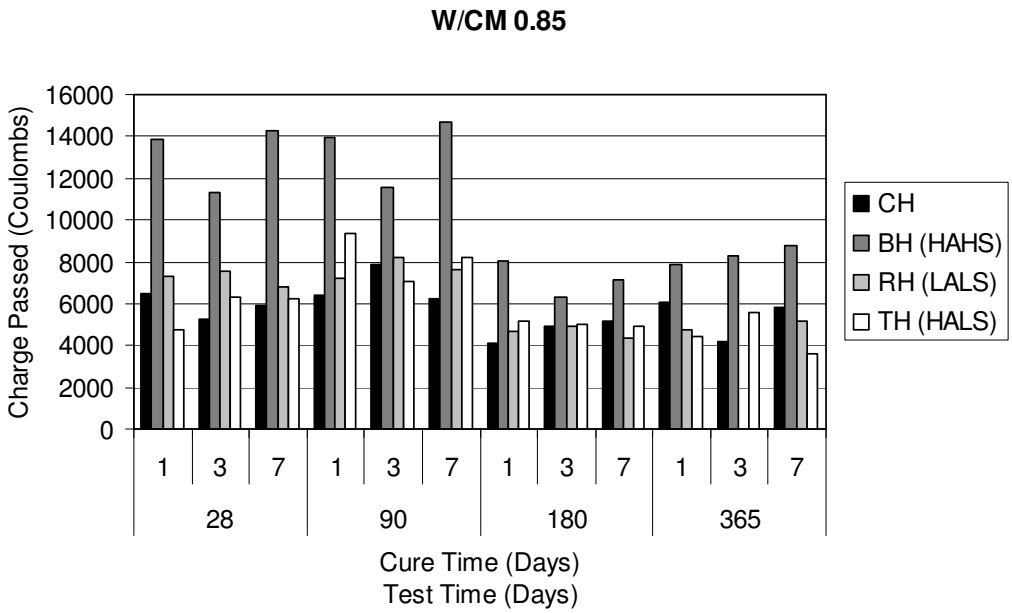

Figure 5.26 Charge Passed for Concrete with W/CM=0.85

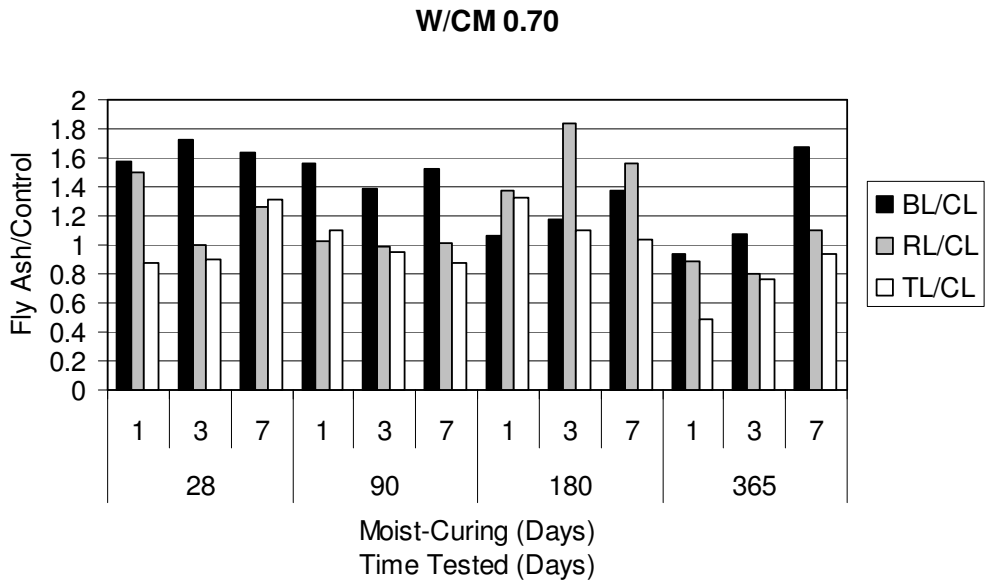

Figure 5.27 Relative Charge Passes between Control and Fly Ash Concrete (W/CM=0.70)

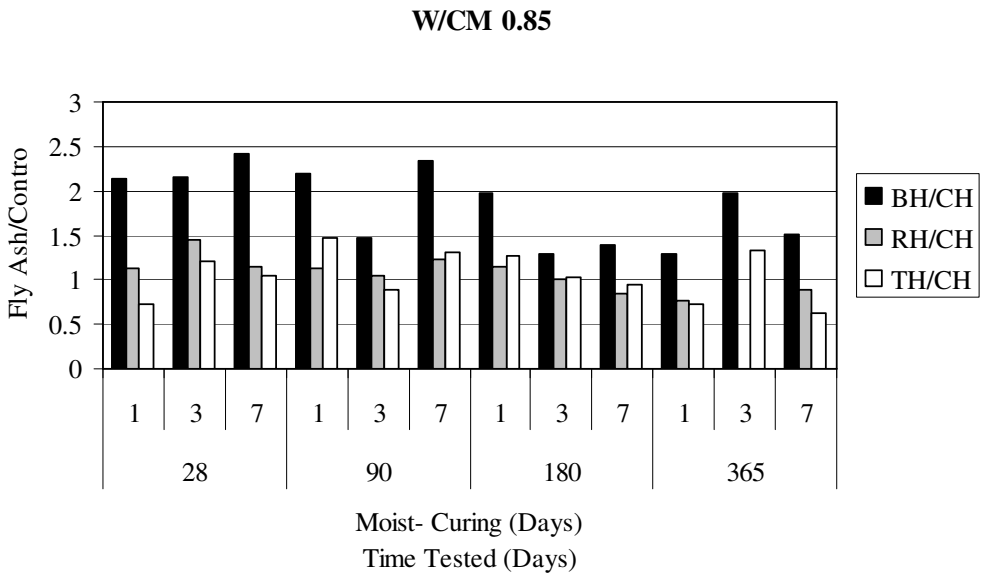

Figure 5.28 Relative Charge Passes between Control and Fly Ash Concrete (W/CM=0.85)

5.3.3 Electrical Resistivity

The electrical resistivity data are presented in Table 5.9. The RCPT measures the electrical charge passed through the specimen during a 6-hour period and is, essentially, a measurement of electrical conductivity. Conductivity is the reciprocal of electrical resistivity and, hence, one might expect a good relationship between electrical resistivity and the RCPT; this can be shown in Figure 5.29. Resistivity measurements at 28 days were not performed on specimens CL, CH, BL (HAHS), BH (HAHS), TL (HALS), and TL (HALS) due to a laboratory miscommunication. Resistivity measurements at 365 days were not performed on specimens RL (LALS) and RH (LALS) due to unavailability of laboratory equipment at time of testing.

Table 5.9 Resistivity (Kohm-cm)

	Time Tested (Days)												
	28				90			180			365		
	Moist-Cured (Days)												
	1	3	7	28	1	3	7	1	3	7	1	3	7
CL	-	-	-	-	2.9	3.0	3.1	3.9	3.7	3.9	3.1	3.0	3.4
CH	-	-	-	-	3.0	3.3	3.0	3.7	3.5	3.6	3.5	4.2	3.1
BL (HAHS)	-	-	-	-	2.0	2.0	2.4	3.7	3.4	2.8	2.7	2.7	2.4
BH (HAHS)	-	-	-	-	1.7	10.2*	1.7	1.9	2.0	2.1	2.4	2.1	2.3
TL (HALS)	-	-	-	-	3.5	2.8	3.4	4.0	3.9	4.4	5.0	4.8	4.3
TH (HALS)	-	-	-	-	2.7	2.8	2.9	2.8	3.3	3.0	3.5	3.6	4.2
RL (LALS)	2.3	3.6	5.3	11.0*	2.4	2.7	2.4	2.8	2.4	2.6	-	-	-
RH (LALS)	2.6	2.4	3.2	3.5	2.5	3.1	2.3	3.5	3.1	3.5	-	-	-

*Suspect results

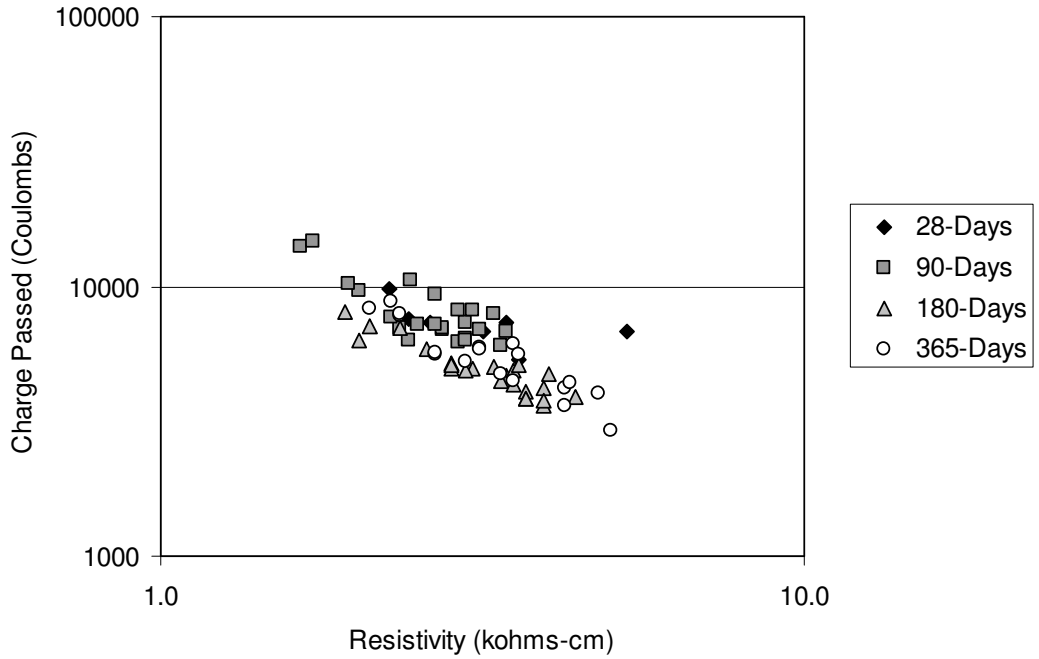

Figure 5.29 Relationships between Resistivity and Rapid Chloride Permeability

5.3.4 Carbonation

Carbonation results are summarized in Table 5.10.

Table 5.10 Depths of Carbonation Data

	Time Tested (Days)								
	90			180			365		
	Time cured (days)								
Depth (mm)	1	3	7	1	3	7	1	3	7
CL	9	5	4	6	5	3	9	7	5
CH	12	8	5	11	7	5	12	10	9
BL (HAHS)	10	8	7	10	8	5	10	9	8
BH (HAHS)	14	9	10	13	9	10	18	16	13
RL (LALS)	15	12	10	11	9	8	15	13	10
RH (LALS)	16	13	11	13	11	9	16	15	14
TL (HALS)	9	6	5	9	6	4	10	7	6
TH (HALS)	12	10	8	9	8	7	15	12	8

Carbonation has been shown to progress at an increased rate in concrete that contains fly ash. This is due to the fact that some of the cement is actually being replaced in the mix and the fly ash is reacting with the calcium hydroxide making less available for the carbonate ions to react with during the carbonation process. This increases the rate of carbonation through the concrete. It can be shown in Figures 5.30, 5.31, and 5.32 that when comparing mixes with the same W/CM, the control specimens showed the lowest depth of carbonation.

It can be seen in Table 5.10 that between 90 and 180 days there is a reduction in depth of carbonation. These specimens were tested during the winter months and

at the time of testing were not allowed to thaw completely giving a false depth of carbonation; therefore these data will not be used for evaluation.

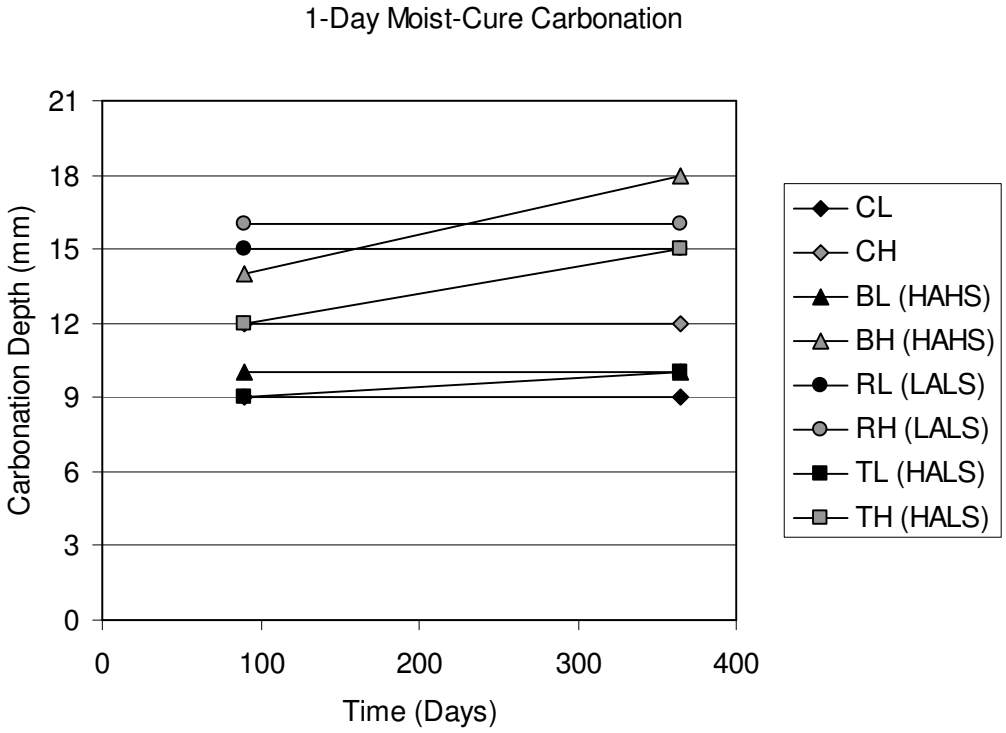

Figure 5.30 1-Day Cure Carbonation

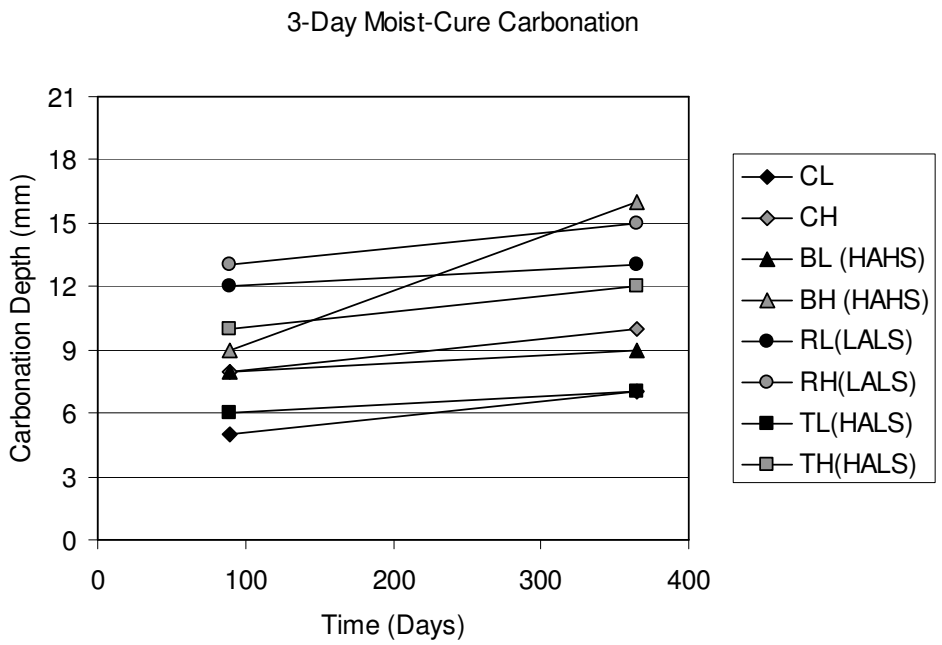

Figure 5.31 3-Day Cure Carbonation

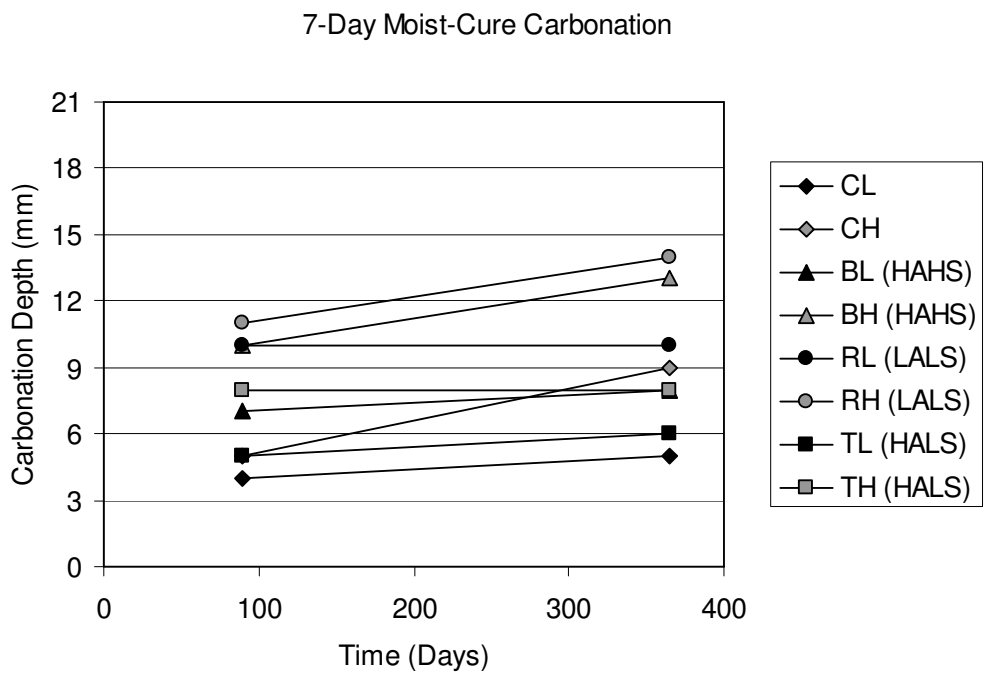

Figure 5.32 7-Day Cure Carbonation

When concrete was tested for depth of carbonation at 90 and 365 days, shown in Figures 5.33 and 5.34 it can be seen in all concrete mixes that as the initial moist-

curing time was increased the depth of carbonation decreased with the exception of BH (HAHS) at 90 days.

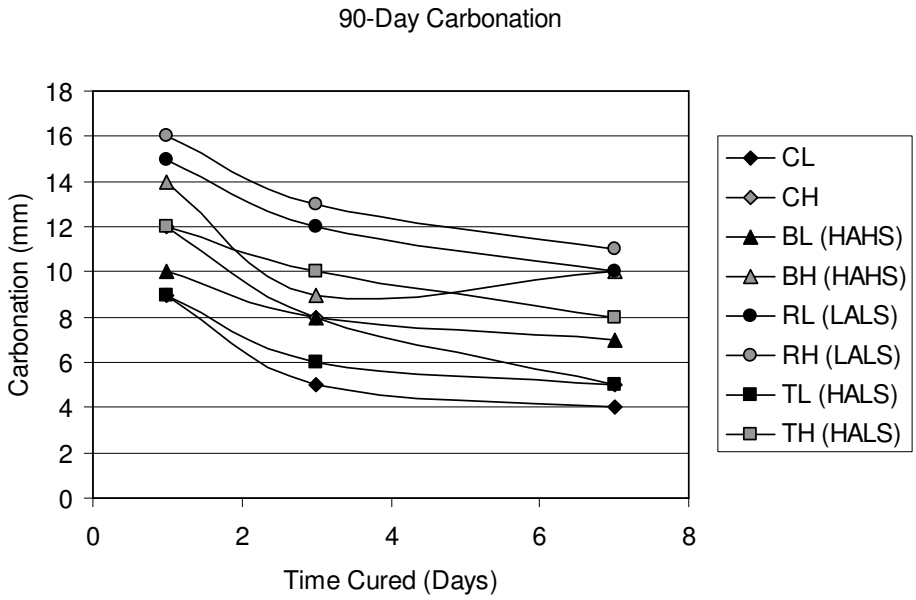

Figure 5.33 90-Day Carbonation

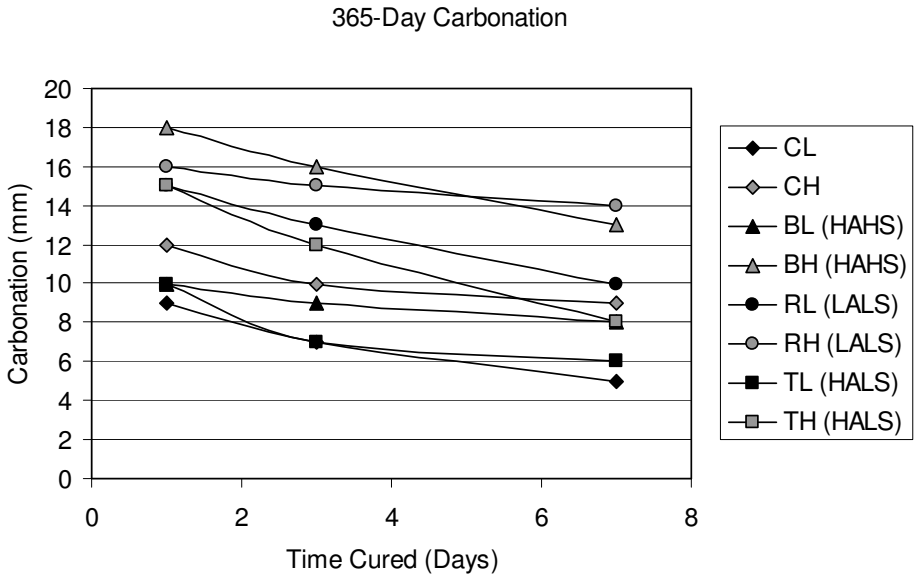

Figure 5.34 365-Day Carbonation

5.3.5 Vapor Transmission

Vapor transmission data are summarized below in Table 5.11.

Table 5.11 Vapor Transmission Data

	WTV g/h/m^2		
Moist-Cured (Days)	1	3	7
CL	1.49	1.35	1.51
CH	1.71	1.36	1.17
BL (HAHS)	1.04	1.39	1.16
BH (HAHS)	1.81	1.9	1.63
RL(LALS)	1.46	1.22	1.25
RH(LALS)	1.84	1.72	1.46
TL(HALS)	1.14	1.12	1.13
TH(HALS)	1.42	1.29	1.28

As with most deleterious mechanisms in concrete, minimizing the movement of water and aggressive chemicals is of utmost importance. There have been many tests developed to determine the potential for the movement of water but their use has been limited by very low permeable concrete. In the case of water vapour transmission, it could take many years to achieve steady flow of moisture through concrete using the conditions used in this test or even in water permeability tests using high-hydraulic pressure. However, due to the mix design and characteristics of the concrete being tested in this study, constant flow of a significant amount of vapour was easily achieved. With a one exception, CL and CH cured for 7 days, concrete produced with the same cementitious materials and cured for the same amount of time with W/CM at 0.70 had a lower flux of water transmitted then W/CM at 0.85. This is shown in Figure 5.35.

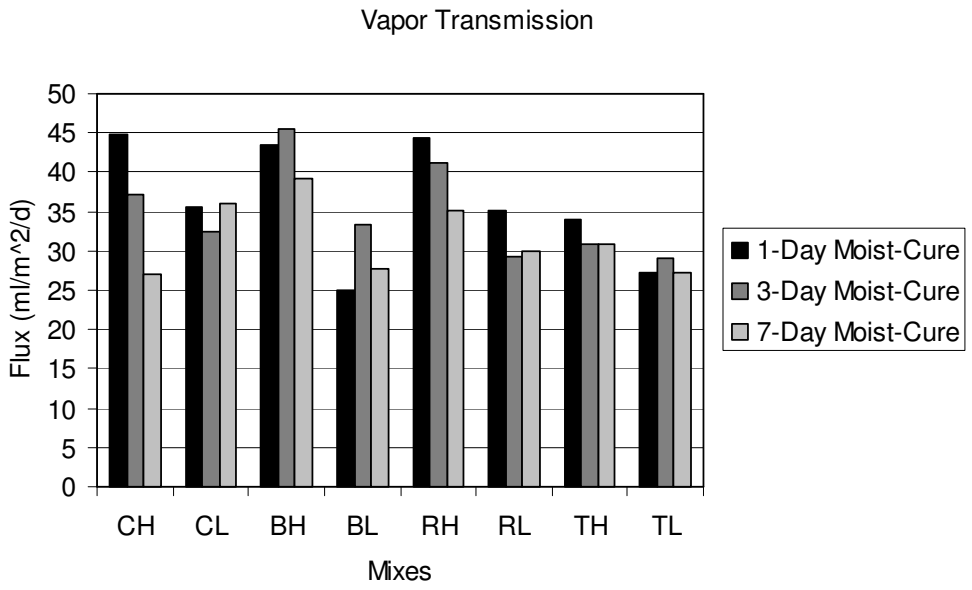

Figure 5.35 Water Vapor Transmission

It can be seen, in Figure 5.36 that all concrete produced with fly ash performed better than the control at a W/CM of 0.70. However, as the W/CM was raised the concrete made with fly ash performed poorly when compared with the control, with the exception of TH concrete that was cured for 1 or 3 days.

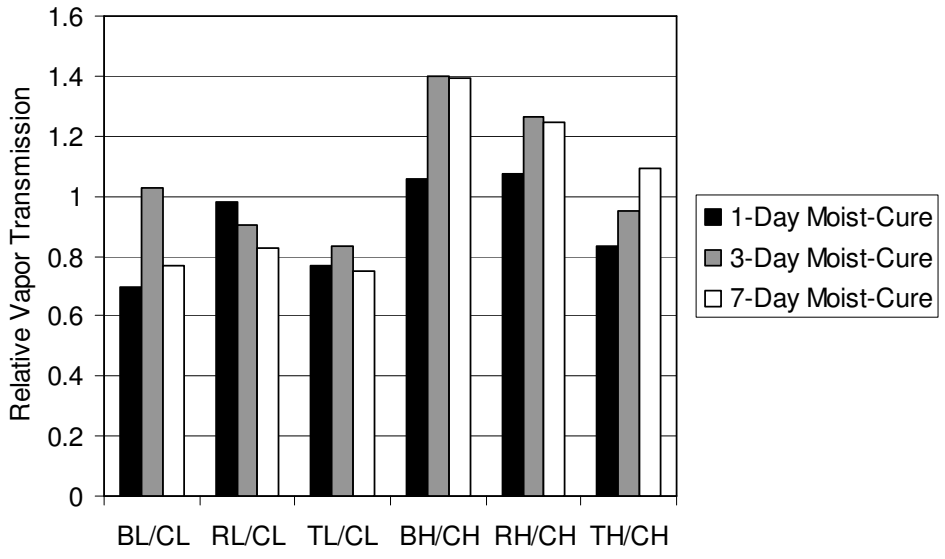

Figure 5.36 Relative Water Vapor Transmission Between Control and Fly Ash Concrete

5.3.6 Rate of Absorption (Sorptivity)

Absorption results are summarized in Table 5.12.

Table 5.12 Absorption Data

	Initial (mm/hr^1/2)		
Moist-Cure (Days)	1	3	7
CL	12.4	11.7	10.8
CH	26.9	20.2	17.5
BL (HAHS)	14.2	10.6	10.3
BH (HAHS)	34.3	19.0	18.5
RL (LALS)	20.2	15.9	13.2
RH (LALS)	37.0	27.4	23.3
TL (HALS)	13.8	9.5	9.1
TH (HALS)	31.4	20.0	21.2

	Secondary (mm/hr^1/2)		
Moist-Cure (Days)	1	3	7
CL	0.23	0.32	0.43
CH	0.15	0.10	0.13
BL (HAHS)	0.19	0.29	0.35
BH (HAHS)	0.13	0.33	0.648*
RL (LALS)	0.43	0.41	0.44
RH (LALS)	0.50	0.47	0.40
TL (HALS)	0.29	1.32*	0.78*
TH (HALS)	0.22	0.26	0.26

* Suspect Values

As would be expected, as shown in Figure 5.37, the concrete made with the same cementitious materials with W/CM =0.70 experienced a lower rate of initial rate of absorption than the concrete made with a W/CM =0.85. Also, as the moist-cure time increased, the rate of initial absorption decreased. It can also be seen that the mixes produced with W/CM of 0.85 and only cured for 1 day show a significant higher in absorption then those cured for longer.

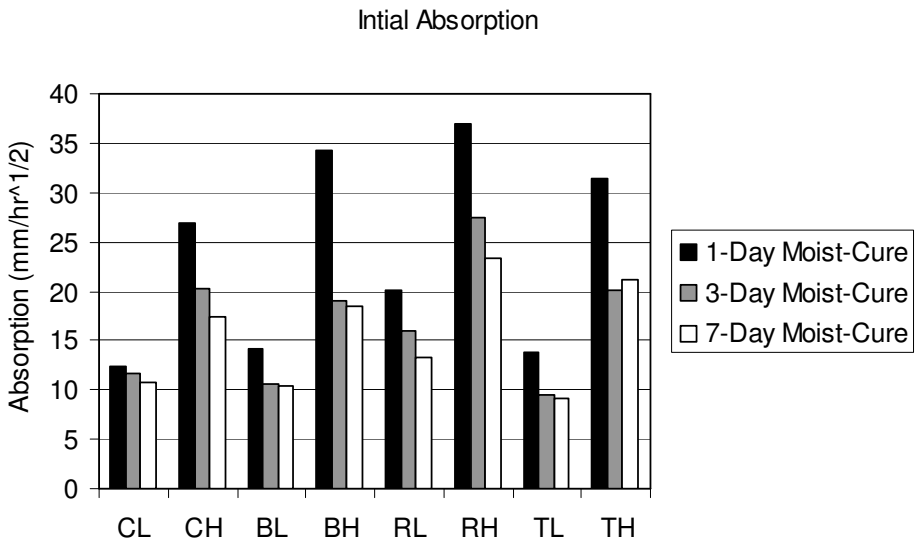

Figure 5.37 Initial Absorption

For the secondary absorption, shown in Figure 5.38, the reverse was true, the high W/CM (0.85) had the lower rate of absorption. This relationship can be attributed to the fact that the specimens absorbed the water necessary for saturation during the initial absorption period. The relationship of the rate of secondary absorption with cure time is not as clear as with the initial absorption. As some of the samples were fully saturated, the secondary rate of absorption will not be looked at any further.

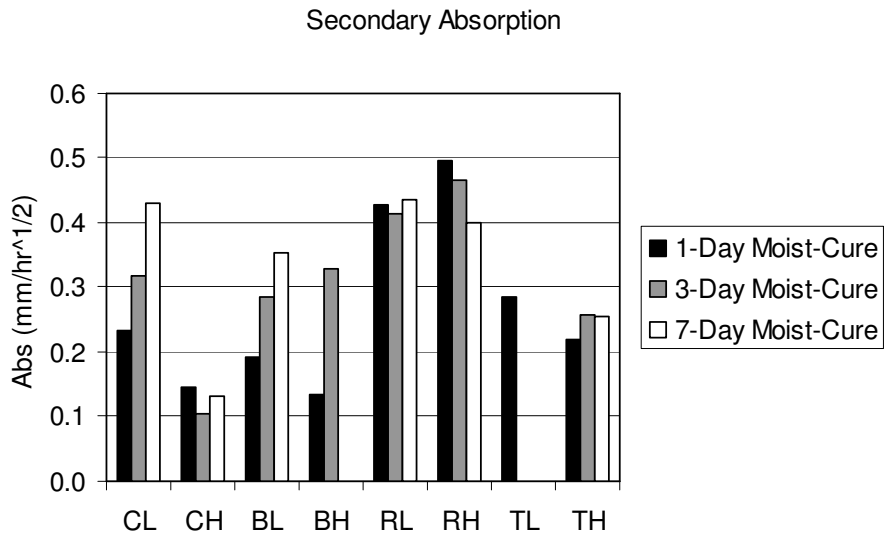

Figure 5.38 Secondary Absorption

When comparing the initial absorption, shown in Figure 5.39, of the control to concrete containing fly ash, for the most part the control performed better. The fly ashes that performed better then the control were BL (HAHS) and TL (HALS) at cure times 3 and 7 days.

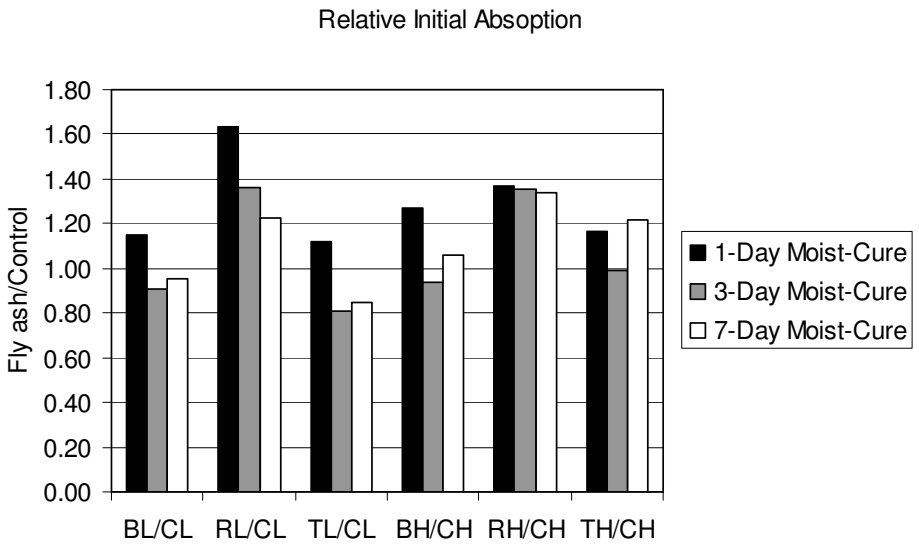

Figure 5.39 Relative Initial Absorption between the Control and Fly Ash Concrete

Parrot (1992) showed that as carbonation occurred in ordinary Portland cement paste there was a reduction in absorption where as in paste produced with 30% fly ash there was an increase in both absorption and capillary porosity. Even though samples are not completely carbonated, samples RH and BH concrete experiences the greatest depth of carbonation and the greatest rate of absorption.

Chang (2003) has also shown that absorption decreases when concrete carbonates and that the relative decrease in absorption rate increased as the W/CM increased.

5.3.7 Rebound Hardness

Rebound hardness results are summarized in Table 5.13.

Table 5.13 Rebound Hardness Data

	28-Day (Cast Surface)				28-Day (Finished Surface)		
Moist-Curing (Days)	1	3	7	Moist-Curing (Days)	1	3	7
CL-28-C	10	11	14	CL-28-F	9	8	12
CH-28-C	10	11	10	CL-28-F	5	6	7
BL-28-C	13	12	13	BL-28-F	8	8	11
BH-28-C	8	6	10	BH-28-F	5	4	8
RL-28-C	8	10	11	RL-28-F	10	5	5
RH-28-C	11	11	13	RH-28-F	7	4	6
TL-28-C				TL-28-F			
TH-28-C				TH-28-F			

	90-Day (Cast Surface)				90-Day (Finished Surface)		
Moist-Curing (Days)	1	3	7	Moist-Curing (Days)	1	3	7
CL-90-C	14	15	15	CL-90-F	9	11	14
CH-90-C	14	15	16	CL-90-F	8	14	13
BL-90-C	11	14	15	BL-90-F	11	12	13
BH-90-C	9	11	12	BH-90-F	9	7	11
RL-90-C	13	13	14	RL-90-F	12	13	13
RH-90-C	15	16	15	RH-90-F	12	12	7
TL-90-C	18	19	17	TL-90-F	16	15	15
TH-90-C	15	18	17	TH-90-F	13	15	15

	180-Day (Cast Surface)				180-Day (Finished Surface)		
Moist-Curing (Days)	1	3	7	Moist-Curing (Days)	1	3	7
CL-180-C	19	17	20	CL-180-F	16	19	18
CH-180-C	21	19	19	CL-180-F	16	18	16
BL-180-C	17	19	20	BL-180-F	18	18	17
BH-180-C	16	16	18	BH-180-F	15	12	13
RL-180-C	16	17	18	RL-180-F	16	16	17
RH-180-C	18	18	17	RH-180-F	15	16	13
TL-180-C	21	19	21	TL-180-F	19	20	20
TH-180-C	17	19	18	TH-180-F	16	15	14

	365-Day (Cast Surface)				365-Day (Finished Surface)		
Moist-Curing (Days)	1	3	7	Moist-Curing (Days)	1	3	7
CL-365-C	22	22	24	CL-365-F	20	20	20
CH-365-C	20	19	24	CL-365-F	16	18	18
BL-365-C	21	20	21	BL-365-F	19	19	20
BH-365-C	19	20	20	BH-365-F	15	13	15
RL-365-C	18	17	20	RL-365-F	16	14	15
RH-365-C	18	18	19	RH-365-F	16	16	17
TL-365-C	19	17	21	TL-365-F	18	17	18
TH-365-C	25	22	25	TH-365-F	22	23	23

It can be shown in Figure 5.40, 5.41, and 5.42 that for both the control concrete and the concrete produced with fly ash there was a general increase in the rebound hardness as the specimens mature and carbonate. Carbonation can increase the rebound hardness by 50% (Mindess et al, 2003). It can also be seen that there was a slight reduction in the rebound hardness as the W/CM increases to 0.85 from 0.70. There were also very slight increases in rebound hardness as the cure time increase from one day to three days and then to seven days.

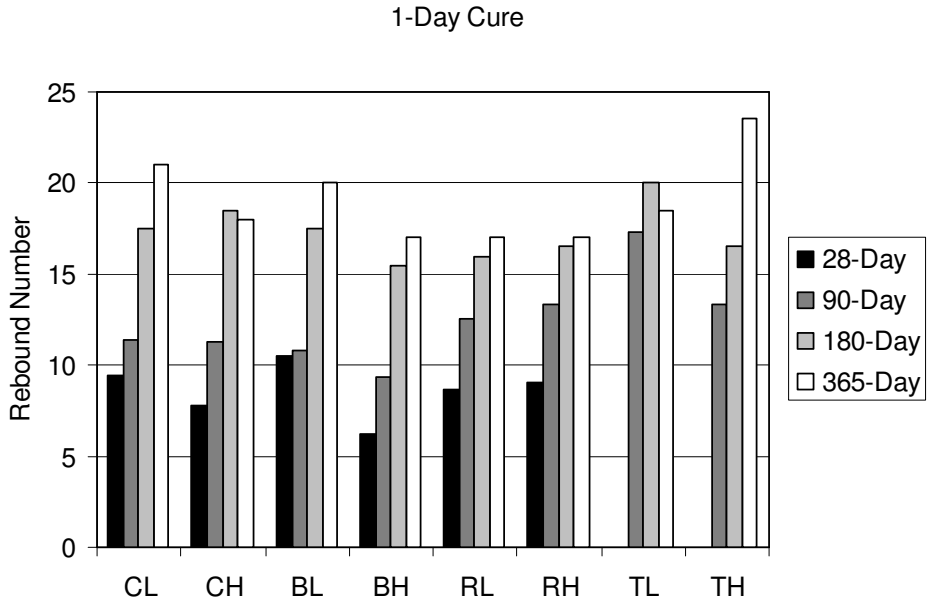

Figure 5.40 1-Day Moist-Cured Rebound Hardness Number

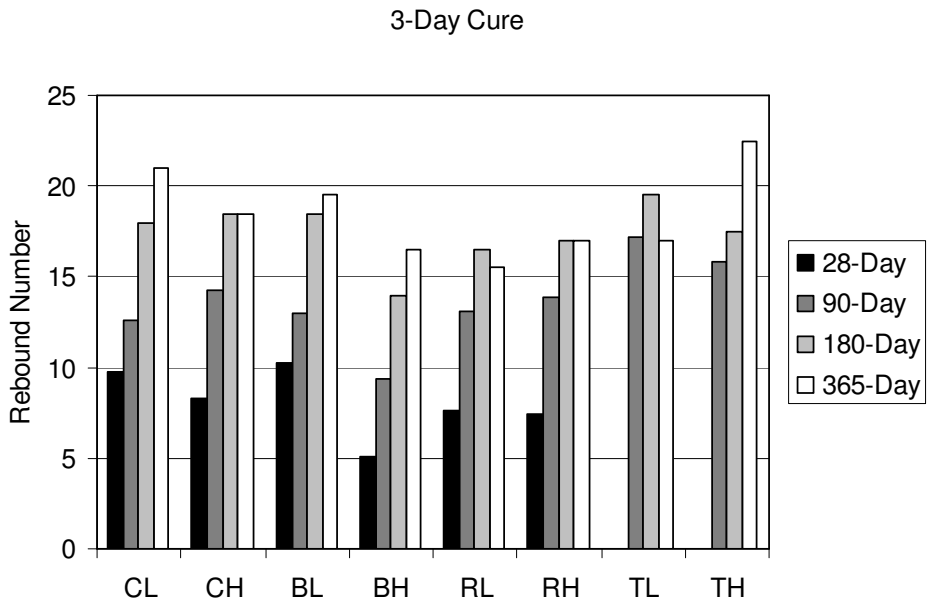

Figure 5.41 3-Day Moist-Cured Rebound Hardness Number

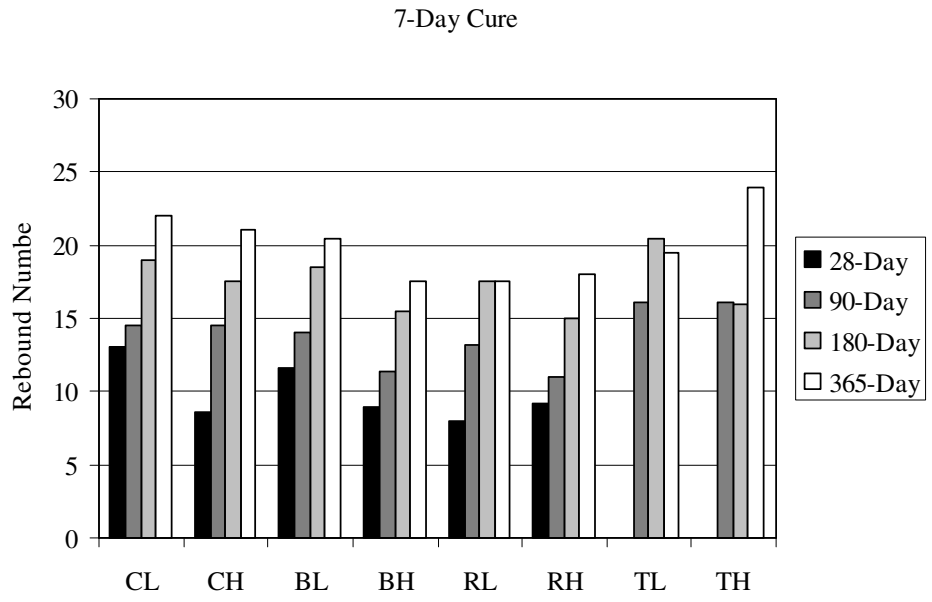

Figure 5.42 7-Day Moist-Cured Rebound Hardness Number

It can be seen in Figures 5.43 and 5.44 that samples produced at both W/CM= 0.7 and 0.85 and produced with OPC and fly ashes, and cured for 1, 3 and 7 days that between 28 and 365 days all had an increase over 50%.

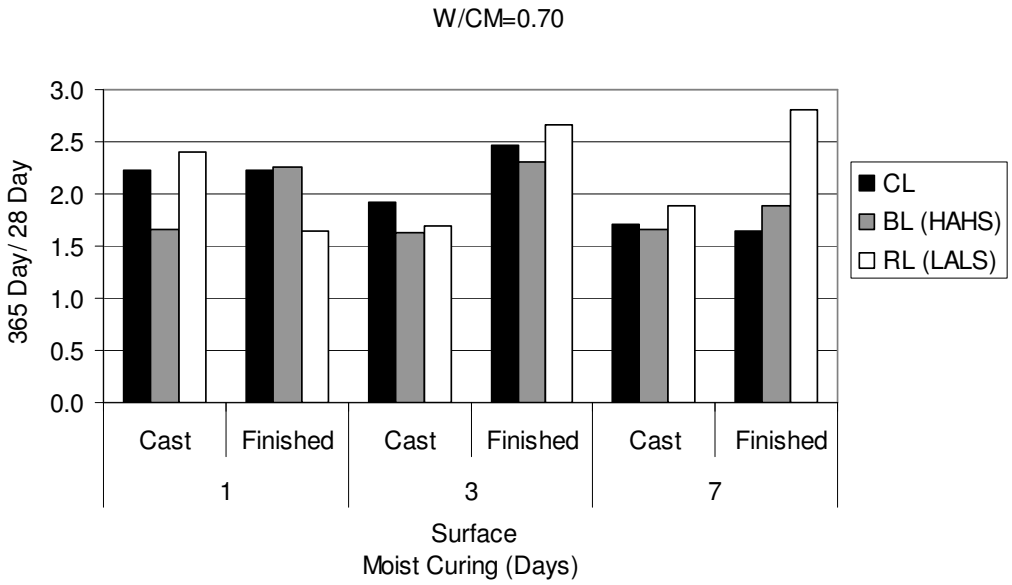

Figure 5.43 Relative Rebound hardness between 28-365 days W/CM 0.7

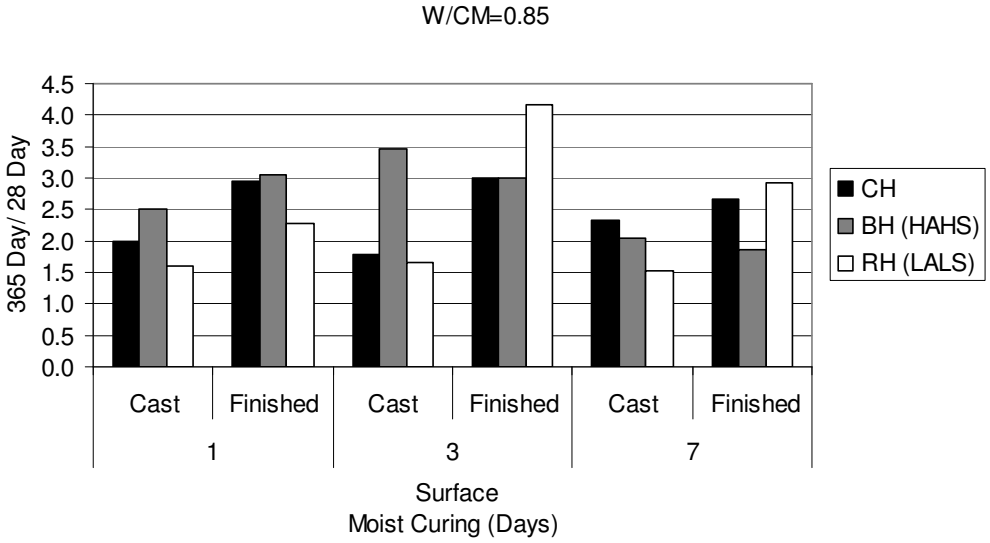

Figure 5.44 Relative Rebound hardness between 28-365 days W/CM 0.7

6.0 Discussion of Results

6.1 Residential Foundations

The investigations of carbonation and the use of fly ash were initiated in response to the deterioration of a large number of residential concrete structures. This deterioration manifested itself in the form of softening of the surface, efflorescence, sub florescence, spalling and scaling. Several mechanisms were identified to have contributed to the failure of the concrete. After these investigations, it was observed that the cementitious matrix of the concrete showed symptoms of popcorn calcite deposition (PCD) as shown in Figure 6.1.

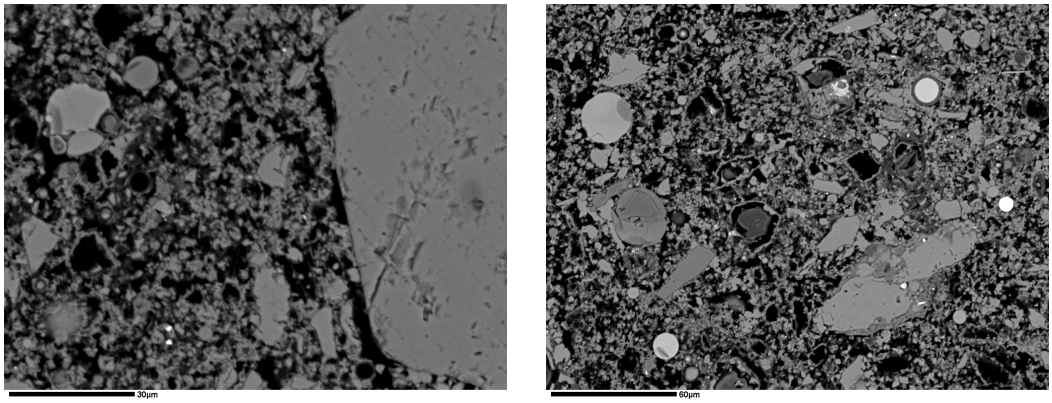

Figure 6.1Backscatter Electron Images of Carbonated Residential Concrete

This resulted in several question being asked. Was this a characteristic of poor quality (high W/CM) concrete or was it a result of the type of fly ash that was used in this case or a combination of the two? Residential concrete typically has high W/CM values equal to or greater than 0.70 but it was suspected that in this case the W/CM may have been as high as 0.90 (some investigators claimed even higher values). The fly ash used had alkali and sulfates contents which were very high compared to typical North American fly ashes. (Seabrook et al, 2003)

As can be observed above in Figure 6.1, a large amount of porosity can be seen where mass water transportation can occur. Seabrook et al. (2003) found the causes of the deterioration to be freeze thaw, internal and physical sulfate attack which all requires moisture to be present therefore when moisture is allowed to move more freely these forms of deterioration can occur much faster.

6.2 Carbonation of Portland Cement Paste and Mortar

It was shown that the only time that extent of PCD (as determined by the percolation of calcium phases) was low in the control paste samples even at W/CM= 0.9. The carbonated control paste still had a continuous matrix of calcium carbonate. The mortar produced for this study was at W/CM=0.7 and the control showed an increase in all mechanical properties after carbonation. This can be seen in Figure 6.2

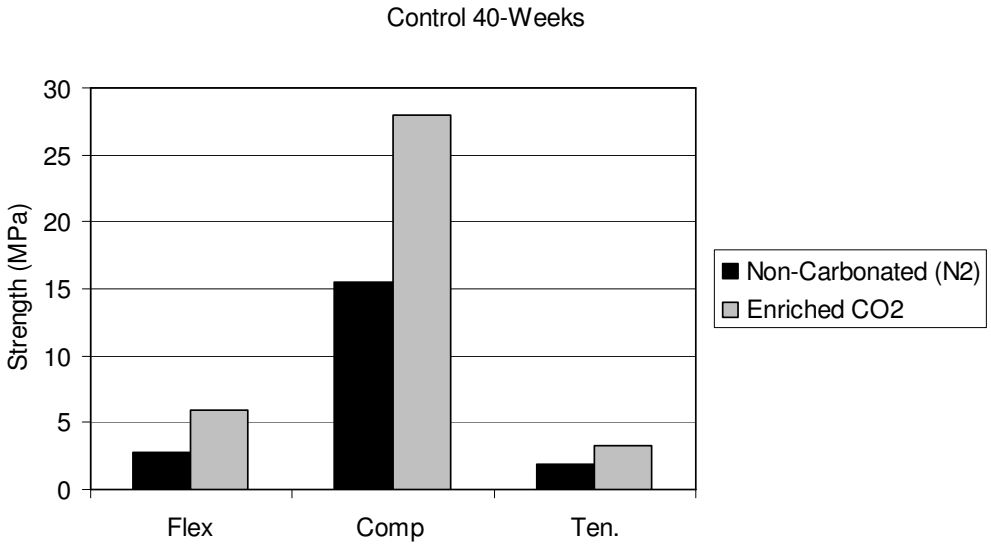

Figure 6.2 Control Mechanical Strengths at 40-Weeks.

This result does not tell us if the control experienced popcorn carbonation, how the mechanical strength would have been affected. The porosity was also determined on mortar samples that experienced carbonation and the control showed a small reduction in total porosity and only a slight increase in capillary (as measured by isopropenol) after carbonation.

Further research is needed at higher W/CM in order to determine whether the mechanical strength will be compromised if Portland cement concrete experiences PCD.

6.3 Fly Ash and Carbonation of Fly Ash Paste and Mortar

When evaluating the pore structure of the paste samples produced with 20% replacement fly ash, there was more evidence of PCD or reduction in the connectivity of the calcium-bearing phases at W/CM=0.7 with the BR (HAHS) fly ash. All fly ash samples exhibited low connectivity at W/CM=0.9. This can be seen in Figure 5.3.

When comparing the fly ash samples to the control, as seen in Figure 5.4, there seems to be a slight increase in percolation in samples RP (LALS) and TB (HALS) at W/CM 0.7, however a drop by 40% in sample BR (HAHS). At W/CM 0.9 all fly ash samples seam to exhibit the same reduction in the connectivity of calcium phases.

When the mechanical properties of the fly ash mortar samples are normalized with respect to the control samples of the same age there is a reduction in the normalized strength of the fly ash sample with age during storage in a CO_2-enriched atmosphere. This is shown in Figure 6.3, 6.4 and 6.5.

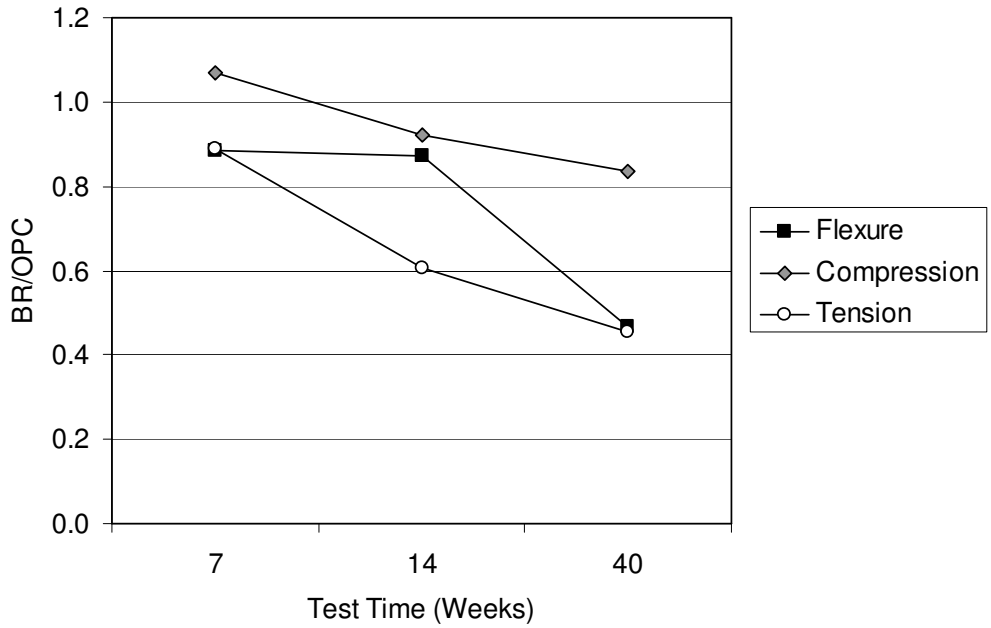

Figure 6.3 Relative Mechanical Strength between MBR (HAHS) and MOPC Stored in CO_2 Enriched Atmosphere

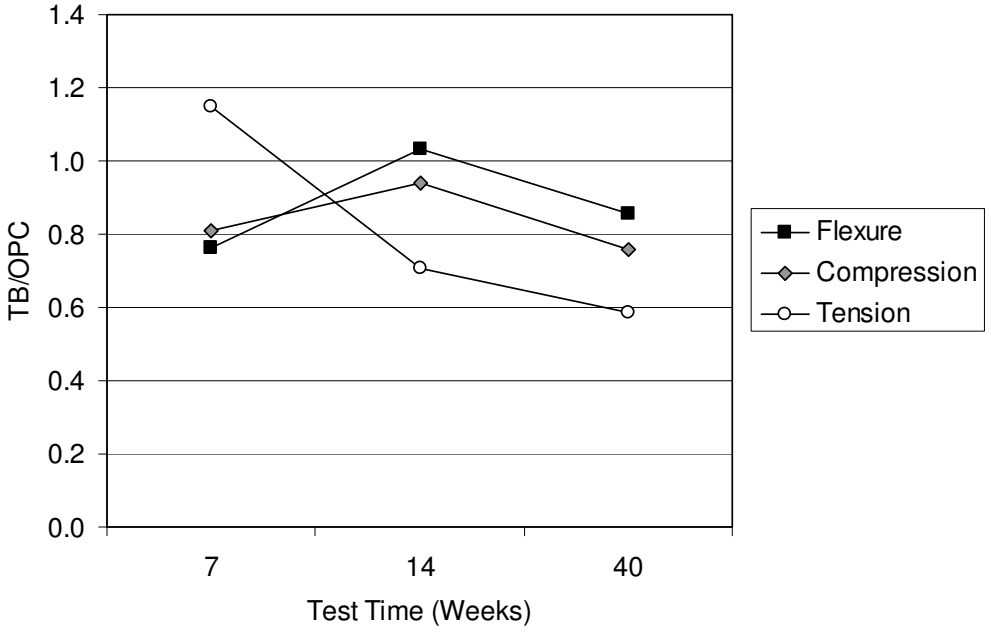

Figure 6.4 Relative Mechanical Strength between MTB (HALS) and MOPC CO_2 Enriched Atmosphere

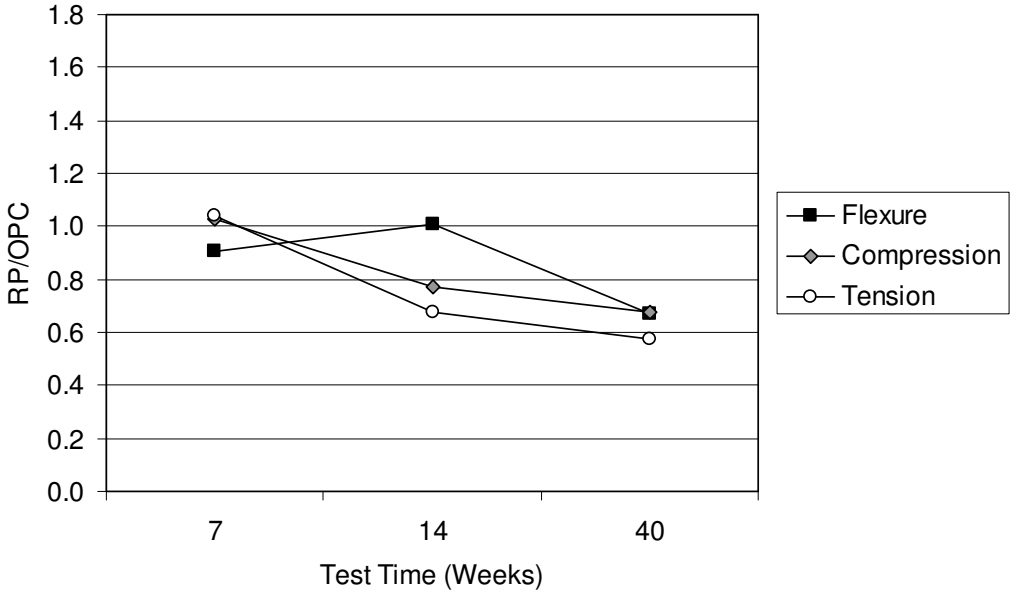

Figure 6.5 Relative Mechanical Strength between MRP (LALS) and MOPC CO_2 Enriched Atmosphere

At 40 weeks of age, based on extensive research done by others on the performance of fly ash, the comparable strengths should be higher than the control.

Even though when the samples made with fly ash to the control show a reduction in relative strength gain, each of the fly ashes experienced an increase in strength after carbonation that can be seen in Figure 6.6 a, b and c.

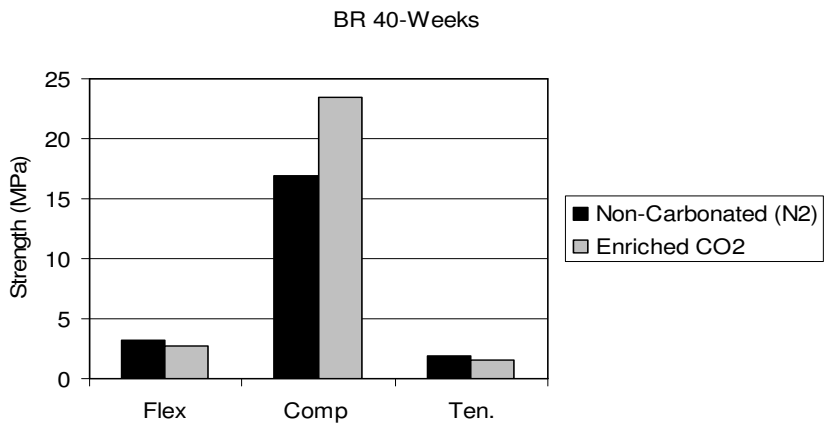

a) BR (HAHS)

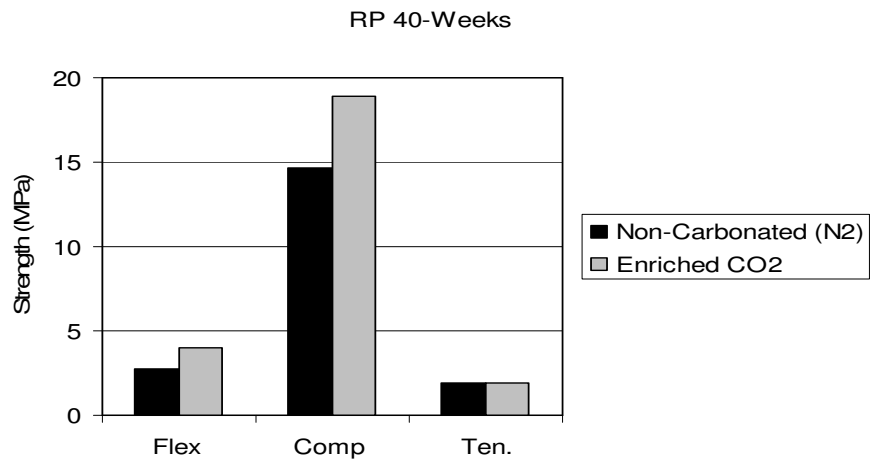

B) RP (LALS)

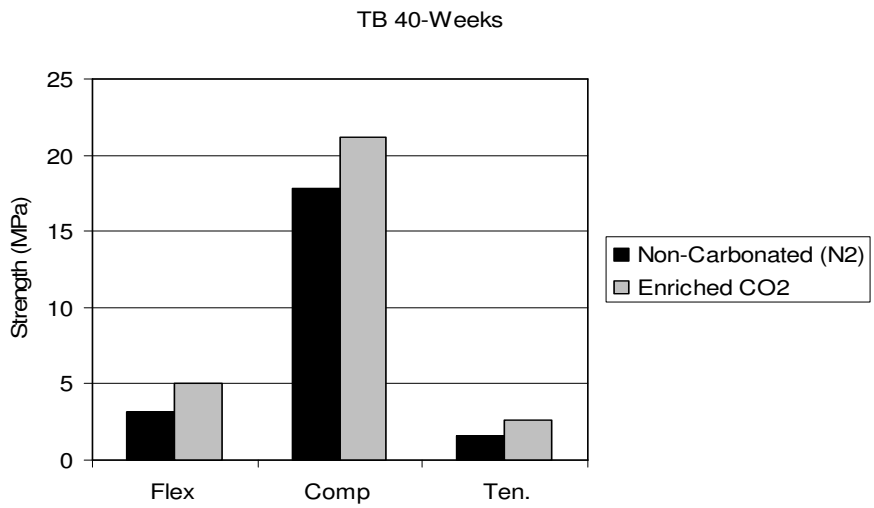

c) TB (HALS)

Figure 6.6 Mechanical Strengths Non carbonated and Carbonated samples at 40-Weeks of a)BR (HAHS), b) RP(LALS) , and c) TB (HALS)

When comparing all samples subjected to wetting and drying cycles and subsequently stored in a humidity controlled tent to those samples that were carbonated at an accelerated pace, there seams to be an even further increase in compressive strength but a reduction in flexural and tensile strength as shown in Figure 6.7. The increase in compressive strength can be attributed to possible future hydration of cement particles however the reduction in the other two properties cannot be explained at this point.

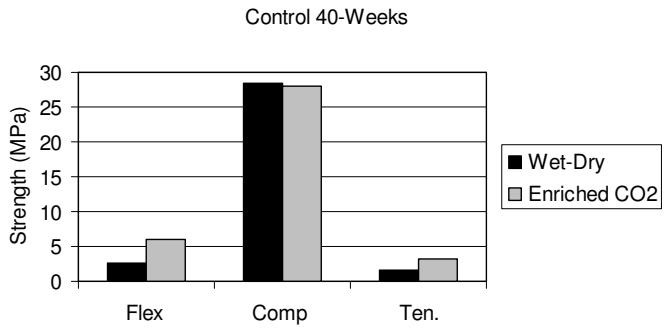

a) OPC

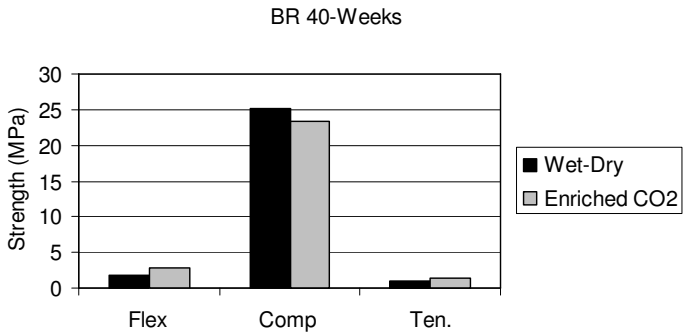

b)BR (HAHS)

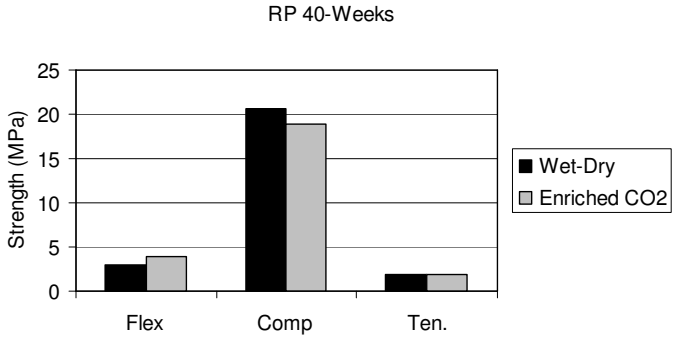

c) RP (LALS)

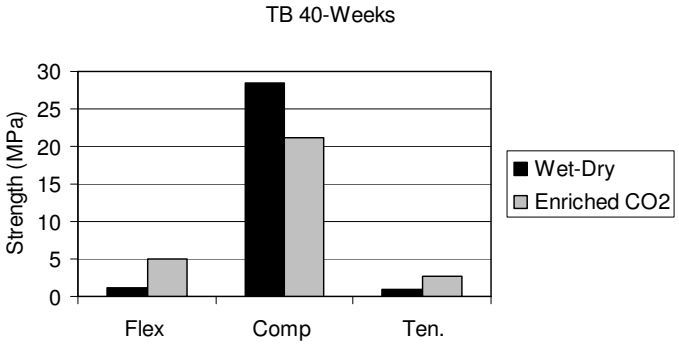

d) TB (HALS)

Figure 6.7 Mechanical Strengths Wet Dry (tent) and Carbonated samples at 40-Weeks of a)OPC , b) BR (HAHS) , c) RP (LALS), and d) TB (HALS)

Even though others have used micro hardness to evaluate the effects of carbonation on microstructure in paste samples, due to the softness of the samples with W/CM = 0.7 and 0.9 the test was difficult to perform and some measurements could not be made..

Further to mechanical strength showing some differences when samples underwent carbonation and wet drying cycles the porosity also showed evidence of change. The data showed that there was a slight reduction in porosity for samples MOPC, MRP (LALS) and MTB (HALS) and a slight increase in MBR (HAHS), however these pores were found to be coarser in all samples with the largest increase in coarser pores being in sample BR (HAHS) indicating more break down of the CSH during carbonation and possibly creating a more disconnected calcium-bearing phase in the carbonated cement paste. These samples were produced at a W/CM = 0.7 and when comparing these to the percolation measurements as shown in Figure 6.8 that as the coarser porosity increased there was a decrease in percolated calcium phases in sample BR (HAHS).

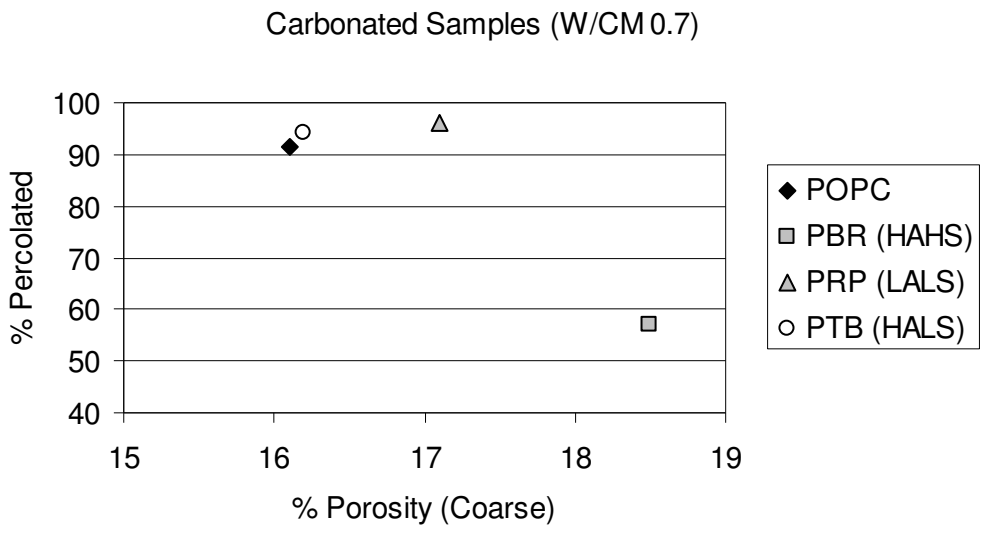

Figure 6.8 Carbonated Samples Relating % Coarse Porosity and %Percolation

The real difference in percolation was noticed at W/CM =0.9 and further possible correlation between porosity and percolation should be evaluated.

6.4 Fly ash Concrete and Mass Transport

There were several different tests performed during this study to evaluate the mass transport system and mechanical strength characteristics which are commonly used to characterize higher quality concrete; such tests include rapid chloride permeability, electrical resistivity, carbonation, water vapor transmission, rate of absorption in addition to the traditional compressive strength testing.

For the compressive strength, all fly ash samples performed worse than the control for all curing periods and for both W/CM = 0.7 and 0.85. This is uncharacteristic of concrete produced with fly ash tested at later ages. Figure 6.9 does show improvements where samples are continuously cured until time of

testing, more so in samples TL (HALS) ,TH (HALS), RL (LALS) and RH (LALS) with little to no difference in samples BL (HAHS) and BH (HAHS).

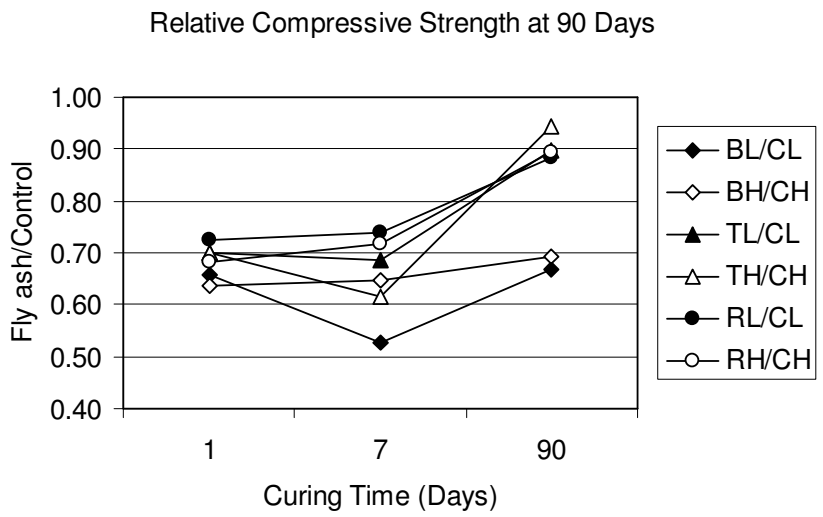

Figure 6.9 Fly Ash compared to Control Compressive Strength at 90 days

The samples were also tested for rapid chloride, as this is a commonly used test to determine transport properties in concrete. This test is generally used to test high performance concrete that has low electrical conductivity. As can been seen in the results of section 5.3.2 the samples all fall above the highest value of 4000 Coulombs according to ASTM 1202. It was experienced in most, if not all samples that the current passed was so high that the samples and solutions in each end of the apparatus increased in temperature to the point of boiling. The effect of high temperature could lead to highly variable results and therefore the results of this testing cannot be used as a reliable measure of performance.

Carbonation measurements on concrete samples were taken and the results are what would be expected such as when the curing was increased or the W/CM was

lowered the carbonation depths decreased. Also with the addition of fly ash the depth of carbonation increased as seen in Figure 6.10. However since these measurements were only taken over a year, the data cannot be projected to determine performance over a longer period of time. Some of the issues observed in the field were after several years after construction. Also, these samples were stored outdoors and the carbonation process is likely to cease during the winter months when the concrete is frozen.

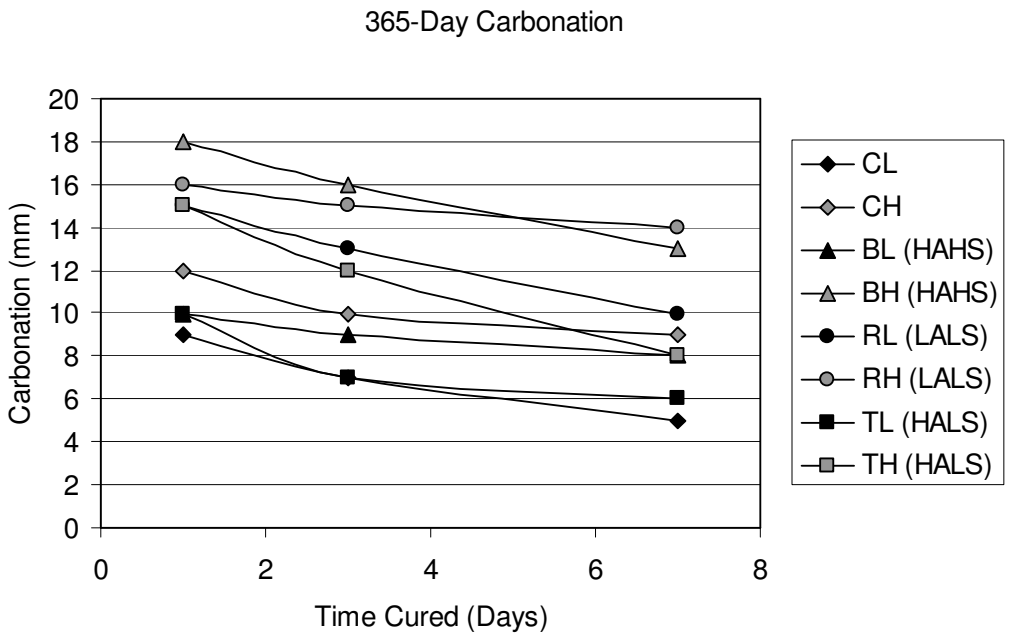

Figure 6.10 Carbonation at 365 day.

Other attempts were made to measure moisture transport by means of vapor transmission and rate of absorption, as mentioned above the more accepted method of RCP testing proved to be too harsh. Even though these results showed common effects of changing W/CM and curing, due to the fact samples were not fully carbonated no interpretations on the data can be made.

6.5 Implications and Limitations of Study

One of the problems with studying concrete durability is that the processes of deterioration usually take years, if not decades, to manifest. This complicates laboratory studies where there is often insufficient time to allow the mechanisms of failure to fully develop. For example, it would take many years for a concrete sample to carbonate significantly for the mechanical properties to be significantly altered. This necessitated working with smaller mortar samples and pastes, which are not always fully representative of concrete. Despite the limitations there is evidence from the paste studies that PCD does occur in fly ash samples with the W/CM = 0.90 and, to a lesser extent, with W/CM = 0.70, and some indication from the mortar studies that this may lead to a reduction in mechanical properties at W/CM = 0.70. Unfortunately, mortar studies were not conducted at the higher W/CM. There is also evidence that PCD and resulting loss in strength are more likely to occur with high alkali-sulfate fly ashes.

Although these findings must be treated with caution, they do highlight the need for further studies to determine if strength loss due to PCD is likely to occur in concrete with high W/CM and whether the process is exacerbated by fly ash. This will require a study of a much longer duration than was possible in this case.

7.0 Conclusion

The following conclusions can be drawn from this study:

1. Samples prepared from basements that experienced severe forms of deterioration were shown to have PCD.

2. As W/CM increased in paste samples with fly ash carbonation led to a decrease in the connectivity of calcium phases; there was only a slight decrease in connectivity in samples produced with OPC.

3. Carbonation showed to have a coarsening effect on the pore size distribution in all samples produced with fly ash but was more evident in samples produced with the BR fly ash that had both high sulfate and high alkali content.

4. Carbonation increased mechanical strength in control samples; however, the increase is only noticeable in the fly ash samples when evaluating compressive strength.

5. Carbonation decreased the strength of fly ash mortars relative to the control mortars; the effect was most pronounced with fly ash BR.

6. Carbonation when combined with wet-dry cycling showed a slightly further increase in compressive strength but showed a lowering of both tensile and flexural strength for all samples.

8.0 Recommendation

After completing this study, the following recommendations are made for further research with regards to fly ash and the effects of carbonation on mechanical properties and pore structure:

1. Use higher water to cementitious material in mortar samples to further investigate the effect of carbonation and fly ash.
2. Perform porosity measurements using mercury intrusion porosimetry to better understand the change in pore size distribution due to carbonation.
3. Investigate this type of carbonation and its effect on the hardened air-void system.
4. Perform various mass transport tests using modified testing to compensate for the increased ability for water to absorb into concrete due to increased W/CM.
5. Perform tests at increased levels of fly ash (e.g. 30 to 60%).

9.0 Reference

ACI Committee 201. (2001) Guide to Durable Concrete. ACI Manual of Concrete Practice 201.2R-01.

American Society for Testing and Material, (2000). Standards on Dics, Vol. 04.02, October 2000, Concrete and Aggregates. West Conshohocken, PA, United States.

ASMT C39 Standard Test Method for Compressive Strength of Cylindrical Concrete Specimens

ASTM C 143/C 143M Test Method for Slump of Hydraulic Cement Concrete.

ASTM C 190-85 Standard Test Method for Tensile Strength of Hydraulic-Cement Mortars

ASTM C 192/C 192M-98 Making and Curing Concrete Test Specimens in The Laboratory.

ASTM C 215 Standard Test Method for Fundamental Transverse, Longitudinal, and Torsional Resonant Frequencies of Concrete

ASTM C 231 Test Method for Air Content of Freshly Mixed Concrete by the Pressure Method

ASTM C 305 Practice for Mechanical Mixing of Hydraulic Cement and Paste Samples of Plastic Consistency

ASMT C 348-02 Standard Test Method for Flexural Strength of Hydraulic-Cement Mortars

ASTM C 349-02 Standard Test Method for Compressive Strength of Hydraulic-Cement Mortars

ASTM C 805 Standard Test Method for Rebound Number for Hardened Concrete

ASTM C 1202 Standard Test Method for Electrical Indication or Concrete's Ability to Resist Chloride Ion Penetration

ASTM C 1585-04 Standard Test Method for Measurement of Rate of Absorption of Water by Hydraulic Cement Concretes.

ASTM E 96-00 Standard Test Method for Water Vapor Transmission of Materials

ASTM E 104-02 Standard Practice for Maintaining Constant Relative Humidity by Means of Aqueous Solution

ASTM E 384 Standard Test Method for Microindentation Harndness of Material.

Ashbridge, A.H., Page, C.L. and Page, M.M. 2002. Effects of metakaolin, water/binder ratio and interfacial transition zones on the microhardness of cement mortars." Cement and Concrete Research, Vol. 32, pp. 1365-1369.

Bentz, D. burn2d.f Algorithm.

Bier, T. 1986. "Influence of type of cement and curing on carbonation and pore structure of HCP." Proceedings of the Materials Research Society, V85, Boston, 18pp.

Canadian Standards Association (CSA), 2003. "Cementitious Materials Compendium", CSA A3000-03, Mississauga, Ontario.

Canadian Standards Association (CSA), 1983. "Concrete construction for housing and small buildings." CSA A438-M1983, Rexdale, Ontario.

Chang, J.J., Yeih, W., Huang, H., Chen, C.T. 2004. Suitability of several current used concrete durability indices on evaluating the corrosion hazard for carbonated concrete,
84: 71-78.

Chang, J.J., Yeih, W., Huang, R., Chi, J.M. 2003. Mechanical Properties of Carbonated Concrete. Journal of the Chinese Institute of Engineers, Vol. 26, No. 4, 513-522.

Chang, J.J. 2001. A Study of the Bond Degradation of rebar due to Cathodic Protection Current. Cement and Concrete Research, **32:** 657-663.

Ghosh, A., and Pratt, P.L. 1981. Studies of the hydration reaction and microstructure of cement – fly ash paste. Proceedings, Annual Meeting of the Materials Research Society, Boston, MA.

Hagelia, P., Sibbick, R.G., Crammond, N.J., and Larsen, C.K. (2003): "Thaumasite and secondary calcite in some Norwegian concretes". Cement and Concrete Composites 25, 1131-1140.

Igarashi, S., Bentur, A., Mindess, S. 1996. Microhardness Testing of Cementitious Materials. Advanced Cement Based Materials, **4**: 48-57.

Joshi, R.C. and Lohtia, R.P. 1997. Fly Ash in Concrete Production, Properties and Uses. Gordon Breach Science Publishers.

Kobayashi, K., Suzuki, K. and Uno, Y. 1994. "Carbonation of concrete structures and decomposition of C-S-H." Cement and Concrete Research, Vol. 24, pp. 55-61.

Lawes G. Scanning Electron Microscopy and X-Ray Microanalysis. Analytical Chemistry by Open Learning, Thames Polytechnica. London. (1987)

Malhotra, V.M., and Mehta, P.k. (2002). "High Performance, High – Volume Fly Ash Concrete". Supplementary Cementing Materials for Sustainable Development Inc.,Ottawa Canada.

Malhotra, V.M., and Ramezanianpour, A.A. (1994). Fly ash in Concrete, Second Edition. Natural Recourses Canada, Ottawa, Ontario, CANMET- Canadian Center for Mineral and Energy Technology.

Marceau, M. L., Nisbet, M. A., and VanGeem, Martha G., Life Cycle Inventory of Portland Cement Manufacture, SN2095b, Portland Cement Association, Skokie, IL, 2006, 69 pages.

Mindess, S., Young, J.F., and Darwin, D. (2003). Concrete, Second Edition. Prentice Hall, Pearson Education, Inc., Upper Saddle River, NJ.

Ngala, V.T., and Page, C.L. 1997. Effects of Carbonation on Pore Structure and Diffusional Properties of Hydrated Cement Pastes. Cement and Concrete Research, Vol 27, No. 7 995-1007.

Ngala, V.T., and Page, C.L, Parrott, L.J., Yu, S.W. 1994. Diffusion in Cementitious Materail:II. Furture Investigations of Chloride and Oxygen Diffusion in Well-Cured OPC and OPC/30% PFA Pastes. Cement and Concrete Research, Vol 25, No.4 819-826

Neville, A M. 1993. Properties of Concrete. Longman Scientific & Technical, Copublished with John Wiley & sons, inc, New York.

Parrott, L.J. (1987) A Review of Carbonation in Reinforced Concrete. A review carried out by C&Ca under a Building Research Establishment contract.

Parrott, L.J., 1992. Varations of Water Absorption Rate and Porosity with Depth From an Exposed Concrete Surface: Effects of Exposure Conditions and Cement Type. Cement and Concrete Research Vol. 22, 1077-1088.

Powers, T.C., Copeland, L.E. and Mann, H.M. 1959. "Capillary continuity or discontinuity in cement pastes." Journal of the PCA Research and Development Laboratories, Vol. 1 (2), pp. 38-48.

Ramachandran, V.S., Feldman, R.F. and Beaudoin, J.J. 1981. Concrete Science, Heydon & Sons, London, 328 p.

Seabrook, P.T., Day, R., Langley W.S., Thomas M.D, 2003. The Role of Fly Ash in the Ontario Basement Case Study. EcoSmart Concrete Project.

Sibbick, T. Crammond, N. 2003. The Petrographical Examination of poporn Calcite Deposition (PCD) Within Concret Mortar, and Its Association With Other Forms of Degradation. Presented at 9Th Euroseminar on Microscopy Applied to Building Materials, Trondheim, Norway. 9-12.

Thaulow, N., Lee, RJ, Wagner, K., Sahu, S., Effects of Calcuim Hydroxide Content on the form, Extent, and Significance of Carbonation. Materials Science of Concrete Special Volume: Calcium Hydroxide in Concrete. The American Ceramic Society, Westervill Ohio. 2001.

Thomas, M.D.A. 2008. Personal Communication.

Urrox, G. Getting started with FORTRAN G77. (2002)

Wierig, H. 1984. “Long time studies on the carbonation of concrete under normal outdoor exposure.” Proceedings of RILEM Seminar, Hannover, pp. 239-249.

Curriculum Vita

Tanya April Owens

Universities attended: St. Francis Xavier 1996-1998 Diploma of Engineering

University of New Brunswick 1998-2001 Bachelor of Science Mathematics

University of New Brunswick 2001-2003 Bachelor of Science Engineering